Hindawi Publishing Corporation
International Journal of Medicinal Chemistry
Volume 2015, Article ID 430248, 54 pages
http://dx.doi.org/10.1155/2015/430248

Review Article

A Review of the Updated Pharmacophore for the Alpha 5 GABA(A) Benzodiazepine Receptor Model

Terry Clayton,[1] Michael M. Poe,[1] Sundari Rallapalli,[1] Poonam Biawat,[1] Miroslav M. Savić,[2] James K. Rowlett,[3] George Gallos,[4] Charles W. Emala,[4] Catherine C. Kaczorowski,[5] Douglas C. Stafford,[6] Leggy A. Arnold,[1,6] and James M. Cook[1,6]

[1]*Department of Chemistry and Biochemistry, University of Wisconsin-Milwaukee, Milwaukee, WI 53201, USA*
[2]*Department of Pharmacology, Faculty of Pharmacy, University of Belgrade, Belgrade, Serbia*
[3]*Department of Psychiatry and Human Behavior, University of Mississippi Medical Center, Jackson, MS 39216, USA*
[4]*Department of Anesthesiology, Columbia University, New York, NY 10032, USA*
[5]*Department of Anatomy and Neurobiology, University of Tennessee Health Science Center, Memphis, TN 38163, USA*
[6]*Milwaukee Institute of Drug Discovery, University of Wisconsin-Milwaukee, Milwaukee, WI 53201, USA*

Correspondence should be addressed to James M. Cook; capncook@uwm.edu

Received 11 February 2015; Revised 16 June 2015; Accepted 2 July 2015

Academic Editor: Hussein El-Subbagh

An updated model of the GABA(A) benzodiazepine receptor pharmacophore of the α5-BzR/GABA(A) subtype has been constructed prompted by the synthesis of subtype selective ligands in light of the recent developments in both ligand synthesis, behavioral studies, and molecular modeling studies of the binding site itself. A number of BzR/GABA(A) α5 subtype selective compounds were synthesized, notably α5-subtype selective inverse agonist PWZ-029 (**1**) which is active in enhancing cognition in both rodents and primates. In addition, a chiral positive allosteric modulator (PAM), SH-053-2′F-R-CH_3 (**2**), has been shown to reverse the deleterious effects in the MAM-model of schizophrenia as well as alleviate constriction in airway smooth muscle. Presented here is an updated model of the pharmacophore for $\alpha5\beta2\gamma2$ Bz/GABA(A) receptors, including a rendering of PWZ-029 docked within the α5-binding pocket showing specific interactions of the molecule with the receptor. Differences in the included volume as compared to $\alpha1\beta2\gamma2$, $\alpha2\beta2\gamma2$, and $\alpha3\beta2\gamma2$ will be illustrated for clarity. These new models enhance the ability to understand structural characteristics of ligands which act as agonists, antagonists, or inverse agonists at the Bz BS of GABA(A) receptors.

1. Introduction

The gamma-amino butyric acid A ($GABA_A$) receptor is a heteropentameric chloride ion channel. This channel is generally made up of two α-subunits, two β-subunits, and a single γ-subunit arranged in an $\alpha\beta\alpha\beta\gamma$ fashion. The $GABA_A$ receptors ($GABA_AR$) are responsible for a myriad of brain functions. Positive allosteric modulators (PAMs) and negative allosteric modulators (NAMs) act on the benzodiazepine (BZ) site of the $GABA_AR$ which can change the conformation of the receptor to inhibit or excite the neurons associated with the ion channel. To date, researchers have been unable to get an X-ray crystal structure of a functional Bz/$GABA_AR$ ion channel. Recently, Miller and Aricescu [1] have reported the crystal structure of a homopentameric $GABA_AR$ containing the β3-subunit at 3 Å resolution. Although this work provides great promise that other heteropentameric $GABA_ARs$ will be crystallized in the near future, molecular modeling and structure-activity-relationships (SARs) still remain key tools to find better subtype-selective binding agents.

2. Subtype Selective Ligands for α5 GABA(A)/Bz Receptors

Interest in BzR/GABA(A) α5 subtypes began years ago when it was realized that $\alpha5\beta3\gamma2$ Bz/GABA(A) subtypes are located

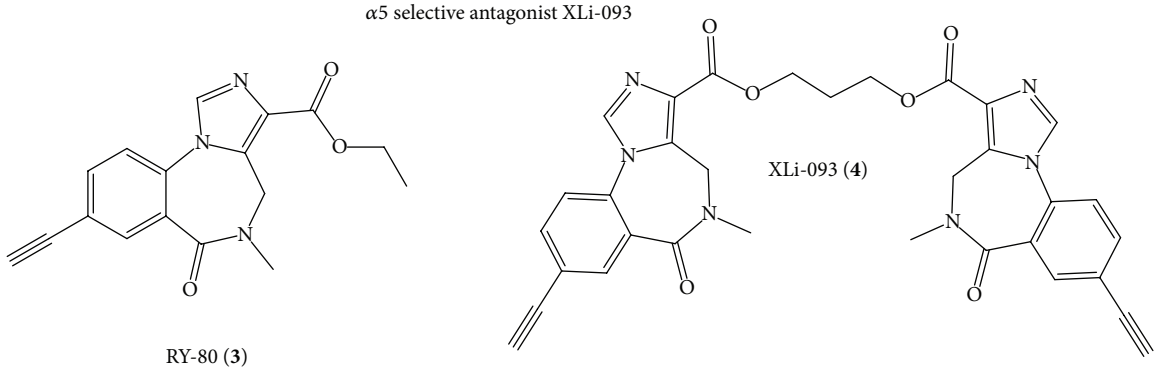

Ligand	$\alpha1$	$\alpha2$	$\alpha3$	$\alpha4$	$\alpha5$	$\alpha6$
RY-80 (**3**)	2834	21.4	25.8	5.3	0.49	28.8
XLi-093 (**4**)	>1000	>1000	858	1550	15	>2000

Figure 1: Alpha 5 selective compounds [13]. This figure is modified from that reported in [13].

primarily in the hippocampus. More recently this interest has been confirmed by the report of Möhler et al. [2–5] on $\alpha5$ "knock-in mice." This group has provided strong evidence that hippocampal extrasynaptic $\alpha5$ GABA(A) receptors play a critical role in associative learning as mentioned above [6–11].

Earlier we synthesized a series of $\alpha5$ subtype selective ligands (RY-023, RY-024, RY-079, and RY-080) based on the structure of Ro 15-4513 and reported their binding affinity [6], as well as several ligands by Atack et al. [12]. These ligands are benzodiazepine receptor (BzR) negative modulators *in vivo* and a number of these compounds have been shown to enhance memory and learning [13]. One of these ligands was shown by Bailey et al. [6] to be important in the acquisition of fear conditioning and has provided further evidence for the involvement of hippocampal GABA(A)/BzR in learning and anxiety [13]. This is in agreement with the work of DeLorey et al. [7] in a memory model with a ligand closely related to $\alpha5$ subtype selective inverse agonists RY-024 and RY-079 including PWZ-029 (**1**).

In order to enhance the $\alpha5$ subtype selectivity, the bivalent form of RY-80 (**3**) was prepared to provide XLi-093 (**4**) [13]. The binding affinity of XLi-093 *in vitro* was determined on $\alpha_{1-6}\beta3\gamma2$ LTK cells and is illustrated in Figure 1. This bivalent ligand exhibited little or no affinity at $\alpha_{1-4,6}\beta3\gamma2$ BzR/GABA(A) subtypes, but this $\alpha5$ ligand had a K_i of 15 nM at the $\alpha5\beta3\gamma2$ subtype [14]. Since this receptor binding study indicated bivalent ligand XLi-093 bound almost exclusively to the $\alpha5$ subtype, the efficacy of this ligand on GABA(A) receptor subtypes expressed in *Xenopus* oocytes was investigated by Sieghart, Furtmueller, Li, and Cook [14, 15]. Analysis of the data indicated that XLi-093 up to a concentration of 1 μM did not trigger chloride flux in any one of the GABA(A) subtypes tested. At 1 μM XLi-093 did not modulate GABA induced chloride flux in $\alpha1\beta3\gamma2$, $\alpha2\beta3\gamma2$, or $\alpha3\beta3\gamma2$ receptors, but very slightly inhibited chloride flux in $\alpha5\beta3\gamma2$ subtypes. At 1 μM, XLi-093 barely influenced benzodiazepine (Valium) stimulation of GABA-induced current in $\alpha1\beta3\gamma2$, $\alpha2\beta3\gamma2$, and $\alpha3\beta3\gamma2$ BzR but shifted the diazepam dose response curve to the right in $\alpha5\beta3\gamma2$ receptors in a very significant manner [16]. Importantly, bivalent ligand XLi-093 was able to dose dependently and completely inhibit diazepam-stimulated currents in $\alpha5\beta3\gamma2$ receptors. This was the first subtype selective benzodiazepine receptor site antagonist at $\alpha5$ receptors. This bivalent ligand XLi-093 provided a lead compound for all of the bivalent ligands in this research [16].

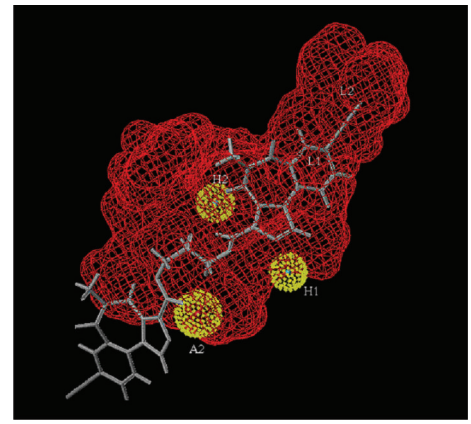

Figure 2: XLi-093 (**4**) aligned in the included volume of the pharmacophore receptor model for the $\alpha5\beta3\gamma2$ subtype [17, 18] (this figure is modified from the figure in Clayton et al., 2007) [23].

Illustrated in Figure 2 is XLi-093 (**4**) aligned excellently within the pharmacophore-receptor model of the $\alpha5\beta3\gamma2$ subtype [14, 16–19]. The fit to the pharmacophore-receptor and the binding data indicate that bivalent ligands will bind to BzR subtypes [14, 19]. It is believed that the dimer enters the binding pocket with one monomeric unit docking while the other monomer tethered by a linker extends out of the protein into the extracellular domain. If this is in fact true that the second imidazole unit is protruding into the extracellular domain of the BzR/GABA(A) $\alpha5$ binding site,

Table 1: Full PDSP panel receptor binding reported (Roth [138]) for XLi-093 and XLi-356.

Cook code	5ht1a	5ht1b	5ht1d	5ht1e	5ht2a	5ht2b	5ht2c	5ht3	5ht5a	5ht6	5ht7	α1A	β1B	α2A	α2B
XLi093	*	Repeat	*	*	*	*	*	*	*	*	*	*	*	*	*
XLi356	*	*	*	*	*	*	*	*	*	*	*	*	*	*	*
Cook code	α2C	Beta1	Beta2	CB1	CB2	D1	D2	D3	D4	D5	DAT	DOR	H1	H2	H3
XLi093	*	*	*	*	*	*	*	*	*	*	*	*	*	*	*
XLi356	*	*	*	*	*	*	*	*	*	*	*	*	*	*	*
Cook code	H4	Imidaz oline	KOR	M1	M2	M3	M4	M5	MDR	MOR	NET	NMDA	SERT	σ1	σ2
XLi093	*	*	***2,024.00***	*	*	*	*	*	*	*	*	*	*	*	*
XLi356	*	*	**6,118.00**	*	*	*	*	*	*	*	*	*	*	*	*

Data ("secondary binding") are K_i values. K_i values are reported in nanomolar concentration, Case Western Reserve University. "*" indicates "primary missed" (<50% inhibition at 10 μM). See full data of the PDSP screen in the report of Clayton [22].

it could have a profound effect on the ligand design. This means other homodimers or even heterodimers may bind to BzR/GABA(A)ergic sites.

In this vein, Wenger, Li, and Cook et al. [13, 20, 21] earlier described preliminary data that XLi-093, an α5 subtype selective antagonist, enhances performance of C57BL/6J mice under a titrating delayed matching to position schedule of cognition, as illustrated in Figure 3 [14, 16–19]. This indicates, however, that this agent does cross the blood brain barrier.

Bivalent ligands have a preferred linker of 3–5 methylene units, between the two pharmacophores (see XLi-093). This was established by NMR experiments run at low temperatures, X-ray crystallography, and molecular modeling of the ligands in question and will be discussed [14, 17, 18].

Based on this data, additional α5-subtype selective ligands have been prepared (see Figure 4). The basic imidazobenzodiazepine structure has been maintained [7]; however substituents were varied in regions around the scaffold based on molecular modeling [6]. These are now the most α5 subtype selective ligands ever reported [22]. Moreover, the ability to increase the subtype selectivity can be done by selecting specific substituents on these ligands to new agents with 400–1000-fold α5-selectivity over the remaining 5 subtypes. *This is an important step forward to understanding the true, unequivocal physiological responses mediated by α5 subtypes in regard to cognition (amnesia), schizophrenia, anxiety, and convulsions, all of which in some degree are influenced by α5 subtypes*. Based on the ligands in Figures 4 and 5, affinity has occurred principally at α5 subtypes. In addition, since XLi-093 bound very tightly only to α5 BzR subtypes, the bivalent nature and functionality presented here can be incorporated into other dimeric ligands.

As shown previously in Figure 3, α5-antagonist XLi-093 (**4**) was shown to enhance cognition. In another study, a reduction of the two acetylenic groups of XLi-093 resulted in ethyl groups [14], providing a new bivalent ligand (XLi-356, **10**) which shows α5-selective binding with very low affinity for α1 subtypes (Figure 5). Efficacy (oocyte) data shows XLi-356 is an α5 negative allosteric modulator [7, 13]. DeLorey et al. have recently shown in mice that XLi-356 does potently reverse scopolamine induced memory deficits [7]. This bivalent α5 inverse agonist enhanced cognition

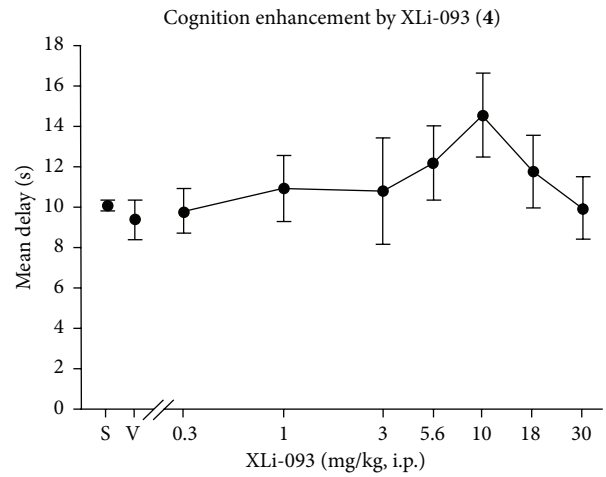

Figure 3: XLi-093 (**4**) effects on cognition enhancement by Wenger et al. (data on statistical significance not shown, unpublished results). Effects of **4** on cognition from the mean delay achieved by C57BL/6J mice titrating delayed matching-to-position schedule.

in agreement with work reported from our laboratory on monovalent inverse agonists RY-10 [6] and RY-23 [7].

The dimers XLi-093 (**4**) and XLi-356 (**10**) were sent to Case Western Reserve (NIMH supported PDSP program, Roth et al.) for full panel receptor binding and they do not bind to other receptors at levels of concern (Table 1).

Although XLi-093 (**4**) was found to be an antagonist at the α5 subtype, XLi-356 (**10**) was found to be a weak agonist-antagonist. XLi-356 was found to reverse scopolamine induced memory deficits in mice. When XLi-356 was looked at in audio cued fear conditioning, the results show no activity. This suggests that the effect of XLi-356 is selective through α5 receptors which are abundant in the hippocampus which is highly associated with contextual memory. Audio cued memory instead is amygdala-based and should not be affected by an α5 subtype selective compound [39–42].

As illustrated in Figure 6, scopolamine (1 mg/kg) reduced freezing (i.e., impairs memory) generally due to coupling the

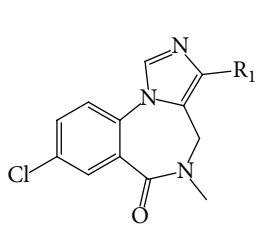

1a–c, **5**, **6**

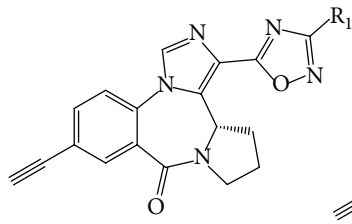

7

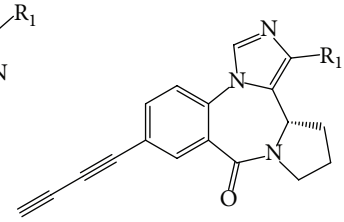

8

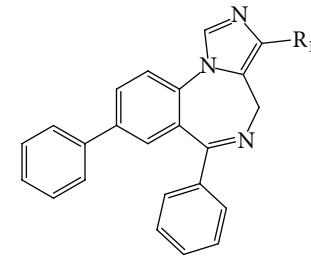

DM-I-81 (**9**)

Ligand	R_1	K_i (nM)[a] $\alpha1$	$\alpha2$	$\alpha3$	$\alpha4$	$\alpha5$	$\alpha6$
1a[b]	CH_2OCH_3	>300	>300	>300	ND	38.8	>300
1b[b]	CH_2OCH_3	920	ND	ND	ND	30	ND
1c[b]	CH_2OCH_3	362.4	180.3	328.2	ND	6.185	ND
5	CH_2Cl	>300	>300	>300	ND	28.5	>300
6	CH_2OEt	>300	>300	>300	ND	82.7	>300
7	CH_3	>89	>70	>91	ND	3.7	>301
8	CO_2Et	>1000	>1000	>1000	>1000	64	>1000
9	CO_2Et	>2000	>2000	>2000	>2000	176	>2000

[a]Data shown here are the means of two determinations which differed by less than 10%. ND: not determined (presumably similar to $\alpha6$).

[b]**1a–c** are binding datasets of PWZ-029 (**1**) from three separate laboratories. This figure is modified from that illustrated in reference [22] to indicate the $\alpha5$ subtype selectivity.

Figure 4: Binding data of selected imidazobenzodiazepines [22].

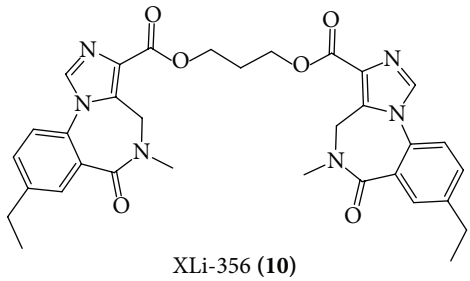

XLi-356 (**10**)

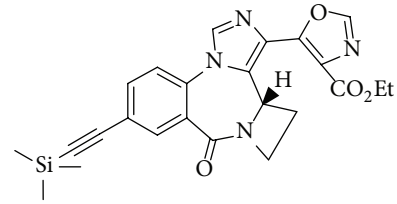

RY-068 (**11**)

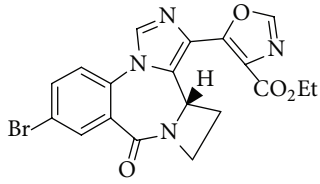

RY-062 (**12**)

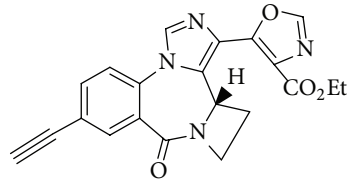

RY-069 (**13**)

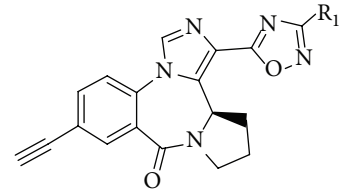

RY-I-29 (**14**)

Ligand	K_i (nM)[a] $\alpha1$	$\alpha2$	$\alpha3$	$\alpha4$	$\alpha5$	$\alpha6$
XLi-356 (**10**)	1852	4203	8545	ND	101	5000
RY-068 (**11**)	>500	877	496	ND	37	>1000
RY-062 (**12**)	>1000	>1000	>500	ND	172	>2000
RY-069 (**13**)	692	622	506	ND	19	>1000
RY-I-29 (**14**)	>1000	>1000	>1000	ND	157	>1000

[a]Data shown here are the means of two determinations which differed by less than 10%. ND: not determined (presumably greater than 1000 nM; similar to $\alpha6$).

Figure 5: Binding data of selected imidazobenzodiazepines substituted with an E-ring as compared to XLi-356 (**10**).

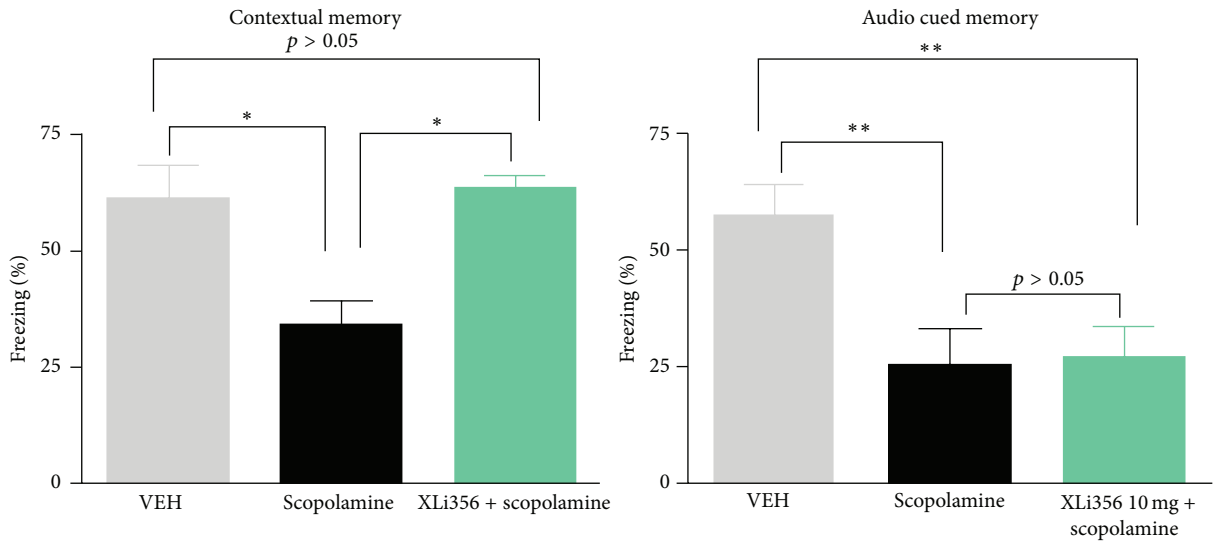

Figure 6: Visual and audio cued data for XLi-356 (**10**). This figure was modified from that in [22].

context (the cage) with a mild shock. XLi-356 (10 mg/kg) attenuated the impairment of memory returning the freezing to the levels on par with subjects dosed with vehicle. In audio cued memory the response was activated by sound, not the context. XLi-356 was not able to reverse this type of memory effect which is amygdala driven. A similar effect was observed for XLi-093 by Harris et al. [43]. XLi-093 is the most selective antagonist for $\alpha5$ subtypes reported to date [13, 43] and is a very useful $\alpha5$ antagonist used by many *in vivo* [22, 44, 45].

Molecular modeling combined with this knowledge was used to generate new lead compounds aimed at the development of $\alpha5$-subtype selective positive and negative allosteric modulators to study cognition as well as amnesia mediated by the hippocampus. All of these compounds have been prepared based on the structure of current $\alpha5$-subtype selective ligands synthesized in Milwaukee [46] (see Figures 4 and 5), as well as the binding affinity (15 nM)/selectivity of bivalent $\alpha5$ antagonist XLi-093 (**4**) [13].

In efforts to enhance $\alpha5$-selectivity in regards to cognition, Cook, Bailey, and Helmstetter et al. have employed RY-024 to study the hippocampal involvement in the benzodiazepine receptor in learning and anxiety [14, 19]. Supporting this Harris, DeLorey et al. show in mice that $\alpha5$ NAMs (**1**) and RY-10 potently reversed scopolamine-induced memory impairment. These $\alpha5$ NAMs provide insight as to how $GABA_A$Rs influence contextual memory, an aspect of memory affected in age associated memory impairment and especially in Alzheimer's disease [13, 62–64]. In addition, Savić et al. have used the $\alpha1$ preferring antagonist, BCCt, in passive avoidance studies, in which midazolam's amnesic effects are shown to be due to interaction of agonist ligands at $\alpha5$ in addition to $\alpha1\beta3\gamma2$ BzR subtypes [24, 65].

3. PWZ-029: A Negative Allosteric Modulator

PWZ-029 (**1**) has been studied extensively as an $\alpha5$-$GABA_A$R inverse agonist and in certain experimental models has been shown to enhance cognition. The binding data from three separate laboratories (Table 2) have all shown that it exhibits remarkable selectivity for the $\alpha5$ subunit-containing receptors, all greater than 60-fold compared to the next subunit.

Table 2: Affinity of PWZ-029 (**1**); K_i (nM)[a].

Code	MW	$\alpha1$	$\alpha2$	$\alpha3$	$\alpha4$	$\alpha5$	$\alpha6$
PWZ-029 (**1**)	291.73	>300	>300	>300	ND	**38.8**	>300
PWZ-029 (**1**)	291.73	920	ND	ND	ND	**30**	ND
PWZ-029 (**1**)	291.73	362	180	328	ND	**6**	ND

[a]Data from three separate laboratories.

Electrophysiological efficacy testing done by Sieghart et al. in oocytes demonstrated that PWZ-029 (**1**) acts as a negative allosteric modulator at the $\alpha5$-subunit, with a very weak agonist activity at the $\alpha1$, $\alpha2$, and $\alpha3$ subunits (Figure 7). At a pharmacologically relevant concentration of 0.1 μM, PWZ-029 exhibits moderate negative modulation at the $\alpha5$-subunit, while showing little or no effect at the $\alpha1$, $\alpha2$, or $\alpha3$-subunits.

Milić et al. reported on the effects of PWZ-029 in the widely used novel object recognition test, which differentiates between the exploration time of novel and familiar objects. As shown by significant differences between the exploration times of the novel and familiar object (Figure 8(a)), as well as the respective discrimination indices (Figure 8(b)), all the three tested doses of PWZ-029 (2, 5 and 10 mg/kg) improved object recognition in rats after the 24 h delay period. Additionally, in the procedure with the 1 h delay between training and testing, the lowest of the tested doses of PWZ-029 (2 mg/kg) successfully reversed the deficit in recognition memory induced by 0.3 mg/kg scopolamine (Figure 9) [25].

The results of the described study showed for the first time that inverse agonism at $\alpha5$-$GABA_A$ receptors may be efficacious in both improving cognitive performance in

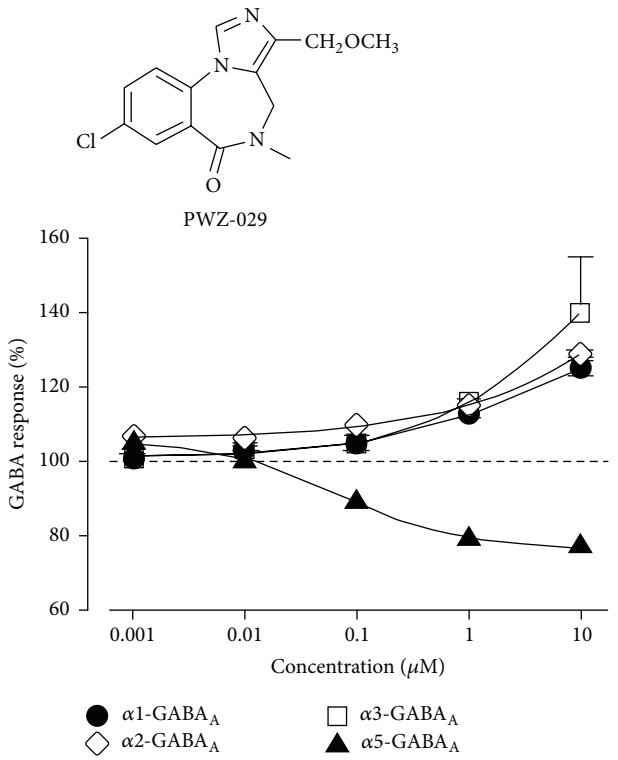

Figure 7: Oocyte electrophysiological data of PWZ-029 (**1**) [24].

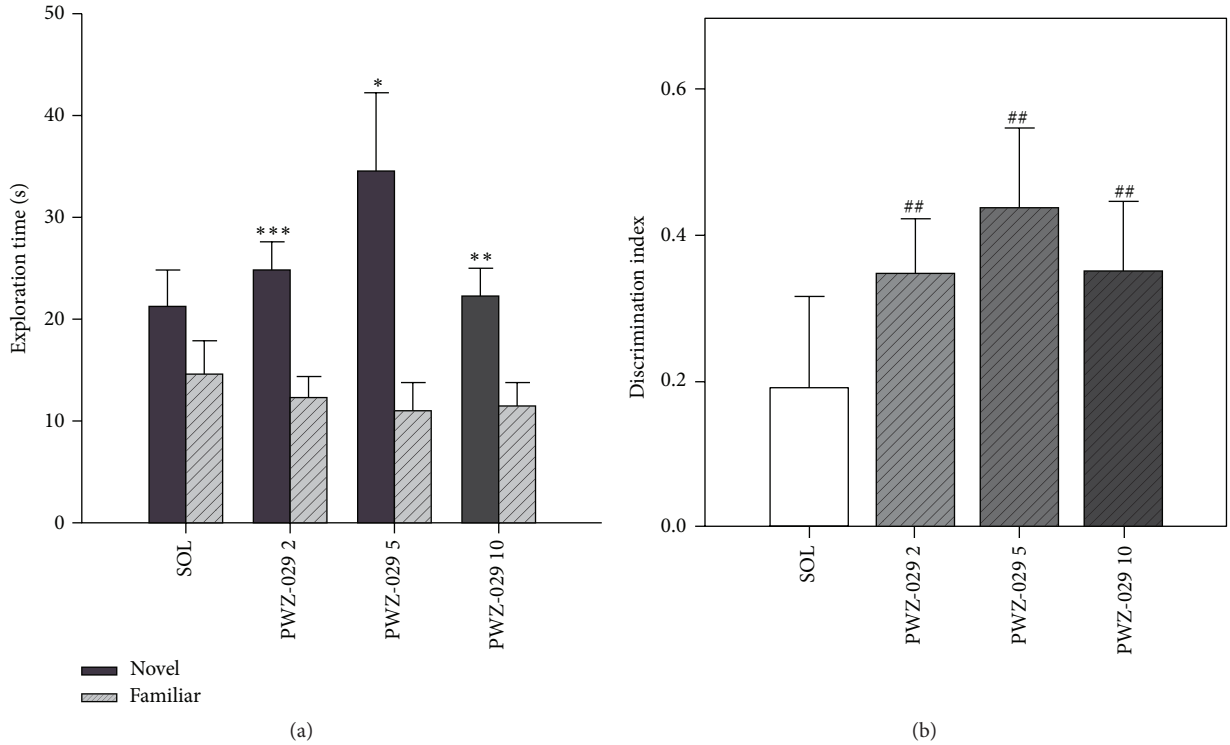

Figure 8: The effects of PWZ-029 (**1**) (2, 5 and 10 mg/kg) on (a) time exploring familiar and novel objects and (b) discrimination indices in the novel object recognition test using a 24 h delay (mean + SEM). Significant differences are indicated with asterisks (paired-samples t-test, novel versus familiar, $^{*}p < 0.05$, $^{**}p < 0.01$, $^{***}p < 0.001$). A significant difference from zero is indicated with hashes (one sample t-test, $^{\#\#}p < 0.01$). The number of animals per each treatment group was 10. SOL = solvent [25].

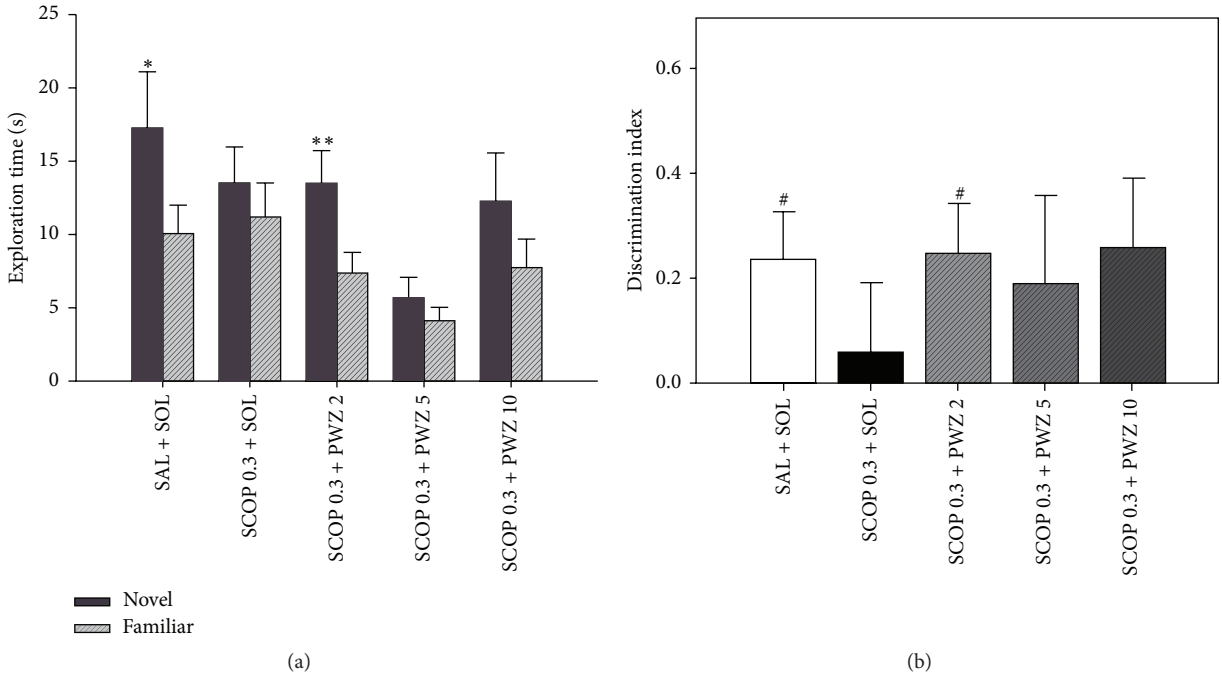

FIGURE 9: The effects of 0.3 mg/kg scopolamine (SCOP 0.3) and combination of 0.3 mg/kg scopolamine and PWZ-029 (**1**) (2, 5, and 10 mg/kg) on the rats' performance in the object recognition task after a 1 h delay: (a) time exploring familiar and novel objects and (b) discrimination index. Data are represented as mean + SEM. Significant differences are indicated with asterisks (paired-samples t-test, novel versus familiar, $^{*}p < 0.05$, $^{**}p < 0.01$). A significant difference from zero is indicated with hashes (one sample t-test, $^{\#}p < 0.05$). The number of animals per each treatment group was 12–15. SAL = saline, SOL = solvent [25].

unimpaired subjects and ameliorating cognitive deficits in pharmacologically impaired subjects, as assessed in two protocols of the same animal model [25].

In a recent by Rowlett et al. [26], negative allosteric modulator PWZ-029 was evaluated in female rhesus monkeys (n = 4) in an Object Retrieval test with Detours (ORD; Figure 10 for details). **1** was administered via i.v. catheters in ORD trained monkeys and evaluated for cognition enhancement. A successful trial was determined by the ability of the subject to obtain a food reward within a transparent box with a single open side, with varying degrees of difficulty ("easy" or "difficult" or "mixed" as a combination of both) based on food placement within the box. In "mixed" trials using PWZ-029, no significant results were observed when compared to vehicle (Figure 11(a)). "Difficult" trials, however, exhibited an increasing dose-dependent curve for successful trials (Figure 11(b)). These results were attenuated by a coadministration α5-antagonist XLi-093 (Figure 11(c)). PWZ-029 was also shown to dose-dependently reverse the cholinergic deficits that were induced by scopolamine (Figure 11(d)) [26].

These findings suggest that PWZ-029 can enhance performance on the ORD task, only under conditions in which baseline performance is attenuated. The effects of PWZ-029 were antagonized in a surmountable fashion by the selective α5-GABA$_A$ ligand, XLi-093, consistent with PWZ-029's effects being mediating via the α5-GABA$_A$ receptor. The results are consistent with the view that α5 GABA$_A$ receptors may represent a viable target for discovery of cognitive enhancing agents.

In addition, we have new data showing that modulation of α5-GABA$_A$Rs by PWZ-029 rescues Hip-dependent memory in an AD rat model [PMID: 23634826] as evidenced by a significant decrease in the latency to reach the hidden platform (memory probe trials) on spatial water maze task (Figure 12). Roche has employed a similar strategy at α5 subtypes and recently has a drug in the clinic to treat symptoms of dementia in Down syndrome patients. It is well known many Down syndrome patients develop Alzheimer's disease or a dementia with a very similar etiology. This is aimed at treating early onset Alzheimer's patients.

4. PWZ-029 Docking within $\alpha5\gamma2$ GABA$_A$ Receptor Subunit Homology Model

These studies with PWZ-029 led to the molecular model rendering of the compound docked within the $\alpha5\gamma2$ BzR subtype (Figures 13–16). The model figures have the following features:

The docking of PWZ-029 within the GABA$_A$/BzR shows the molecule bound and interacting with specific amino acids. The A and B rings of the benzodiazepine framework undergo a π-stacking interaction with HIS 105, indicated by the magenta coloring. At the other end of the molecule the methoxy lone pair and imidazole nitrogen lone pair act as a hydrogen bond acceptors with THR 210 and TYR 213, respectively. These interactions are shown by the aqua-blue descriptors.

Methods

ORD task examples of different types of trials

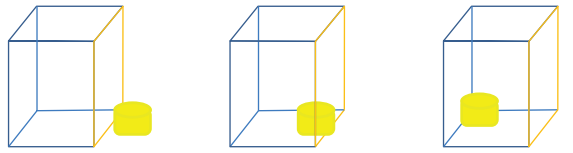

Easy-right outside Easy-right inside Difficult-right deep

Note: open side indicated with orange lines

Mixed trials		
Type of trial	Position of opening	Position of food
Easy	Left	Outside
Easy	Right	Outside
Easy	Front	Outside
Easy	Left	Outside
Easy	Front	Outside
Easy	Left	Inside
Difficult	Right	Deep
Easy	Left	Inside
Easy	Right	Inside
Easy	Left	Inside
Difficult	Right	Deep
Difficult	Left	Deep
Difficult	Right	Deep
Easy	Left	Inside
Easy	Right	Inside

Difficult trials		
Type of trial	Position of opening	Position of food
Difficult	Left	Deep
Difficult	Right	Deep
Difficult	Left	Deep
Difficult	Right	Deep
Difficult	Left	Deep
Difficult	Left	Deep
Difficult	Right	Deep
Difficult	Left	Deep
Difficult	Right	Deep
Difficult	Left	Deep
Difficult	Left	Deep
Difficult	Right	Deep
Difficult	Left	Deep
Difficult	Right	Deep
Difficult	Left	Deep

Subjects:

Rhesus monkeys (*Macaca mulatta*)

$N = 5$

Implanted with chronic i.v. catheters

Procedure:

Object retrieval with detours (ORD)

15 trials per session
Easy, difficult, and mixed trials (see diagram)

Tests:

(i) PWZ-029 · mixed trials

(ii) PWZ-029 · difficult trials

(iii) PWZ-029 + XLi-093 · difficult trials

(iv) Scopolamine · mixed trials

(v) PWZ-029 + scopolamine · mixed trials

Measurements: % correct trials—trial in which food is obtained with the first reach

Errors: barrier reaches (hand in contact with closed side of box) and incomplete trials (food grasped but dropped)

Figure 10: ORD methods and procedure [26].

5. Subtype Selective Agonists for $\alpha5$ $GABA_A$/Bz Receptors

Möhler has proposed that $\alpha5$ selective inverse agonists or $\alpha5$ selective agonists might enhance cognition [5, 13, 16–18, 86]. This is because of the extrasynaptic pyramidal nature of $\alpha5\beta3\gamma2$ subtypes, located almost exclusively in the hippocampus. Because of this, a new "potential agonist" which binds solely to $\alpha5\beta3\gamma2$ subtypes was designed by computer modeling (see Figure 17). This ligand (DM-I-81, **9**) has an agonist framework and binds only to $\alpha5\beta3\gamma2$ subtypes [13, 17, 18, 86]. The binding potency at $\alpha5$ subtypes is 176 nM. Although the 8-pendant phenyl of DM-I-81 was lipophilic and bound to the L_2 pocket, additional work on the 8-position of this scaffold has been abandoned and generally left as an acetylene or halide function, with a few exceptions. The steric bulk of the 8-phenyl moiety was felt detrimental to activity and potency which may have led to the weak binding affinity.

6. Alpha 5 Positive Allosteric Modulators in Schizophrenia

In addition to inverse agonists, a number of other $\alpha5$-$GABA_AR$ positive allosteric modulators (PAMs) have been synthesized. These compounds, such as SH-053-2′F-R-CH_3 (**2**), have been shown to decrease the firing rate of synapses controlling cognition and can be used to treat schizophrenia.

The following is reported by Gill, Cook, and Grace et al. [27–38].

There are a number of novel benzodiazepine-positive allosteric modulators (PAMs), selective for the $\alpha5$ subunit of the $GABA_A$ receptor, including SH-053-2′F-R-CH_3 (**2**), which has been tested for its ability to effect the output of the HPC (hippocampal) in methylazoxymethanol-(MAM-) treated animals, which can lead to hyperactivity in the dopamine system [27–38]. In addition, the effect of this compounds (**2**) response to amphetamine in MAM-animals on the hyperactive locomotor activity was examined. Schizophrenic-like symptoms can be induced into rats when treated prenatally with DNA-methylating agent, methylazoxymethanol, on gestational day (GD) 17. These neurochemical outcomes and changes in behavior mimic those found in schizophrenic patients. Systemic treatment with (**2**) resulted in a reduced number of spontaneously active DA (dopamine) neurons in the VTA (ventral tegmental area) of MAM animals (Figure 18) to levels seen in animals treated with vehicle (i.e., saline). To confirm the location of action, **2** was also directly infused into the ventral HPC (Figure 19)

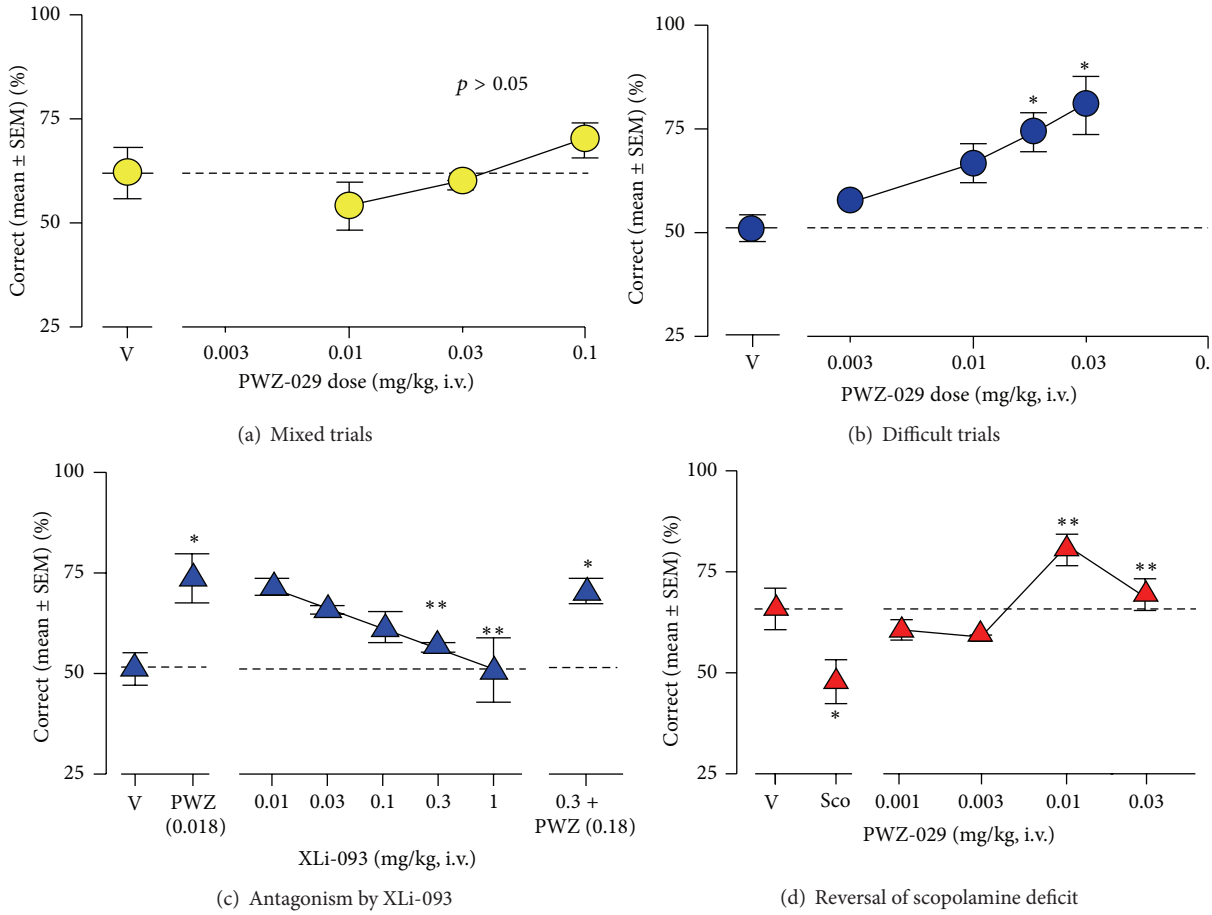

Figure 11: Cognitive-enhancing effects of PWZ-029 in the rhesus monkey Object Retrieval with Detours (ORD) task (n = 5 monkeys). (a) Effects of PWZ-029 on ORD tests consist of both easy and difficult trials: (b) PWZ-029 enhanced performance on the ORD task when tested with difficult trials only; (c) enhancement of ORD performance by 0.018 mg/kg of PWZ-029 was attenuated by the α5 $GABA_A$-preferring antagonist XLi-093 and this antagonism was surmountable by increasing the PWZ-029 dose; (d) PWZ-029 reversed performance impaired by 0.01 mg/kg of scopolamine [26]. $^{*}p < 0.05$ versus vehicle, $^{**}p < 0.05$ versus Scopolamine.

and was shown to have the same effect. Moreover, HPC neurons in both SAL and MAM animals showed diminished cortical-evoked responses following α5-$GABA_A$R PAM treatment. This study is important for it supports a treatment of schizophrenia that targets abnormal HPC output, which in turn normalized dopaminergic neuronal activity [27–38]. This is a novel approach to treat schizophrenia.

The pathophysiology of schizophrenia has identified hippocampal (HPC) dysfunction as a major mediator as reported by many including Anthony Grace [27–38]. This included morphological changes, reduced HPC volume, and GAD67 expression [27, 28] that have been reported after death in the brains of patients with schizophrenia. Both HPC activation and morphology changes have been identified that can precede psychotic symptoms or correlate with severity of cognitive deficits [29–33]. This has been shown in a cognitive test during baseline and activation.

Many animal models of schizophrenia were essential to behavioral pathology and have delivered new knowledge about the network disturbances that contribute to CNS disorder. This study shows that the offspring of MAM-treated animals showed both structural and behavioral abnormalities. These were consistent with those observed in patients with schizophrenia. The animals had reduced limbic cortical and HPC volumes with increased cell packing density and showed increased sensitivity to psychostimulants [34–36]. In addition, the startle response in prepulse inhibition was reduced in MAM-treated animals and deficits in latent inhibition were observed [35]. Furthermore, a pathological rise in spontaneous dopamine (DA) activity by the ventral tegmental area (VTA) was observed that can be attributed to aberrant activation within the ventral HPC [36]. It was suggested that reductions in parvalbumin- (PV-) stained interneurons might be the reason for the hyperactivation of the HPC and disruption of normal oscillatory activity in the HPC and cortex of MAM animals [38, 61]. At least this is the prevailing hypothesis at the moment put forth by many investigators (see references cited in [27–38]).

Selective α5-$GABA_A$R positive allosteric modulator (**2**) was successful in reversing the pathological increase in tonic DA transmission in methylazoxymethanol rats by targeting abnormal hippocampal activity. In addition, the α5-PAM was

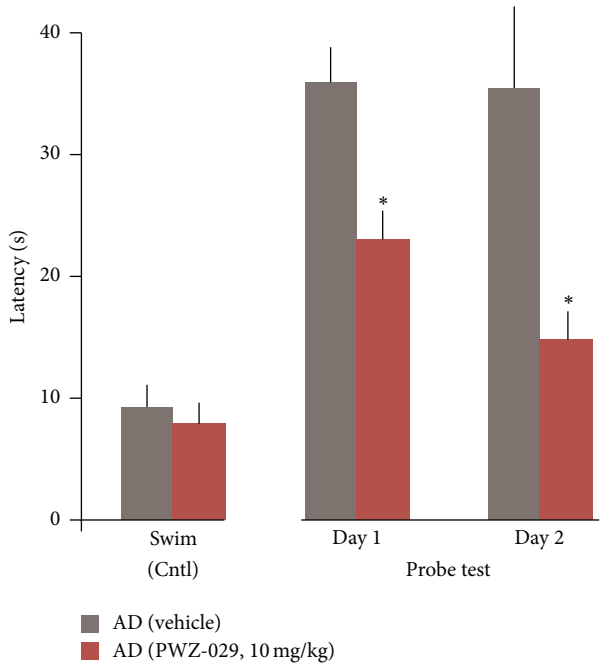

Figure 12: PWZ-029 rescues spatial memory deficits in AD model as evidenced by a decrease in the latency to reach the hidden platform (probe test) in the water maze relative to vehicle (VEH, $^{*}p < 0.05$).

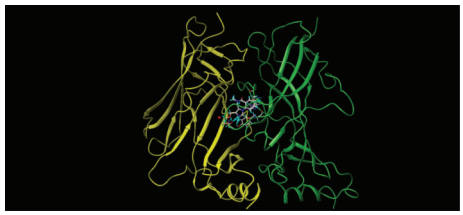

Figure 13: PWZ-029 docked within $\alpha5\gamma2$ BzR binding site (BS).

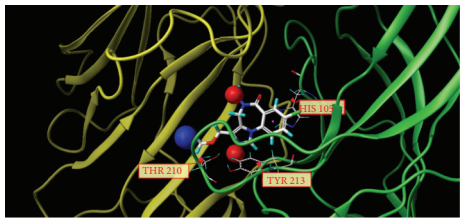

Figure 14: PWZ-029 docked with amino acid residues.

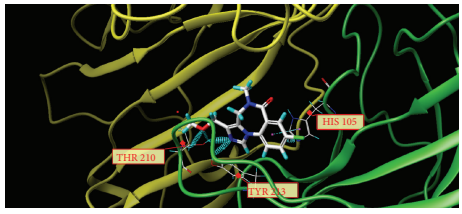

Figure 15: PWZ-029 docked with A.A. residue interactions.

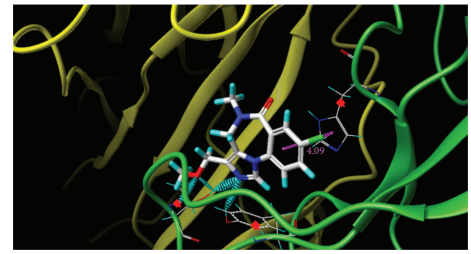

Figure 16: PWZ-029 docked with interactions. (1) HIS 105 π-stacking interaction with centroid of PWZ-029. (2) TYR 213 phenol OH hydrogen bonding to imidazole nitrogen lone pair. (3) THR 210 OH and lone pair on methoxy of PWZ029. (4) $\alpha5$ ribbon being green. (5) $\gamma2$ ribbon being yellow. (6) Hydrogen bonding being aqua blue. (7) π-stacking being magenta.

able to reduce the behavioral sensitivity to psychostimulants observed in MAM rats (Figures 20 and 21). This suggests that novel $\alpha5$-partial allosteric modulators should be effective in alleviating dopamine-mediated psychosis. However, if this drug can also restore rhythmicity within HPC-efferent structure, it may also affect other aspects of this disease state such as cognitive disabilities and negative symptoms. This study, using the MAM-model to induce symptoms of schizophrenia, shows that the use of $\alpha5$-$GABA_AR$ targeting compounds could be an effective treatment in schizophrenic patients. The selective targeting solely of $\alpha5\beta3\gamma2$ subunits, as opposed to unselective BZDs such as diazepam, could provide relief from the psychotic symptoms without producing adverse effects such as sedation [27–38].

As reported by Gill, Grace et al. [36, 38, 47–61].

Often initial antipsychotic drug treatments (APD) for schizophrenia are ineffective, requiring a brief washout period prior to secondary treatment. The impact of withdrawal from initial APD on the dopamine (DA) system is unknown. Furthermore, an identical response to APD therapy between normal and pathological systems should not be assumed. In another study by Gill, Grace et al., $\alpha5$ positive allosteric modulator SH-053-2′F-R-CH_3 (**2**) was used in the MAM neurodevelopmental model of schizophrenia which was used to study impact of withdrawal from repeated haloperidol (HAL) on the dopamine system [36, 38, 47–61].

The following studies were designed to provide insight as to why a new drug to treat schizophrenia may be effective in Phase II clinical trials but fail in Phase III because of the large number of patients required for the study. Many of these patients in Phase III studies have altered neuronal pathways in the CNS because of long-term treatment with antipsychotics (sometimes 10–20 years) [36, 38, 47–61].

Importantly, spontaneous dopamine activity reduction was observed in saline rats withdrawn from haloperidol with an enhanced locomotor response to amphetamine, indicating the development of dopamine supersensitivity. In addition, PAM treatment, as well as ventral HPC inactivation, removed the depolarization block of DA neurons in withdrawn HAL treated SAL rats. In contrast, methylazoxymethanol rats withdrawn from HAL displayed a reduction in spontaneous dopamine activity and enhanced locomotor response that

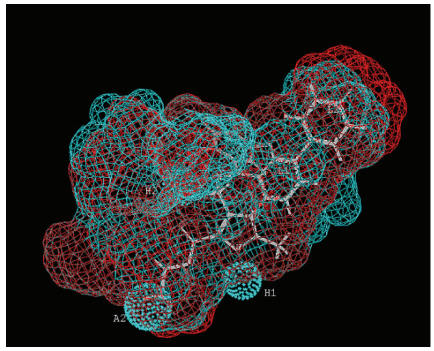

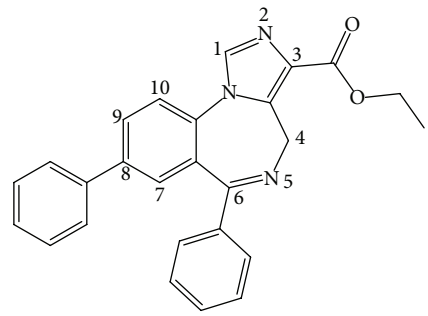

9

DM-I-81 aligned in the included volume of the pharmacophore/receptor model for the $\alpha1\beta3\gamma2$ (blue) and $\alpha5\gamma3\beta2$ (red) subtypes

Binding data	$\alpha1$	$\alpha2$	$\alpha3$	$\alpha4$	$\alpha5$	$\alpha6$
DM-I-81 (**9**)	>2000	>2000	>2000	>2000	176	>2000

Figure 17: The $\alpha5$ selective agonist DM-I-81 (**9**), bound within the $\alpha1$ and $\alpha5$ subtypes. Binding data shown as K_i (nM).

was unresponsive to PAM treatment with SH-053-2′F-R-CH_3 or ventral HPC inactivation [36, 38, 47–61].

Prior HAL treatment withdrawal can restrict the efficacy of subsequent pharmacotherapy in the MAM model of schizophrenia. This is an extremely important result indicating that testing a new drug for schizophrenia in humans treated for years with both typical and atypical antipsychotics may result in a false negative with regard to treatment. Studies that support this hypothesis follow here [36, 38, 47–61].

Novel therapeutics for the treatment of schizophrenia that exhibit initial promise in preclinical trials often fail to demonstrate sufficient efficacy in subsequent clinical trials. In addition, relapse or noncompliance from initial treatments is common, necessitating secondary antipsychotic intervention [47, 48]. Studies have shown that between 49 and 74% of schizophrenia patients discontinue the use of antipsychotic drug (APD) treatments within 18 months due to adverse side-effects [48, 49]. Current pharmacotherapies for schizophrenia target the pathological increase in dopamine system activity, as mentioned above. Common clinical practice for secondary antipsychotic application involves a brief withdrawal period from the initial APD. Unfortunately, the success of even secondary treatments is far from being optimal with the rehospitalization of patients being a common occurrence. The impact of repeated antipsychotic treatment and subsequent withdrawal on the dopamine system has not been adequately assessed [36, 38, 47–61].

As indicated above, schizophrenia is a complex chronic psychiatric illness characterized by frequent relapses despite ongoing treatment. The search for more effective pharmacotherapies for the treatment of schizophrenia continues unabated. It is not uncommon for novel pharmaceuticals to demonstrate promise in preclinical trials but fail to show an adequate response in subsequent clinical trials. Indeed, evaluating the benefits of one APD versus another is complicated by clinical trials beset with high attrition rates and poor efficacy in satisfactorily reducing rehospitalization [47, 49–52].

Previous work from the Gill, Grace et al.'s laboratory [36, 38, 47–61] with the MAM model of schizophrenia has identified a potential novel therapeutic, a $\alpha5$GABAAR PAM. The dopamine system pathology in the MAM model is likely the result of excessive output from the ventral HPC [36]. The $\alpha5$GABAAR PAM was identified as a potential therapeutic due to the relatively selective expression of $\alpha5$GABAAR in the ventral HPC and its potential for reducing HPC activity [53–60]. When either administered systemically or directly infused into the ventral HPC, the $\alpha5$GABAAR PAM (SH-053-2′F-R-CH_3) was effective in reducing the dopamine system activation in MAM rats [38]. Anthony Grace, Gill et al. showed $\alpha5$GABAAR PAM treatment was also effective in reducing the enhanced behavioral response to amphetamine in MAM rats, as stated above. Data from the present study sought to delineate whether the $\alpha5$GABAAR PAM (SH-053-2′F-R-CH_3) would remain effective in MAM rats withdrawn from prior neuroleptic treatment, a common occurrence in the patient population. In both SAL and MAM rats, there was a reduction in the spontaneous activity of dopamine neurons in the VTA after 7 days withdrawal from repeated HAL treatment. However, MAM rats continued to exhibit a greater activation of the dopamine system in comparison to SAL rats. Treatment with the $\alpha5$GABAAR PAM was no longer effective in reducing the activity of dopamine neurons in the VTA in withdrawn HAL treated MAM rats. In contrast, $\alpha5$GABAAR PAM treatment in the withdrawn HAL treated SAL rats instead increased the spontaneous activity of dopamine in the VTA (Figures 22–25) [36, 38, 47–61].

Similar to the effects seen following $\alpha5$GABAAR PAM treatment, ventral HPC inactivation in withdrawn HAL treated SAL rats restored normal dopamine system activity by increasing the number of spontaneously active dopamine neurons. The disparate effect of withdrawal from HAL on

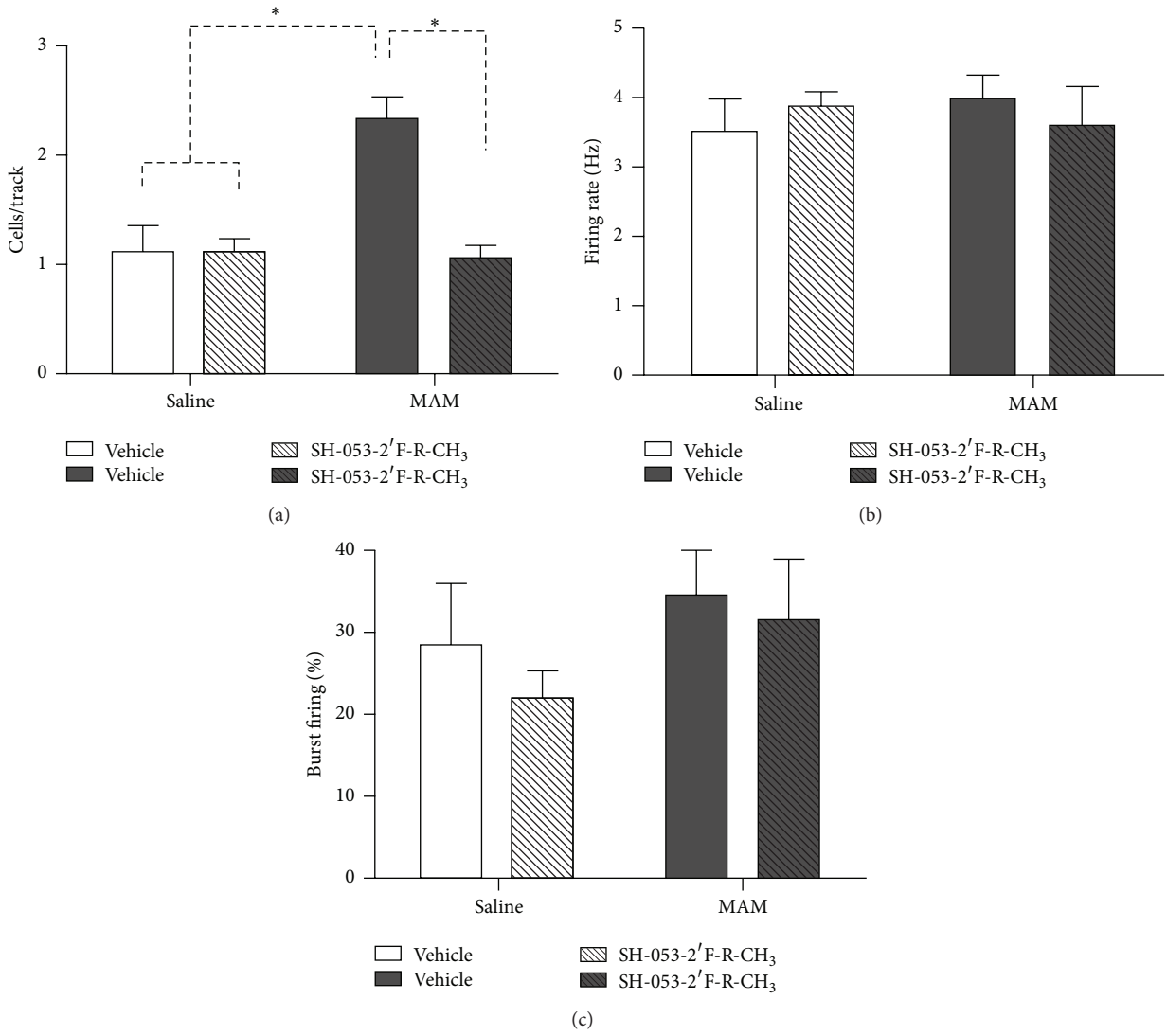

FIGURE 18: Treatment with SH-053-2′F-R-CH_3 (0.1 mg/kg, i.v.; patterned bars) normalizes the aberrant increase in the number of spontaneously firing dopamine neurons (expressed as cells/track) in methylazoxymethanol acetate- (MAM-) treated animals (a). There was no effect of SH-053-2′F-R-CH_3 treatment in control animals (open bars, (a)–(c)) or on firing rate and burst activity in MAM animals (dark bars; (b)-(c)) ($^*p < 0.05$, two-way ANOVA, Holm-Sidak *post hoc*; $N = 5$–7 rats/group) [27–38].

the dopamine system between SAL and MAM rats provides a vital clue for the inconsistencies between preclinical trials for novel therapeutics that utilize normal subjects and subsequent clinical trials in a patient population [36, 38, 47–61].

The data suggests underlying dopamine system pathology alters the impact of withdrawal from prior repeated HAL in the MAM model of schizophrenia. In addition, subsequent novel APD treatment loses efficacy following withdrawal from repeated HAL in MAM animals. This certainly has relevance to Phase III clinical trials of new drugs to treat schizophrenia [36, 38, 47–61].

7. $GABA_A$ $\alpha5$ Positive Allosteric Modulators Relax Airway Smooth Muscle

Emala, Gallos, et al. [66–75] have found that novel $\alpha5$-subtype selective $GABA_A$ positive allosteric modulators relax airway smooth muscle from rodents and humans. The clinical need for new classes of bronchodilators for the treatment of bronchoconstrictive diseases such as asthma remains a major medical issue. Few novel therapeutics have been approved for targeting airway smooth muscle (ASM) relaxation or lung inflammation in the last 40 years [66]. In fact, several asthma-related deaths are attributed, in part, to long-acting β-agonists (LABA) [67]. Adherence to inhaled corticosteroids, the first line of treatment for airway inflammation in asthma, is very poor [68, 69]. Therapies that break our dependence on β-agonism for ASM relaxation would be a novel and substantial advancement.

These ASM studies were undertaken due to a pressing clinical need for novel bronchodilators in the treatment of asthma and other bronchoconstrictive diseases such as COPA. There are only three drug classes currently in clinical

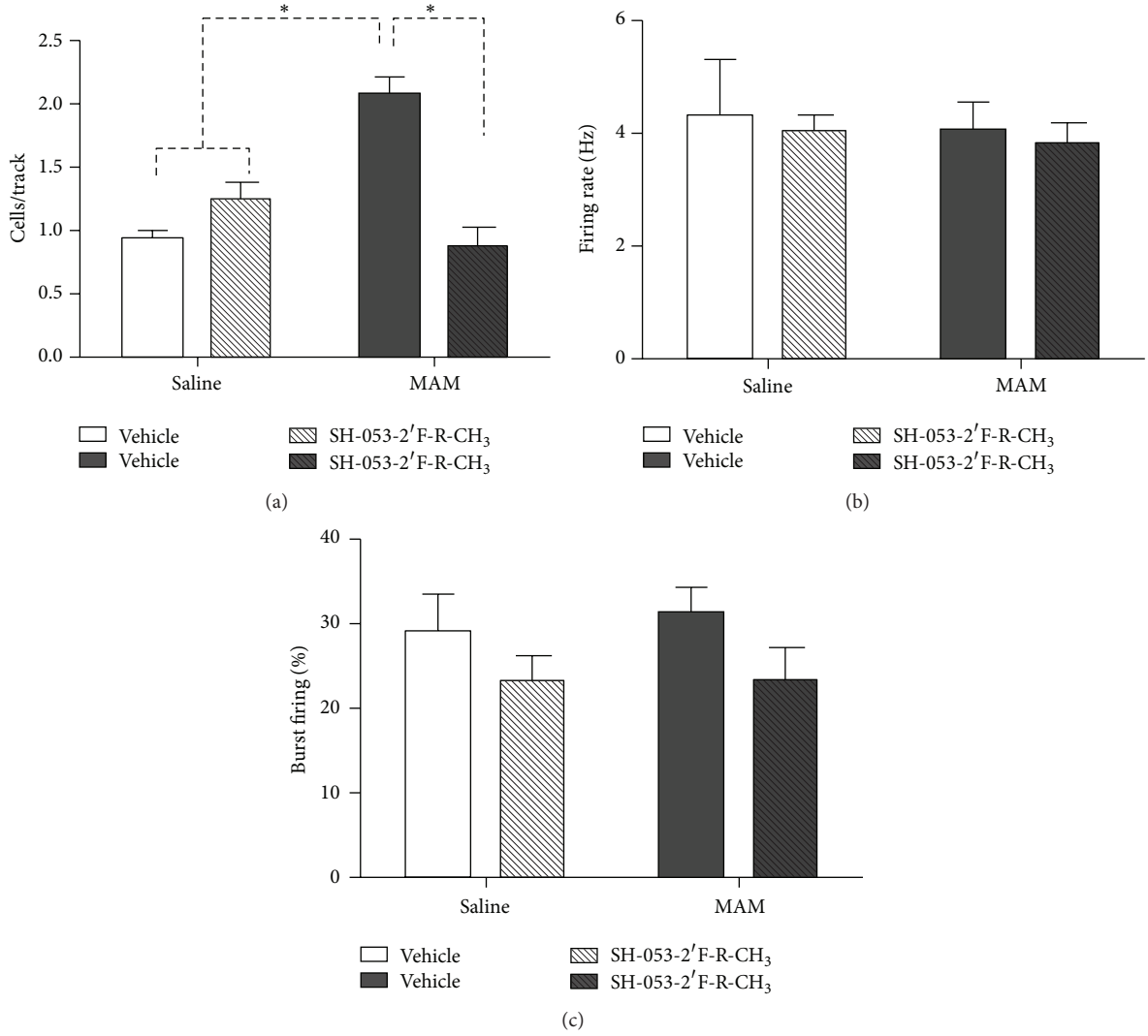

Figure 19: Hippocampal (HPC) infusion of SH-053-2′F-R-CH_3 (1 μM/side; patterned bars) normalizes the aberrant increase in the number of spontaneously firing dopamine neurons (expressed as cells/track) in methylazoxymethanol acetate- (MAM-) treated animals (a). There was no effect of SH-053-2′F-R-CH_3 treatment in control animals (open bars, (a)–(c)) or on firing rate in MAM animals (dark bars; (b)). Hippocampal (HPC) infusion of SH-053-2′F-R-CH_3 significantly reduced the percentage of spikes occurring in bursts of dopamine (DA) neurons in MAM and control animals (c) ($^*p < 0.05$, two-way ANOVA, Holm-Sidak *post hoc*; $N = 7$ rats/group) [27–38].

use as acute bronchodilators in the United States (methylxanthines, anticholinergics, and β-adrenoceptor agonists) [70]. Thus, a novel therapeutic approach that would employ cellular signaling pathways distinct from those used by these existing therapies involves modulating airway smooth muscle (ASM) chloride conductance via $GABA_A$ receptors to achieve relaxation of precontracted ASM [71, 72]. However, widespread activation of all $GABA_A$ receptors may lead to undesirable side effects (sedation, hypnosis, mucus formation, etc.). Thus, a strategy that selectively targets a subset of $GABA_A$ channels, those containing α subunits found to be expressed in airway smooth muscle, may be a first step in limiting side effects. Since human airway smooth muscle contains only α4 or α5 subunits [72], ligands with selectivity for these subunits are an attractive therapeutic option. Concern regarding nonselective $GABA_A$ receptor activation is not limited to the airway or other peripheral tissues. $GABA_A$ receptor ligands are classically known for their central nervous system effects of anxiolysis, sedation, hypnosis, amnesia, anticonvulsion, and muscle relaxant effects. Such indiscriminate activation of $GABA_A$ receptors in the CNS is exemplified by the side effects of classical benzodiazepines (such as diazepam) which were the underpinning for the motivation of a search for benzodiazepine (BZD) ligands that discriminate among the α subunits of $GABA_A$ receptors [73–75].

A novel approach to identify novel benzodiazepine derivatives to selectively target $GABA_A$ channels containing specific α subunits was developed by Cook et al. in the 1980s that employed a pharmacophore receptor model based on the binding affinity of rigid ligands to BDZ/$GABA_A$ receptor sites (as reviewed in 2007 [23]). From this series

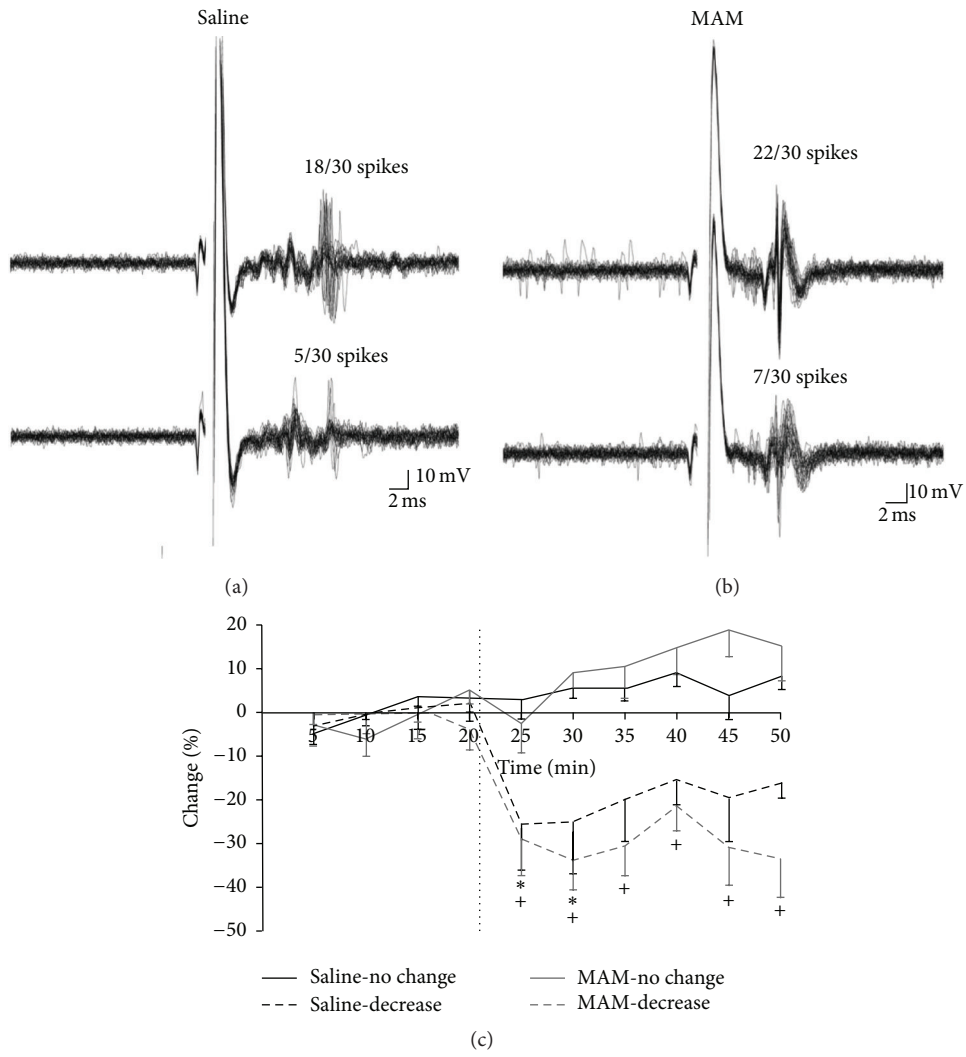

Figure 20: Extracellular recording traces illustrate the reduction in evoked responses in the ventral hippocampal (HPC) to entorhinal cortex stimulation in both MAM- and saline-treated animals (a, b). Treatment with SH-053-2′F-R-CH_3 (0.1 mg/kg, i.v.) decreases the evoked excitatory response (dashed lines) of ventral HPC neurons to entorhinal cortex stimulation in both MAM- and saline-treated animals (c) ($^{*}p < 0.05$ for saline and $^{+}p < 0.05$, two-way repeated measures ANOVA, Holm-Sidak *post hoc*) [27–38].

of receptor models for $\alpha_{1-6}\beta3\gamma2$ subtypes a robust model for $\alpha5$ subtype selective ligands emerged, the result of which included the synthesis of a novel $\alpha5\beta3\gamma2$ partial agonist modulator, SH-053-2′F-R-CH_3 (**2**). The discovery of this and related ligands selective for $\alpha5$ BDZ/$GABA_A$-ergic receptors and the realization that only $\alpha4$ and $\alpha5$ subunits are expressed in $GABA_A$ channels on human airway smooth muscle yielded an ideal opportunity for targeting these $\alpha5$-subunit containing $GABA_A$ channels for bronchorelaxation [66–75].

The $GABA_A\alpha5$ subunit protein was first localized to the ASM layer of human trachea while costaining for the smooth muscle specific protein α actin (Figure 26). The first panel of Figure 26 shows $GABA_A$ $\alpha5$ protein stained with fluorescent green and blue fluorescent nuclear staining (DAPI). The second panel is the same human tracheal smooth muscle section simultaneously stained with a protein specific for smooth muscle, α actin, and the third panel is a merge of the first two panels showing costaining of smooth muscle with $GABA_A$ $\alpha5$ and α actin proteins. The fourth panel is a control omitting primary antibodies but including nuclear DAPI staining [66–75].

After demonstrating the protein expression of $GABA_A$ receptors containing the $\alpha5$ subunit, functional studies of isolated airway smooth muscle were performed in tracheal airway smooth muscle from two species. Human airway smooth muscle suspended in an organ bath was precontracted with a concentration of acetylcholine that was the EC_{50} concentration of acetylcholine for each individual airway smooth muscle preparation. The induced contraction was then relaxed with a β-agonist (isoproterenol) in the absence or presence of the $GABA_A$ $\alpha5$ ligand SH-053-2′F-R-CH_3 (**2**). Figure 27(a) shows that the amount of relaxation

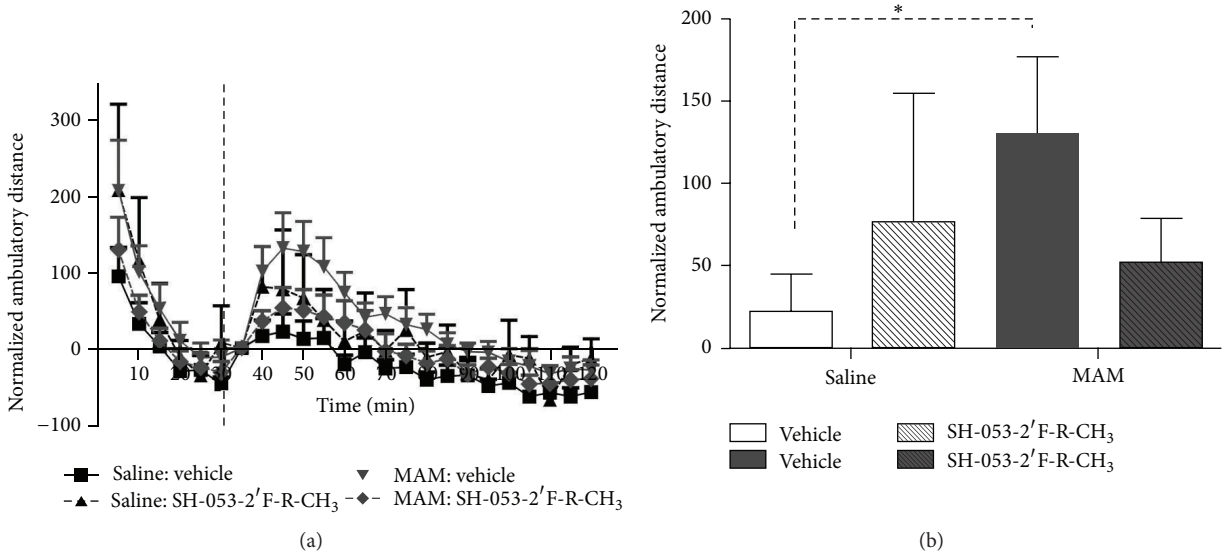

FIGURE 21: Treatment with SH-053-2′F-R-CH_3 (10 mg/kg, i.p.) reduced the aberrant increased locomotor response to D-amphetamine (0.5 mg/kg i.p.) observed in MAM rats (a). MAM animals demonstrated a significantly larger peak locomotor response than both saline-treated animals and MAM animals pretreated with the alpha-5 PAM (b) (there was a significant difference between MAM-vehicle and all other groups, $^{*}P < 0.05$, two-way repeated measures ANOVA, Holm-Sidak *post hoc*) [27–38].

induced by 10 nM isoproterenol was significantly increased if 50 μM SH-053-2′F-R-CH_3 (**2**) was also present in the buffer superfusing the airway smooth muscle strip. Studies were also performed in airway smooth muscle from another species, guinea pig, that measured direct relaxation of a different contractile agonist, substance P. As shown in Figure 27(b), the amount of remaining contractile force 30 minutes after a substance P-induced contraction was significantly reduced in airway smooth muscle tracheal rings treated with SH-053-2′F-R-CH_3 (**2**) [66–75].

Following these studies in intact airway smooth muscle, cell based studies were initiated in cultured human airway smooth muscle cells to directly measure plasma membrane chloride currents and the effects of these currents on intracellular calcium concentrations. SH-053-2′F-R-CH_3 (**2**) induced a Cl^- current *in vitro* using conventional whole cell patch clamp techniques [66–75]. These electrophysiology studies were then followed by studies to determine the effect of these plasma membrane chloride currents on intracellular calcium concentrations following treatment of human airway smooth muscle cells with a ligand whose receptor couples through a Gq protein pathway, a classic signaling pathway that mediates airway smooth muscle contraction.

SH-053-2′F-R-CH_3 (**2**) attenuated an increase in intracellular calcium concentrations induced by a classic Gq-coupled ligand, bradykinin (Figure 28(a)) [66–75]. The attenuation by SH-053-2′F-R-CH_3 (**2**) was significantly blocked by the $GABA_A$ antagonist gabazine (Figure 28(b)) indicating that SH-053-2′F-R-CH_3 (**2**) was modulating $GABA_A$ receptors for these effects on cellular calcium [66–75].

The major findings of these studies are that human airway smooth muscle expresses α5 subunit containing $GABA_A$ receptors that can be pharmacologically targeted by a selective agonist. The $GABA_A$ α5 subunit selective ligand SH-053-2′F-R-CH_3 (**2**) relaxed intact guinea pig airway smooth muscle contracted with substance P and augmented β-agonist-mediated relaxation of intact human airway smooth muscle. The mechanism for these effects was likely mediated by plasma membrane chloride currents that contributed to an attenuation of contractile-mediated increases in intracellular calcium, a critical event in the initiation and maintenance of airway smooth muscle contraction [66–75].

8. Recent Discovery of Alpha 5 Included Volume Differences: L_4 Pocket as Compared to Other Bz/GABAergic Subtypes

The findings in both the MAM-model of schizophrenia and the relaxation of airway smooth muscle have led to the study of SH-053-2′F-R-CH_3 and related compounds bound within the α5-$GABA_A$/BzR (Figure 29). The SH-053-R-CH_3 (**15**) and SH-053-S-CH_3 (**16**) isomers have been previously described [23]. These compounds along with SH-053-2′F-R-CH_3 and SH-053-2′F-S-CH_3 have been tested for binding affinity and show selectivity for the α5-subunit (Table 3).

From examination of Figure 30 and Tables 3 and 4, it is clear the (R)-isomers bound to the α5 subtype while the (S)-isomers were selective for α2/α3/α5 subtypes.

From this data, these compounds were then used in examining the α5-binding pocket, most specifically the fluoroseries. In regard to molecular modeling, depicted in Figure 30 is the included volume and ligand occupation of the SH-053-2′F-S-CH_3 (**17**) and SH-053-2′F-R-CH_3 (**2**) enantiomers in the α5 subtype as well as the α2 subtype. It

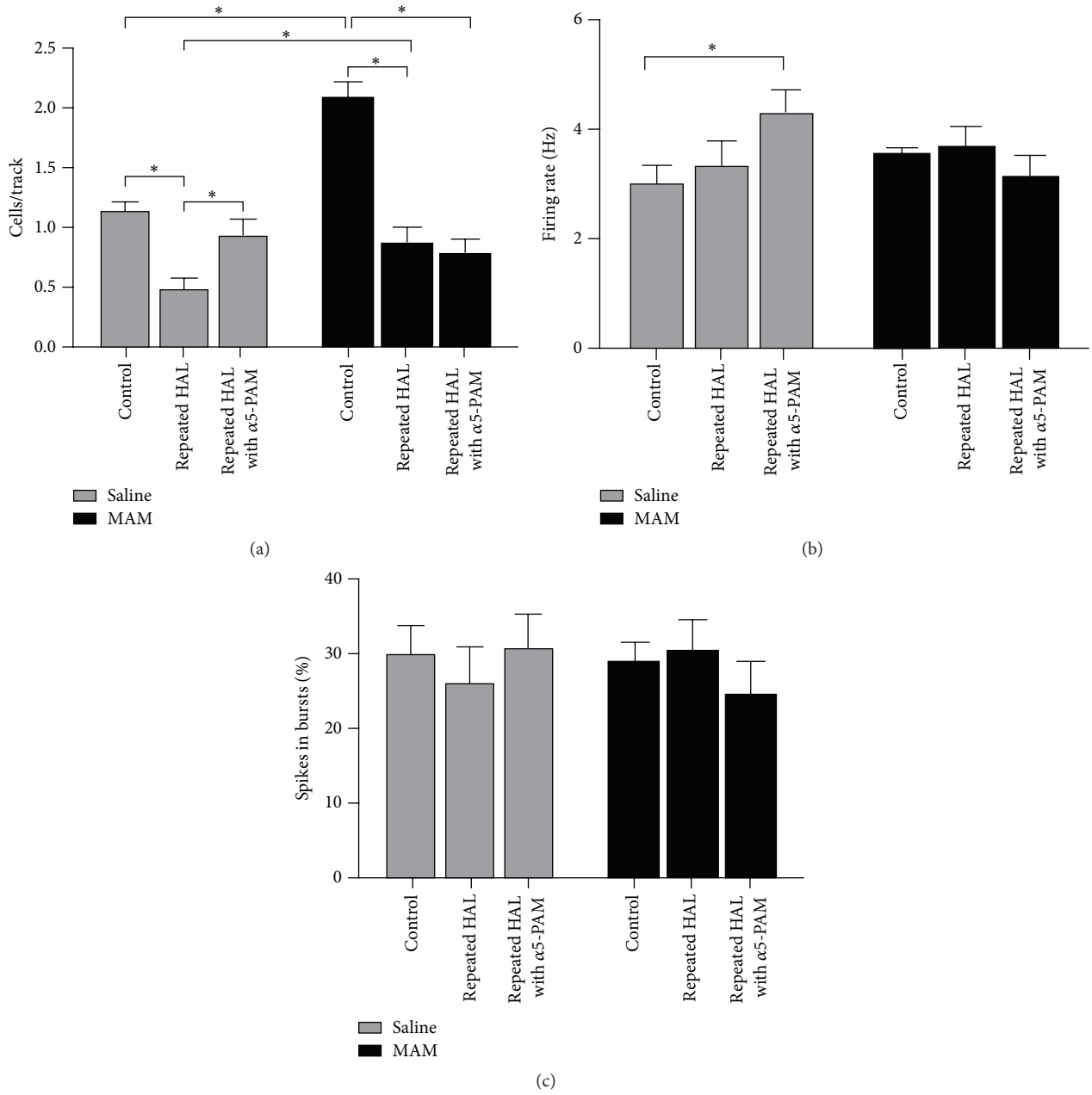

FIGURE 22: Repeated haloperidol treatment caused a reduction in the number of spontaneously active dopamine neurons in both SAL and MAM rats injected with vehicle compared to untreated control animals. Treatment with SH-053-2′F-R-CH_3 (0.1 mg/kg, i.v.) reversed the haloperidol-induced reduction in cells/track in SAL, but not MAM, rats (a). Repeated haloperidol treatment had no effect on the firing rate of dopamine neurons recorded in SAL or MAM rats treated with vehicle. However, SH-053-2′F-R-CH_3 caused an increase in firing rate of dopamine neurons in repeatedly haloperidol-treated SAL rats (b). Repeated haloperidol treatment, as well as SH-053-2′F-R-CH_3 injection, had no impact on the percentage of spikes occurring in bursts for dopamine neurons recorded in SAL and MAM rats (c) [36, 38, 47–61]. $^*p < 0.05$.

is clear a new pocket (L_4) has been located in the α5 subtype permitting **2** as well as **17** to bind to the α5 subtype. Examination of both ligands in the α2 subtype clearly illustrates the analogous region in the α2 subtype is not present and thus does not accommodate **2** for the pendant phenyl which lies outside the included volume in the space allocated for the receptor protein itself [23].

9. BzR GABA(A) Subtypes

In terms of potency, examination of the values in Table 4 [87], it is clear the R-isomer (**2**) shows more selectivity towards the α5-subunit, while the S-isomer (**17**) is potent at the α2/3/5 subunits. It is important, as postulated earlier [23], that the major difference in GABA(A)/Bz receptors subtypes stems

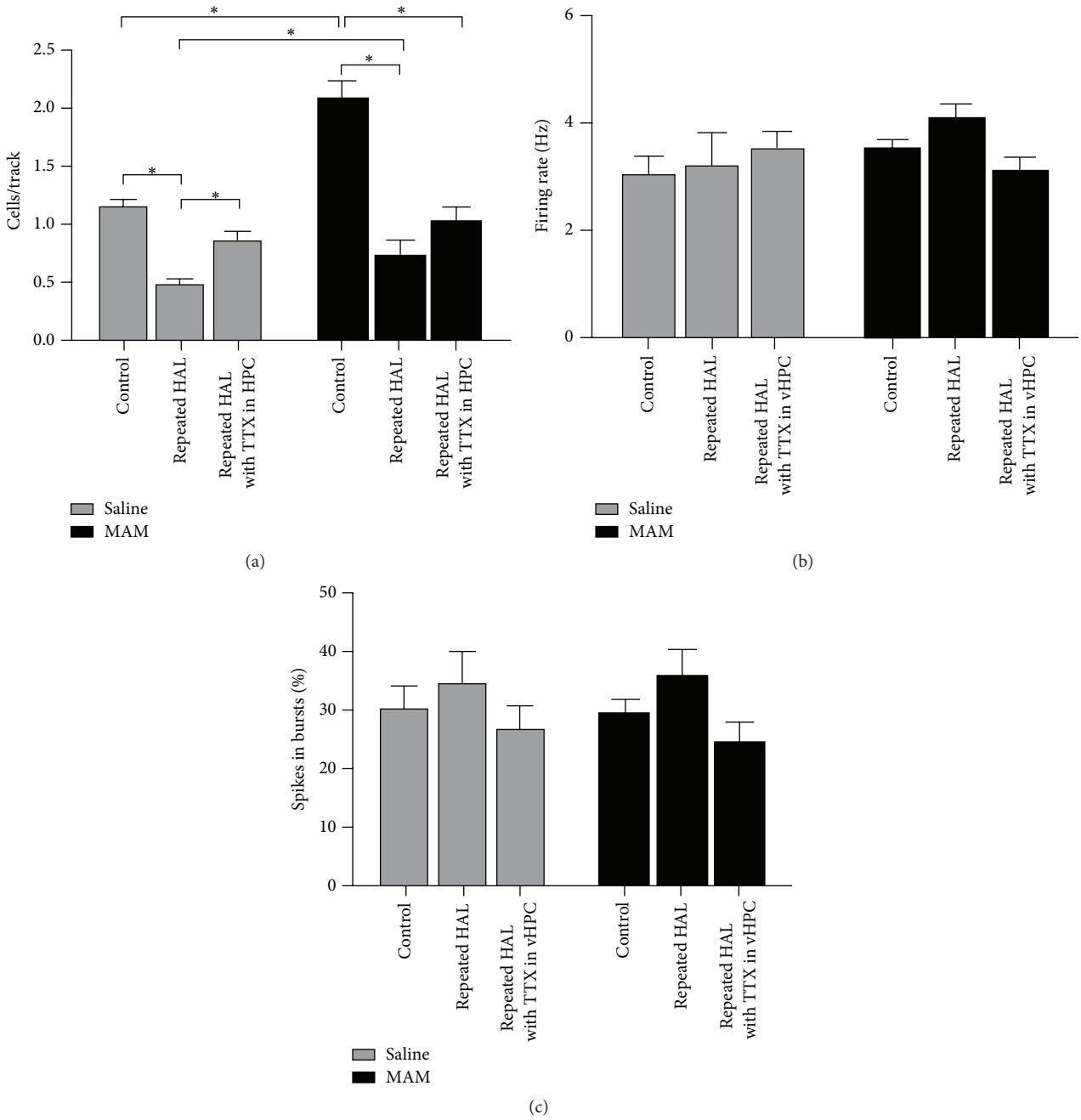

Figure 23: Repeated haloperidol treatment caused a reduction in the number of spontaneously active dopamine neurons in both SAL and MAM rats microinfused with vehicle in the ventral HPC compared to untreated control animals. Infusion of TTX in the ventral HPC reversed the haloperidol-induced reduction in cells/track in SAL, but not MAM, rats (a). Repeated haloperidol treatment had no effect on the firing rate of dopamine neurons recorded in SAL or MAM rats infused with vehicle or TTX in the ventral HPC (b). Repeated haloperidol treatment had no effect on the percentage of spikes occurring in bursts for dopamine neurons recorded in SAL or MAM rats infused with vehicle or TTX in the ventral HPC (c) [36, 38, 47–61]. $^{*}p < 0.05$.

from differences in asymmetry in the lipophilic pockets L_1, L_2, L_3, L_4, and L_{Di} in the pharmacophore/receptor model and indicates even better functional selectivity is possible with asymmetric BzR ligands.

The synthetic switching of chirality at the C-4 position of imidazobenzodiazepines to induce subtype selectivity was successful. Moreover, increase of the potency of imidazobenzodiazepines can be achieved by substitution of the 2′-position hydrogen atom with an electron rich atom (fluorine) on the pendant phenyl ring in agreement with Haefely et al. [88], Fryer [89, 90], and our own work [22, 91]. The biological data on the two enantiomeric pairs of benzodiazepine ligands

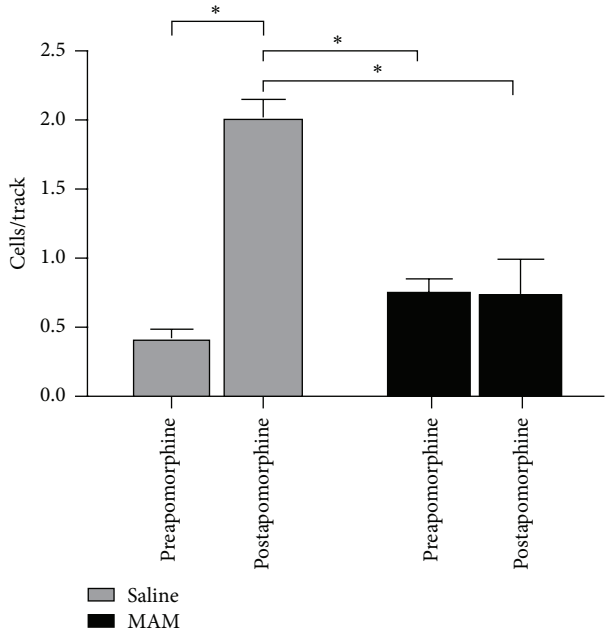

Figure 24: Administration of apomorphine (80 mg/kg i.v.) increased the number of spontaneously active dopamine neurons in SAL rats withdrawn from repeated HAL, while having no effect on the number of active dopamine neurons in MAM rats withdrawn from repeated HAL [36, 38, 47–61]. $^{*}p < 0.05$.

Table 3: Binding affinity at $\alpha x\beta 2\gamma 2$ $GABA_A$ receptor subtypes (values are reported in nM).

Compound[a]	$\alpha 1$	$\alpha 2$	$\alpha 3$	$\alpha 4$	$\alpha 5$	$\alpha 6$
SH-053-R-CH_3, (**15**)	2026	2377	1183	>5000	949.1	>5000
SH-053-S-CH_3, (**16**)	1666	1263	1249	>5000	206.4	>5000
SH-053-2′F-R-CH_3, (**2**)	759.1	948.2	768.8	>5000	95.17	>5000
SH-053-2′F-S-CH_3, (**17**)	350	141	1237	>5000	19.2	>5000

[a]Data shown here are the means of two determinations which differed by less than 10%.

Table 4: Oocyte electrophysiological data of benzodiazepines[a] [87].

Compound	$\alpha 1$	$\alpha 2$	$\alpha 3$	$\alpha 5$
SH-053-2′F-R-CH_3 (**2**)	111/154	124/185	125/220	183/387
SH-053-2′F-S-CH_3 (**17**)	116/164	170/348	138/301	218/389

[a]Efficacy at $\alpha x\beta 3\gamma 2$ $GABA_A$ receptor subtypes as % of control current at 100 nM and 1 μM concentrations. Data presented as percent over baseline (100) at concentrations of 100 nM/1 μM.

confirm the ataxic activity of BZ site agonists is mediated by $\alpha 1\beta 2/3\gamma 2$ subtypes, as reported in [23, 91–93]. The antianxiety activity in primates of the S isomers was preserved with no sedation. In only one study in rodents was any sedation observed; the confounding sedation was observed in both the S isomer (functionally selective for $\alpha 2$, $\alpha 3$, and $\alpha 5$ receptor subtypes) and R isomer (essentially selective for $\alpha 5$ subtype) and may involve at least, in part, agonist activity at $\alpha 5$ BzR subtypes. There are some $\alpha 5$ BzR located in the spinal cord which might be the source of the decrease in locomotion with SH-053-2′F-R-CH_3 and SH-053-2′F-S-CH_3; however, this is possibly some type of stereotypical behavior. Hence in agreement with many laboratories including our own [23, 92, 93] the best potential nonsedative, nonamnesic, antianxiety agents stem from ligands with agonist efficacy at $\alpha 2$ subtypes essentially silent at $\alpha 1$ and $\alpha 5$ subtypes (to avoid sedation) [91]. It must be pointed out again; however, in primates Fischer et al. [87] observed a potent anxiolytic effect with no sedation with the 2′F-S-CH_3 (**17**) isomer, while the 2′F-R-CH_3 (**2**) isomer exhibited only a very weak anxiolytic effect.

Numerous groups have done modeling and SAR studies on different classes of compounds which have resulted in a few different pharmacophore models based on the benzodiazepine binding site (BS) of the $GABA_A$ receptor [94]. These models are employed to gain insight in the interactions between the BS and the ligand. These have been put forth by Loew [7, 95, 96], Crippen [97, 98], Codding [76, 77, 99–101], Fryer [89, 90, 94], Gilli and Borea [102–105], Tebib et al. [106], and Gardner [107], as well as from Professors Sieghart, Cromer, and our own laboratory [21, 39, 40, 76, 78–82, 108–118].

The Milwaukee-based pharmacophore/receptor model is a comprehensive building of the BzR using radioligand binding data and receptor mapping techniques based on 12 classes of compounds [20, 23, 39, 40, 42, 111, 119–122]. This model (Figure 31) [79] has brought together previous models which have used data from the activity of antagonists, positive allosteric modulators, and negative allosteric modulators and included the new models for the "diazepam-insensitive" (DI) sites [123]. Four basic anchor points, H_1, H_2, A_2, and L_1, were assigned, and 4 additional lipophilic regions were defined as L_2, L_3, L_{Di}, and the new L_4 (see captions in Figure 31 for details); regions S_1, S_2, and S_3 represent negative areas of steric repulsion. As previously reported, the synthesis of both partial agonists and partial inverse agonists has been achieved by using parts of this model [99, 100, 104, 105, 119, 124–127].

The cloning, expression, and anatomical localization of multiple GABA(A) subunits have facilitated both the identification and design of subtype selective ligands. With the availability of binding data from different recombinant receptor subtypes, affinities of ligands from many different structural classes of compounds have been evaluated.

Illustrated in Figure 31 is the [*3,4-c*]quinolin-3-one CGS-9896 (**18**) (dotted line), a diazadiindole (**19**) (thin line), and diazepam (**20**) (thick line) fitted initially to the inclusive pharmacophore model for the BzR. Sites H_1 (Y210) and H_2 (H102) represent hydrogen bond donor sites on the receptor protein complex while A_2 (T142) represents a hydrogen bond acceptor site necessary for potent inverse activity *in vivo*. L_1, L_2, L_3, L_4, and L_{Di} are four lipophilic regions in the binding pharmacophore. Descriptors S_1, S_2, and S_3 are regions of negative steric repulsion.

Based on SAR data obtained for these ligands at 6 recombinant BzR subtypes [128–132], an effort has been undertaken to establish different pharmacophore/receptor models for BzR subtypes. The alignment of the twelve different structural classes of benzodiazepine receptor ligands was earlier based on the least squares fitting of at least three points. The coordinates of the four anchor points (A_2, H_1, H_2, and L_1) employed in the alignment are outlined in Figure 32.

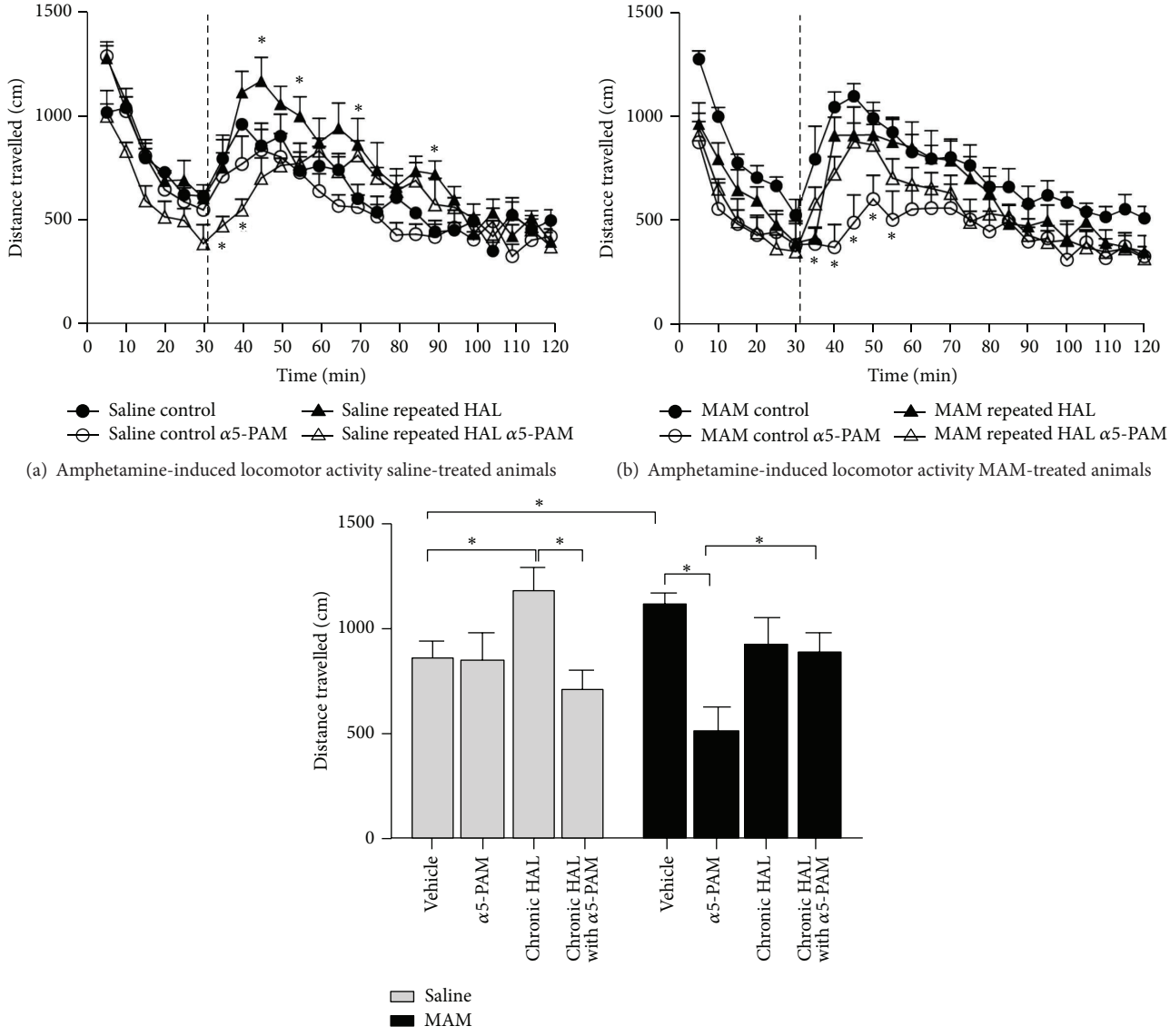

(a) Amphetamine-induced locomotor activity saline-treated animals

(b) Amphetamine-induced locomotor activity MAM-treated animals

(c) Postamphetamine average peak distance travelled

FIGURE 25: Repeated haloperidol treatment causes an enhancement in the locomotor response to D-amphetamine (0.5 mg/kg, i.p.) in SAL animals that is reduced by pretreatment with SH-053-2′F-R-CH$_3$ (10 mg/kg, i.p.) (a). MAM rats treated repeatedly with haloperidol exhibit a locomotor response following D-amphetamine similar to untreated MAM rats. However, repeated haloperidol treatment blocks the effect of SH-053-2′F-R-CH$_3$ pretreatment in decreasing the locomotor response in MAM rats (b). Untreated MAM rats demonstrated a significantly larger peak locomotor response than untreated SAL rats. In addition, SH-053-2′F-R-CH$_3$ pretreatment significantly reduced the peak locomotor response in untreated MAM rats, while having no effect in repeatedly haloperidol-treated MAM rats. In contrast, repeated haloperidol treatment enhanced the peak locomotor response to amphetamine in SAL rats that was reduced by SH-053-2′F-R-CH$_3$ pretreatment (c) [36, 38, 47–61]. $^*P < 0.05$.

Herein are described the results from ligand-mapping experiments at recombinant BzR subtypes of 1,4-benzodiazepines, imidazobenzodiazepines, β-carbolines, diindoles, pyrazoloquinolinones, and others [126]. Some of the differences and similarities among these subtypes can be gleaned from this study and serve as a guide for future drug design.

10. α1 Updates

10.1. Beta-Carbolines. A series of 3,6-disubstituted β-carbolines was prepared and evaluated for their *in vitro* affinity at $\alpha x\beta 3\gamma 2$ GABA(A)/BzRr subtypes by radioligand binding assays in search of $\alpha 1\beta 3\gamma 2$ subtype selective compounds (Figure 33). A potential therapeutic application of such antagonist analogs is to treat alcohol abuse [133, 134]. Analogues of βCCt (**21**) were synthesized *via* a carbonyldiimidazole-mediated method by Yin et al. [85] and the related 6-substituted β-carboline-3-carboxylates including WYS8 (**27**) were synthesized from 6-iodo βCCt (**29**). Bivalent ligands (**42** and **43**) were also synthesized to increase the scope of the structure-activity relationships (SAR) to larger ligands. An

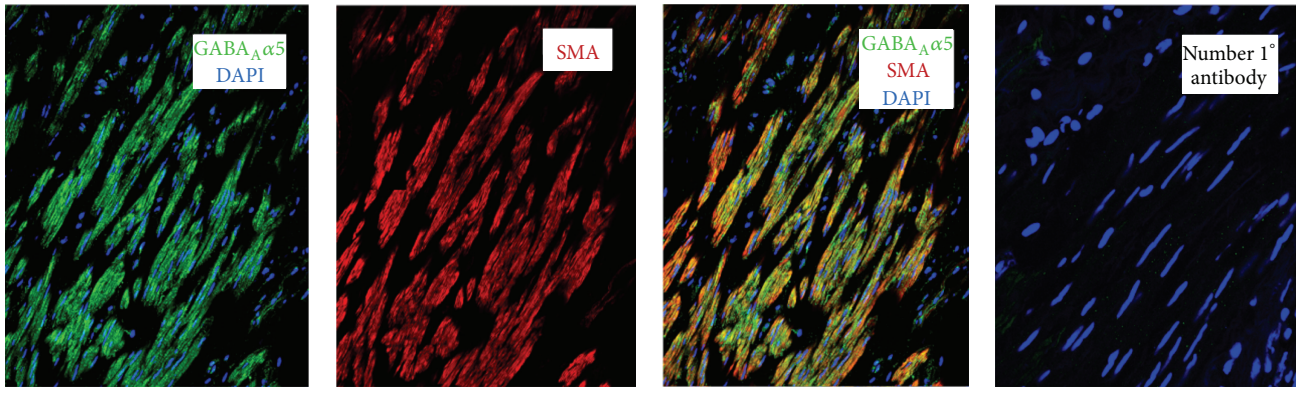

FIGURE 26: Protein expression of the GABA$_A$ α5 subunit in intact human trachea-bronchial airway smooth muscle. Representative images of human tracheal airway smooth muscle sections using confocal microscopy are depicted following single, double, and triple immunofluorescence labeling. The antibodies employed were directed against the GABA$_A$ α5 subunit (green), α-smooth muscle actin (SMA; red), and/or the nucleus via DAPI counterstain (blue). Panels illustrate the following staining parameters from left to right: (1st) costaining of DAPI and GABA$_A$ α5 subunit; (2nd) α-SMA staining alone; (3rd) triple-staining of GABA$_A$ α5, α-SMA, and DAPI; (4th) DAPI nucleus counterstain, with primary antibodies omitted as negative control. Modified from [66–75].

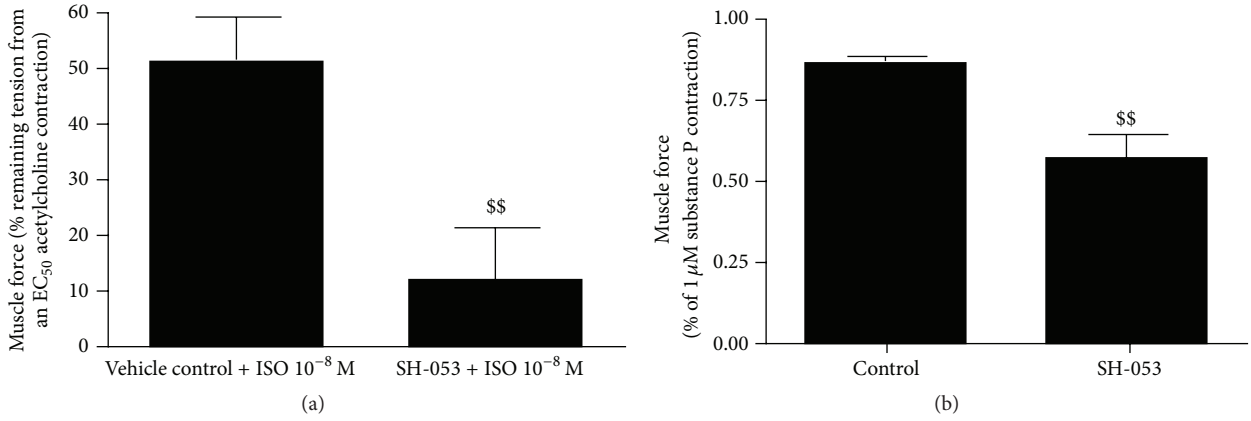

FIGURE 27: SH-053-2′F-R-CH$_3$ (**2**) mediated activation of α5 subunit containing GABA$_A$ channels induces relaxation of precontracted airway smooth muscle. (a) SH-053-2′F-R-CH$_3$ (**2**) (SH-053) potentiates β-agonist-mediated relaxation of human airway smooth muscle. Cotreatment of human airway smooth muscle strips with SH-053-2′F-R-CH$_3$ (**2**) (50 μM) significantly enhances isoproterenol (10 nM) mediated relaxation of an acetylcholine EC$_{50}$ contraction compared to isoproterenol alone (N = 8/group, \$\$ = $p < 0.01$). Modified from [66–75]. (b) SH-053-2′F-R-CH$_3$ (**2**) activation of α5 containing GABA$_A$ receptors induces direct relaxation of substance P-induced airway smooth muscle contraction. Compiled results demonstrating enhanced spontaneous relaxation (expressed as % remaining force at 30 minutes following a 1 μM substance P mediated contraction) following treatment with SH-053-2′F-R-CH$_3$ (**2**) compared to treatment with vehicle control (n = 4-5/group, \$\$ = $p < 0.01$) [66–75].

initial SAR on the first analogs demonstrated that compounds with larger side-groups at C6 were well tolerated as they projected into the L_{Di} domain (see **42** and **43**) [85]. Moreover, substituents located at C3 exhibited a conserved stereo interaction in lipophilic pocket L_1, while N2 likely participated in hydrogen bonding with H_1. Three novel β-carboline ligands (**21**, **23**, and **27**) permitted a comparison of the pharmacological properties with a range of classical benzodiazepine receptor antagonists (flumazenil, ZK93426) from several structural groups and indicated these β-carbolines were "near GABA neutral antagonists." Based on the SAR, the most potent (*in vitro*) α1 selective ligand was the 6-substituted acetylenyl βCCt (WYS8, **27**). In a previous study both **21** and **23** were able to reduce the rate at which rats self-administrated alcohol in alcohol preferring and HAD rats but had little or no effect on sucrose self-administration [85].

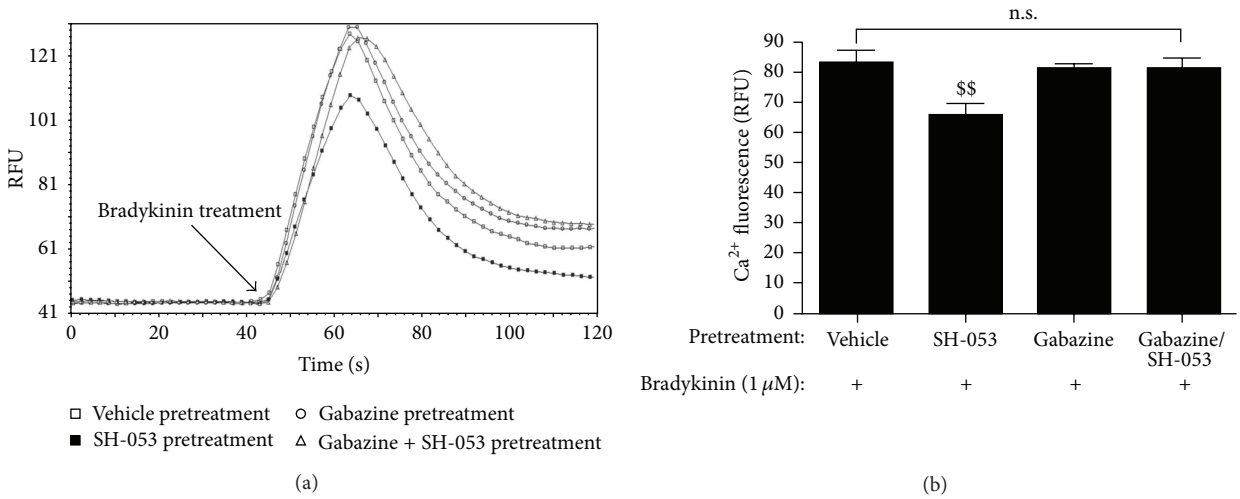

FIGURE 28: SH-053-2′F-R-CH_3 (**2**) mediated activation of α5 containing $GABA_A$ receptors attenuates bradykinin-induced elevations in cytosolic Ca^{2+} in human airway smooth muscle cells. (a) Representative Fluo-4 Ca^{2+} fluorescence (RFU) tracing illustrating pretreatment with SH-053-2′F-R-CH_3 (**2**) (SH-053) (10 μM) reduces cytosolic Ca^{2+} response to bradykinin (1 μM). This effect is reversed in the presence of gabazine (200 μM, $GABA_A$ receptor antagonist). Modified from [66–75]. (b) Compiled results illustrating SH-053-2′F-R-CH_3 (**2**) pretreatment of $GABA_A$ α5 receptors on human airway smooth muscle cells attenuates bradykinin-induced elevations in intracellular Ca^{2+} compared to levels achieved following pretreatment with vehicle control ($$ = $p < 0.01$). While gabazine-mediated blockade of $GABA_A$ channels does not significantly affect bradykinin-induced intracellular calcium increase compared to vehicle control, gabazine treatment did reverse SH-053-2′F-R-CH_3 (**2**) ability to attenuate bradykinin-induced elevations in intracellular calcium thereby illustrating a $GABA_A$ channel specific effect (n.s. = not significant). Modified from [66–75].

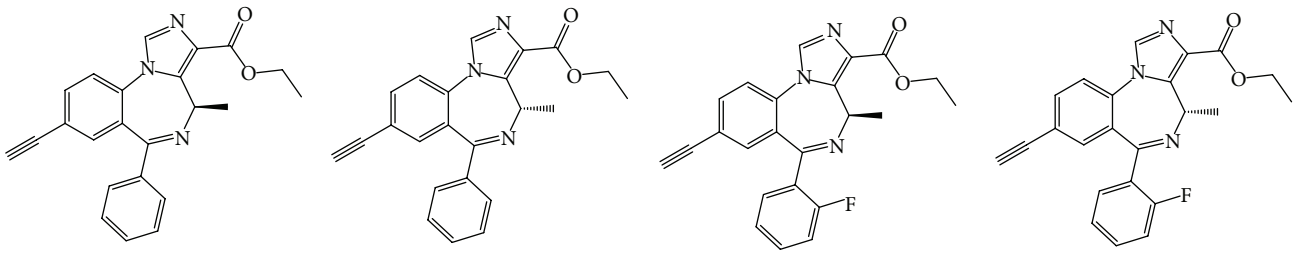

SH-053-R-CH_3, **15** SH-053-S-CH_3, **16** SH-053-2′F-R-CH_3, **2** SH-053-2′F-S-CH_3, **17**

FIGURE 29: Structures of enantiomers with 2′H (**15**, **16**) and 2′F (**2**, **17**).

3-PBC (**23**) was also active in baboons [134]. This data has been used in updating the pharmacophore model in the α1-subtype.

11. The Updated Included Volume Models

Illustrated in Figure 34 is the included volume of the updated pharmacophore receptor model of the $\alpha1\beta3\gamma2$ subtype of Clayton [22]. The current model for the $\alpha1\beta3\gamma2$ subtype has several new features. The cyclopropyl group of CD-214 extended 2 Å past the A_2 descriptor slightly increasing its volume. The trimethylsilyl group of QH-II-82 and WYS7 illustrates how well bulky groups are tolerated near the entrance of the binding pocket. Despite not being as potent, dimers of beta carbolines, WYS2 and WYS6, bound to α1 subtypes at 30 nM and 120 nM, respectively. Their ability to bind, albeit weakly, supports the location of the binding site entrance from the extracellular domain. The included volume of the $\alpha1\beta3\gamma2$ subtype was previously 1085.7 cubic angstroms. The volume has now been measured as 1219.2 cubic angstroms. Volume measurements should be used carefully as the binding site is not enclosed and the theoretical opening near L_{DI} is not clearly demarcated. Dimers were excluded from the included volume exercise because although they bound to the receptor, they represented compounds which were felt to extend outside the receptor binding pocket when docked to the protein. Where appropriate,

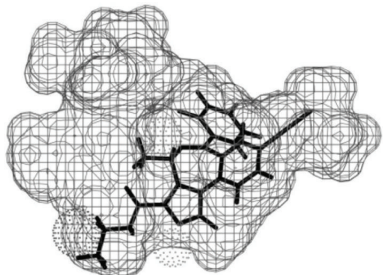

SH-053-2′F-S-CH_3 **17** fits the pharmacophore in the included volume of the alpha 2 subtype

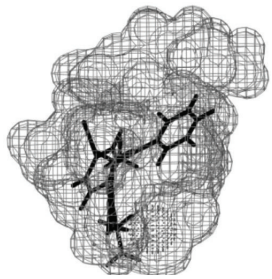

The left image of figure rotated 90°. It can be clearly seen that **17** fits within the included volume

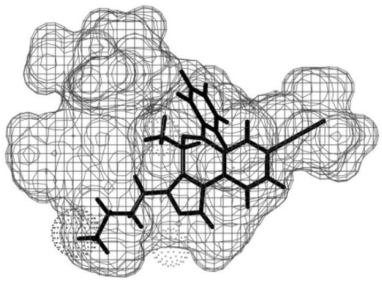

SH-053-2′F-R-CH_3 **2** does not fit the pharmacophore in the included volume of the alpha 2 subtype

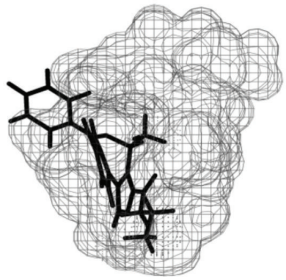

The left image of figure rotated 90°. It can be clearly seen that the conformation of **2** is such that the pendant 6-phenyl sticks outside the included volume

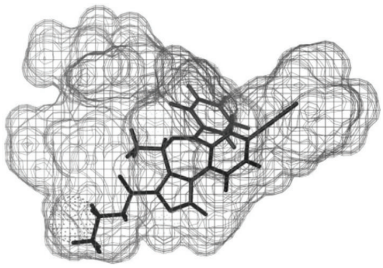

SH-053-2′F-S-CH_3 **17** fits the pharmacophore in the included volume of the alpha 5 subtype

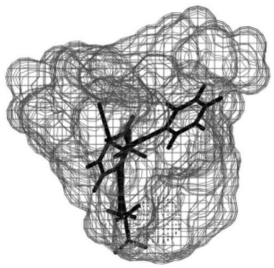

The left image of figure rotated 90°. It can be clearly seen that **17** fits within the included volume

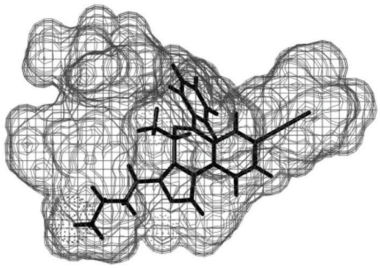

SH-053-2′F-R-CH_3 **2** fits the pharmacophore in the included volume of the alpha 5 subtype

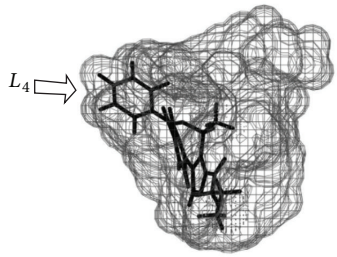

The left image of figure rotated 90°. It can be clearly seen that **2** fits within the included volume

FIGURE 30: Included volume and ligand occupation of the SH-053-2′F-S-CH_3 **17** and SH-053-2′F-R-CH_3 **2** enantiomers in the $\alpha 5$ and $\gamma 2$ pharmacophore/receptor models. This figure was modified and reproduced from that reported by Clayton et al. in [22, 23].

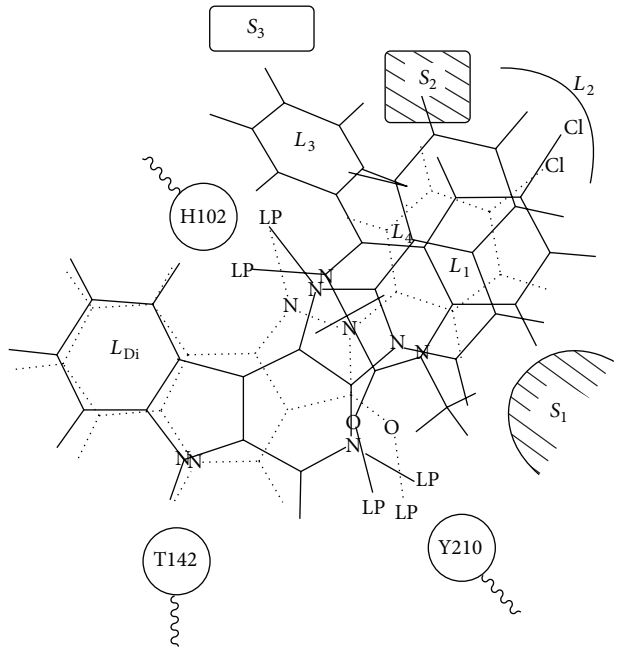

FIGURE 31: The two-dimensional representation of the Milwaukee-based unified pharmacophore with 3 amino acids in the binding site based on the rigid ligand template [23, 39, 42, 76–80]. This figure has been modified from that reported for PAMs, NAMs, and antagonists in [22, 23].

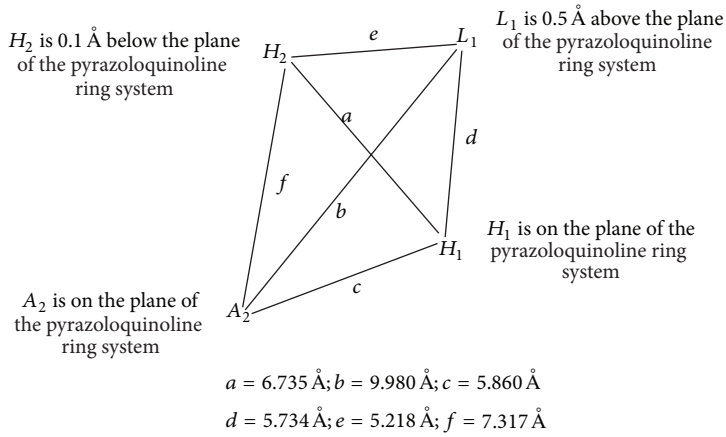

FIGURE 32: The schematic representation of the descriptors for the initial inclusive BzR pharmacophore based on the rigid ligands (diindoles) [79, 81–84]. This figure has been modified from that reported in [79].

their monomers were included in the included volume analysis. Ligands considered for the included volume in Table 5 exhibited potent binding at $\alpha 1$ subtypes ($K_i \leq 20$ nM) but were not necessarily subtype selective. The binding data for ligands at α_{2-6}-subtypes follow (Tables 6–10; structures located in Clayton [22] and Supporting Information, Appendix III in Supplementary Material available online at http://dx.doi.org/10.1155/2015/430248).

12. The $\alpha 1\beta 3\gamma 2$ Receptor Subtype

The focus of this research was aimed at diazepam sensitive receptors; additional features to the $\alpha 4\beta 3\gamma 2$ and $\alpha 6\beta 3\gamma 2$ receptors were not identified (see Table 5, Figures 34 and 35). The major new feature identified for the $\alpha 5\beta 3\gamma 2$ receptor was a new L_4 pocket. This new lipophilic pocket was identified with SH-053-R-CH_3 (**15**) and SH-053-S-CH_3 (**16**) chiral enantionmers as well as the 2′F analogs [74, 135, 136].

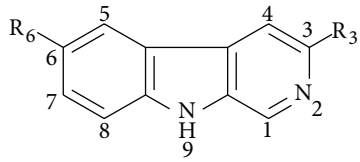

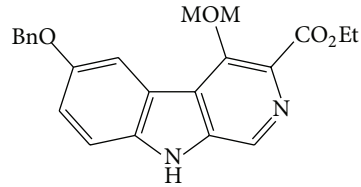

ZK-93423

Ligands	R_6	R_3	$\alpha1$	$\alpha2$	$\alpha3$	$\alpha4$	$\alpha5$	$\alpha6$
21(βCCt)	**H**	**CO_2tBu**	**0.72**	**15**	**18.9**	**1000**	**111**	**>5,000**
22(βCCE)	**H**	**CO_2Et**	**1.2**	**4.9**	**5.7**	**ND**	**26.8**	**2,700**
23(3-PBC)	H	OnPr	5.3	52.3	68.8	1000	591	>1,000
24(WYB14)	TMS—≡	CO_2tBu	6.8	30	36	2000	108	1000
25(WY-B-25)	TMS—≡	$CO_2CH_2CF_3$	17	59	88	200	1444	>3000
26(WY-B-99-1)	TMS—≡	CO_2Et	4.4	4.5	5.58	2000	47	2000
27(WYS8)	H—≡	CO_2tBu	**0.972**	**111**	**102**	**2000**	**1473**	**1980**
28(WY-B-26-2)	H—≡	$CO_2CH_2CF_3$	4.5	44.6	42.7	2000	124	2000
29(iodo-βCCt)	I	CO_2tBu	14.4	44.9	123	>4000	65.3	>4000
30(WY-B-20)	I	$CO_2CH_2CF_3$	12	39	47	2000	122	3000
31(iodo-βCCE)	I	CO_2Et	4.8	31	34	1000	286	1000
32(WY-B-08)	I	$CO_2CH_2(CF_3)_2$	78	301	131	3000	681	3000
33(WYS13)		CO_2tBu	2.4	13	27.5	NA	163	5000
34(WYB27-1)		$CO_2CH_2CF_3$	26	143	117	3000	127	2000
35(WYS12)		CO_2tBu	37	166	314	NA	2861	5000
36(WYB27-2)		$CO_2CH_2CF_3$	9.2	13	72	2000	449	2000
37(WYS15)		CO_2tBu	3.63	2.02	44.3	NA	76.5	5000
38(WYB29-2)		$CO_2CH_2CF_3$	25	137	125	2000	299	2000
39(CMA57)	F	COC_3H_7	3.7	27	40	NA	254	>2500
40(CM-A-82a)	$C(CH_3)_3$	CO_2tBu	2.78	8.93	24.5	1000	7.49	1000
41(CM-A-87)	F	CO_2tBu	1.62	4.54	14.7	1000	4.61	1000
42(WY-S-2)	Bcct—≡—Bcct		30	124	100	>300	>300	>4000
43(WY-S-6)	Bcct—≡≡—Bcct		120	1059	3942	5000	5000	5000

[a]Affinity of compounds at GABA(A)/BzR recombinant subtypes was measured by competition for [^{3}H]flunitrazepam or [^{3}H] Ro-15-4513 binding to HEK cell membranes expressing human receptors of composition $\alpha1\beta3\gamma2$, $\alpha2\beta3\gamma2$, $\alpha3\beta3\gamma2$, $\alpha4\beta3\gamma2$, $\alpha5\beta3\gamma2$, and $\alpha6\beta3\gamma2$ [85]. Data represent the average of at least three determinations with a SEM of ±5%.

Figure 33: [a]Affinities (K_i = nM) of 3,6-disubstituted β-carbolines at $\alpha x\beta3\gamma2$ (x = 1–3, 5, 6) receptor subtypes [85]. The structures versus code numbers of all ligands in the tables of this review can be found in the Ph.D. thesis of Terry Clayton (Ph.D. thesis, University of Wisconsin-Milwaukee, Milwaukee, WI, December, 2011) [22] and in the Supporting Information.

Table 5: These ligands bound with potent affinity for $\alpha 1$; ligands bound with K_i values <20 nM at this subtype.

Cook code[a]	$\alpha 1$	$\alpha 2$	$\alpha 3$	$\alpha 4$	$\alpha 5$	$\alpha 6$
WY-TSC-4 (WYS8)	0.007	0.99	1.63		51.04	
SH-TSC-2 (BCCT)	0.03	0.0419	0.035		69.32	
QH-II-090 (CGS-8216)	0.05	0.08	0.12		0.25	17
XLI-286	0.051	0.064	0.118		0.684	
QH-II-077	0.06	0.08	0.05		0.12	4
QH-II-092	0.07	0.03	0.04	ND	0.17	ND
JYI-57	0.076	0.076	0.131	ND	0.036	ND
QH-II-085	0.08	0.06	0.02	ND	0.08	ND
XHE-II-024	0.09	0.18	0.32	14	0.24	11
PWZ-007A	0.11	0.1	0.09	ND	0.2	10
CGS8216	0.13	ND	ND	ND	ND	46
SPH-121	0.14	1.19	1.72	ND	4	479
QH-II-075	0.18	0.21	0.25	ND	1.3	40
PZII-028	0.2	ND	0.2	ND	0.32	1.9
CGS9895	0.21	ND	ND	ND	ND	9.3
PWZ-0071	0.23	0.17	0.12	ND	0.44	17.31
XHE-III-24	0.25	ND	8	222	10	328
JYI-42	0.257	0.146	0.278	ND	0.256	ND
CGS9896	0.28	ND	ND	ND	ND	181
JYI-64 (C17H12N4FBr)	0.305	1.111	0.62	ND	0.87	5000
PZII-029	0.34	ND	0.79	ND	0.52	10
BRETAZENIL	0.35	0.64	0.2	ND	0.5	12.7
FG8205	0.4	2.08	1.16	ND	1.54	227
YT-5	0.421	0.6034	36.06	ND	1.695	ND
6-PBC	0.49	1.21	2.2	ND	2.39	1343
QH-146	0.49	ND	0.76	ND	7.7	10000
DM-II-90 (C17H12N4BrCl)	0.505	1	0.63	ND	0.37	5000
SPH-165	0.63	2.79	4.85	ND	10.4	1150
BCCt	0.72	15	18.9	ND	110.8	5000
SH-I-048A	0.774	0.1723	0.383	ND	0.11	ND
alprazolam	0.8	0.59	1.43	ND	1.54	10000
Ro15-1788	0.8	0.9	1.05	ND	0.6	148
WYS10 C14H9F3N2O2	0.88	36	25.6	ND	548.7	15.3
WY-B-15	0.92	0.83	0.58	2080	4.42	646
WY-A-99-2 (WYS8)	0.972	111	102	2000	208	1980
XHE-III-06a	1	2	1	5	1.8	37
Xli366 C22H21N3O2	1	ND	ND	ND	ND	ND
JYI-59 (C22H13N3O2F4)	1.08	2.6	11.82	ND	11.5	5000
WYSC1 C16H16N2O2	1.094	5.44	12.3	ND	69.8	21.2
MLT-I-70	1.1	1.2	1.1	ND	40.3	1000
SVO-8-30	1.1	5.3	5.3	2.8	0.6	15
BCCE	1.2	4.9	5.7	ND	26.8	2700
XHE-III-04	1.2	2	1.1	219	0.4	500
XLi350 C17H11ClN2O	1.224	1.188	ND	ND	2.9	ND
XHE-III-49	1.3	5.5	4.2	38.7	11.3	85.1
PWZ-009A1	1.34	1.31	1.26	ND	0.84	2.03
DM-239	1.5	ND	0.53	ND	0.14	6.89
XLi351 C21H21ClN2OSi	1.507	0.967	ND	ND	1.985	ND
XLi352 C18H13ClN2O	1.56	0.991	ND	ND	1.957	ND

Table 5: Continued.

Cook code[a]	$\alpha 1$	$\alpha 2$	$\alpha 3$	$\alpha 4$	$\alpha 5$	$\alpha 6$
TG-4-39	1.6	34	24	5.6	1.4	23
TG-II-82	1.6	2.9	2.8	ND	1	1000
CM-A87	1.62	4.54	14.73	1000	4.61	1000
QH-II-082	1.7	1.8	1.6	ND	6.1	100
JYI-49 (C20H12N3O2F4Br)	1.87	2.38	ND	ND	6.7	3390
LJD-III-15E	1.93	14	19	ND	70.8	1000
SPH-38	2	5.4	10.8	ND	18.5	3000
XHE-I-093	2	7.1	8.9	1107	20	1162
MSA-IV-35	2.1	16	21	ND	995	3000
JYI-19 (C23H23N3O3S)	2.176	205	ND	ND	34	12.7
FLUNITRAZEPAM	2.2	2.5	4.5	ND	2.1	2000
YCT-5	2.2	11.46	16.3	ND	200	10000
TJH-IV-51	2.39	17.4	14.5	ND	316	10000
WYS13 C20H18N2O3	2.442	13	27.5	ND	163	5000
YT-III-25	2.531	5.786	5.691	ND	0.095	ND
XHE-III-14	2.6		10	13	2	7
WYS9 C16H15IN2O2	2.72	22.2	23.1	ND	562	122
JYI-47	2.759	2.282	0.511	ND	0.427	ND
CM-A82a	2.78	8.93	24.51	1000	7.49	1000
TG-4-29	2.8	3.9	2.7	2.1	0.18	3.9
XLi268 C17H13BrN4	2.8145	0.6862	ND	ND	0.6243	ND
JYI-54 (C24H15N3O3F4)	2.89	172	6.7	ND	57	1890
MMB-II-74	3	24.5	41.7	500	125.7	1000
MMB-III-016	3	1.97	2	1074	0.26	211
MMB-III-16	3	1.97	2	1074	0.26	211
QH-II-080b	3	3.7	4.7	ND	24	1000
YCT-7A	3	23.8	30.5	ND	240	10000
JYI-32 (C20H15N3O2BrF)	3.07	4.96	ND	ND	2.92	52.24
Ro15-4513	3.3	2.6	2.5	ND	0.26	3.8
XHE-II-017	3.3	10	7	258	17	294
XLi-JY-DMH ANX3	3.3	0.58	1.9	ND	4.4	5000
MLT-II-18	3.4	11.7	11	ND	225	10000
TJH-V-88	3.41		30	ND	140.9	10000
XLI-2TC	3.442	1.673	44.08	ND	1.121	
WYS15 C22H20N2O2	3.63	2.02	44.3	ND	76.5	5000
CM-A57	3.7	27	40	ND	254	1000
XHE-II-006b	3.7	15	12	1897	144	1000
JYI-60	3.73	1.635	4.3	ND	1.7	5000
RY-008	3.75	7.2	4.14	ND	1.11	44.3
MLT-II-18	3.9	12.2	24.4	ND	210	10000
OMB-18	3.9	1.2	3.4	1733	0.8	5
WY-B-09-1	3.99	8	32	1000	461	2000
SHU-1-19	4	12	7	48	14	84
ZK 93423	4.1	4.2	6	ND	4.5	1000
WY-B-23-2 (WYS11)	4.2	37.7	39	2000	176	69.4
WY-B-23-2 (WYS11)	4.2	37.7	73	ND	176	69.4
WY-B-99-1	4.4	4.5	5.58	2000	47	2000
WY-B-26-2	4.45	44.57	42.66	2000	124	2000
XHE-II-006a	4.7	4.4	20	1876	89	3531

Table 5: Continued.

Cook code[a]	α1	α2	α3	α4	α5	α6
CM-B01	4.8	31	34	1000	286	1000
PWZ-085	4.86	13	8.5	ND	0.55	40
MLT-II-16	5.05	10.41	18.4	ND	260	10000
3 PBC	5.3	52.3	68.8	ND	591	1000
MA-3-PROPOXYL	5.3	52.3	68.8	ND	591	1000
TJH-IV-43	5.42	30.19	48.9	ND	475	10000
DMCM	5.69	8.29	4	ND	1.04	134
DM-139	5.8	ND	169	ND	9.25	325
XHE-II-073A (R ENRICHED)	5.9	11	10	15	1.18	140
MSR-I-032	6.2	18.7	4	ND	3.3	74.9
JYI-70 (C19H13N4F)	6.3	2.1	ND	ND	0.56	5000
XLi343 C20H19ClN2OSi	6.375	17.71	ND	ND	150.5	ND
3 EBC	6.43	25.1	28.2	ND	826	1000
DM-146	6.44	ND	148	ND	4.23	247
DM-215	6.74	ND	7.42	ND	0.293	8.28
ZG69A	6.8	16.3	9.2	ND	0.85	54.6
ZG-69a (Ro15-1310)	6.8	16.3	9.2	ND	0.85	54.6
WY-B-14 (WYS7)	6.84	30	36	2000	108	1000
YT-II	6.932	0.8712	3.518	ND	5.119	ND
SVO-8-67	7	41	26	15	2.3	191
MLT-II-34	7.04	15.95	22.3	ND	158	1000
SPH-195	7.2	168.5	283.5	ND	271	10000
XHE-I-065	7.2	17	18	500	57	500
ZG-234	7.25	22.14	9.84	ND	0.3	5.25
SH-I-04	7.3	6.136	5.1	ND	7.664	ND
XHE-I-038	7.3	5	34	ND	132	1000
XHE-III-13	7.3	ND	7.1	880	1.6	311
WY-B-25	7.6	40	66	2000	263	2000
CM-A49 (R)	7.7	32.5	43	ND	69	1000
SVO-8-14	8	25	8	6.9	0.9	14
TG-4-29	8.3	10.2	6.9	ND	0.4	7.61
XHE-II-002	8.3	18	13	3.9	1.5	11
WY-B-14 (WYS7)	8.5	165	245	ND	1786	5000
XHE-II-011	9	60	39	3233	90	1000
WY-B-27-2	9.19	111	72	2000	449	2000
QH-II-063	9.4	9.3	31	ND	7.7	3000
JC184 C13H9BrN2OS	9.606	10.5	ND	ND	6.709	ND
ZG-208	9.7	11.2	10.9	ND	0.38	4.6
RY-I-31	10	45	19	ND	6	1000
WY-B-23-1	10	33	43	1000	189	2000
RY-098	10.1	22.2	16.5	ND	1.68	100
Hz148 C18H15N3	10.98	5000	ND	ND	256	5000
SVO-8-20	11	40	28	19	8.6	138
XHE-II-073B (S-ENRICHED)	11	17	12	33	2.1	269
SH-I-085	11.08	4.866	13.75	ND	0.24	ND
PWZ-096	11.1	36	16.9	ND	1.07	51.5
ZG-168	11.2	10.7	9.2	ND	0.47	9.4
CM-A77	11.51	51.9	105.16	1000	42.62	1000
WY-B-20	12	39	47	2000	122	3000
ABECARNIL	12.4	15.3	7.5	ND	6	1000

Table 5: Continued.

Cook code[a]	$\alpha1$	$\alpha2$	$\alpha3$	$\alpha4$	$\alpha5$	$\alpha6$
SH-I-89S	12.78	8.562	8.145	ND	3.23	ND
ZG-213	12.8	49.8	30.2	ND	3.5	22.5
EDC-I-071	12.9	83.1	ND	ND	314	5000
MMB-III-14	13	13	6.9	333	1.1	333
DM-173	13.1	ND	38.1	ND	0.78	118
XLI-348	13.56	11.17	1.578	ND	82.05	ND
EDC-I-093	13.6	423	ND	ND	2912	5000
diazepam	14	20	15	ND	11	ND
XLi223 C22H20BrN3O2	14	8.7	18	1000	10	2000
WYSC2 C15H11F3N2O2	14.14	113	170	ND	518	61.2
SH-I-030	14.42	11.04	19.09	ND	1.89	ND
CM-A100	14.49	44.91	123.8	1000	65.31	1000
RY-033	14.8	56	25.3	ND	1.72	22.9
HJ-I-037	15.07	8.127	28.29	ND	0.818	ND
YT-6	15.31	87.8	60.49	ND	1.039	ND
EDC-II-044	15.4	ND	293	ND	323	1000
CM-A58	16	120	184	ND	1000	1012
QH-II-067a	16	31	52	ND	199	3000
CD-214	16.4	48.2	42.5	ND	9.8	168
JYI-06 (C23H23N3O4)	16.5	5.48	5000	ND	12.6	5000
CM-A50 (S)	17	59	88	ND	144	1000
RY-061	17	13	6.7	ND	0.3	31
ZG-224	17.1	33.7	50	ND	2.5	30.7
ZG-63A	17.3	21.6	29.1	ND	0.65	4
DM-II-30 (C20H13N3O2BrF3)	17.6	13.4	28.51	ND	7.8	5000
CM-A64	18	60	116	ND	216	1000
RY-071	19	56	91	ND	7.2	266
WZ-113	19.2	13.2	13.4	ND	11.5	300
YT-III-23	19.83	23.65	19.87	ND	1.105	ND
CM-E09b	20	22	19	55	0.45	69
MMB-II-90	20	24	5.7	9	0.25	36

[a]Affinity of compounds at $GABA_A$/BzR recombinant subtypes was measured by competition for [^{3}H]flunitrazepam or [^{3}H] Ro15-4513 binding to HEK cell membranes expressing human receptors of compositions $\alpha1\beta3\gamma2$, $\alpha2\beta3\gamma2$, $\alpha3\beta3\gamma2$, $\alpha4\beta3\gamma2$, $\alpha5\beta3\gamma2$, and $\alpha6\beta3\gamma2$ [139]. Data represent the average of at least three determinations with a SEM of ±5%. The structures of these ligands are in the Ph.D. thesis of Clayton (2011) [22] and Supporting Information.

13. The $\alpha2\beta3\gamma2$ Receptor Subtype

See Table 6 and Figures 36 and 37.

14. The $\alpha3\beta3\gamma2$ Receptor Subtype

See Table 7 and Figures 38 and 39.

15. The $\alpha4\beta3\gamma2$ Receptor Subtype

See Table 8 and Figures 40 and 41.

16. The $\alpha5\beta3\gamma2$ Receptor Subtype

The multiple volume contours displayed in Figures 34–47 were created using the mvolume function (multiple volume contour function) in Sybyl and compounds with binding affinity at the receptor less than or equal to 20 nM. To create the overlays, first, the display (dsp) and contour (cnt) files were created for the $\alpha5\beta3\gamma2$ receptor subtype and the $\alpha1\beta3\gamma2$ receptor subtype by overlaying the compounds for each of these receptors (see Table 9 and Figures 42–45). Using the mvolume function, a logical expression was entered to create the surfaces making up the union as well as the included volume for each receptor subtype itself. It is clear from the

Table 6: Ligands with potent affinity for $\alpha 2$; ligands bound with K_i values <20 nM at this subtype. The structures of these ligands are in the Ph.D. thesis of Clayton (2011) [22].

Cook code[a]	$\alpha 1$	$\alpha 2$	$\alpha 3$	$\alpha 4$	$\alpha 5$	$\alpha 6$
QH-II-092	0.07	0.03	0.04	ND	0.17	ND
SH-TSC-2 (BCCT)	0.03	0.0419	0.035	ND	69.32	ND
QH-II-085	0.08	0.06	0.02	ND	0.08	ND
XLI-286	0.051	0.064	0.118	ND	0.684	ND
JYI-57	0.076	0.076	0.131	ND	0.036	ND
QH-II-090 (CGS-8216)	0.05	0.08	0.12	ND	0.25	17
QH-II-077	0.06	0.08	0.05	ND	0.12	4
PWZ-007A	0.11	0.1	0.09	ND	0.2	10
JYI-42	0.257	0.146	0.278	ND	0.256	ND
PWZ-0071	0.23	0.17	0.12	ND	0.44	17.31
SH-I-048A	0.774	0.1723	0.383	ND	0.11	ND
XHE-II-024	0.09	0.18	0.32	14	0.24	11
QH-II-075	0.18	0.21	0.25	ND	1.3	40
XLi-JY-DMH ANX3	3.3	0.58	1.9	ND	4.4	5000
alprazolam	0.8	0.59	1.43	ND	1.54	10000
YT-5	0.421	0.6034	36.06	ND	1.695	ND
BRETAZENIL	0.35	0.64	0.2	ND	0.5	12.7
XLi268 C17H13BrN4	2.8145	0.6862	ND	ND	0.6243	ND
WY-B-15	0.92	0.83	0.58	2080	4.42	646
YT-II	6.932	0.8712	3.518	ND	5.119	
Ro15-1788	0.8	0.9	1.05	ND	0.6	148
XLi351 C21H21ClN2OSi	1.507	0.967	ND	ND	1.985	ND
WY-TSC-4 (WYS8)	0.007	0.99	1.63	ND	51.04	ND
XLi352 C18H13ClN2O	1.56	0.991	ND	ND	1.957	ND
DM-II-90 (C17H12N4BrCl)	0.505	1	0.63	ND	0.37	5000
JYI-64 (C17H12N4FBr)	0.305	1.111	0.62	ND	0.87	5000
XLi350 C17H11ClN2O	1.224	1.188	ND	ND	2.9	ND
SPH-121	0.14	1.19	1.72	ND	4	479
MLT-I-70	1.1	1.2	1.1	ND	40.3	1000
OMB-18	3.9	1.2	3.4	1733	0.8	5
6-PBC	0.49	1.21	2.2	ND	2.39	1343
YT-III-271	32.54	1.26	2.35	ND	103	ND
PWZ-009A1	1.34	1.31	1.26	ND	0.84	2.03
DM-II-72 (C15H10N20BrCl)	5000	1.37	ND	ND	2.02	5000
JYI-60 (C17H11N2OF)	3.73	1.635	4.3	ND	1.7	5000
XLI-2TC	3.442	1.673	44.08	ND	1.121	ND
QH-II-082	1.7	1.8	1.6	ND	6.1	100
TC-YT-II-76	101.1	1.897	5.816	ND	11.99	ND
MMB-III-016	3	1.97	2	1074	0.26	211
MMB-III-16	3	1.97	2	1074	0.26	211
XHE-III-06a	1	2	1	5	1.8	37
XHE-III-04	1.2	2	1.1	219	0.4	500
WYS15 C22H20N2O2	3.63	2.02	44.3	ND	76.5	5000
FG8205	0.4	2.08	1.16	ND	1.54	227
JYI-70 (C19H13N4F)	6.3	2.1	ND	ND	0.56	5000
JYI-47	2.759	2.282	0.511	ND	0.427	ND
JYI-49 (C20H12N3O2F4Br)	1.87	2.38	ND	ND	6.7	3390
FLUNITRAZEPAM	2.2	2.5	4.5	ND	2.1	2000
JYI-59 (C22H13N3O2F4)	1.08	2.6	11.82	ND	11.5	5000

Table 6: Continued.

Cook code[a]	α1	α2	α3	α4	α5	α6
Ro15-4513	3.3	2.6	2.5	ND	0.26	3.8
SPH-165	0.63	2.79	4.85	ND	10.4	1150
YT-II-76	95.34	2.797	0.056	ND	0.04	ND
TG-II-82	1.6	2.9	2.8	ND	1	1000
QH-II-080b	3	3.7	4.7	ND	24	1000
TG-4-29	2.8	3.9	2.7	2.1	0.18	3.9
PS-1-34B C20H17N4BrO	ND	4.198	3.928	ND	ND	ND
ZK 93423	4.1	4.2	6	ND	4.5	1000
XHE-II-006a	4.7	4.4	20	1876	89	3531
WY-B-99-1	4.4	4.5	5.58	2000	47	2000
CM-A87	1.62	4.54	14.73	1000	4.61	1000
OMB-19	22	4.6	20	3333	3.5	40
SH-I-085	11.08	4.866	13.75	ND	0.24	ND
BCCE	1.2	4.9	5.7	ND	26.8	2700
JYI-32 (C20H15N3O2BrF)	3.07	4.96	ND	ND	2.92	52.24
XHE-I-038	7.3	5	34	ND	132	1000
SVO-8-30	1.1	5.3	5.3	2.8	0.6	15
SPH-38	2	5.4	10.8	ND	18.5	3000
WYSC1 C16H16N2O2	1.094	5.44	12.3	ND	69.8	21.2
JYI-06 (C23H23N3O4)	16.5	5.48	5000	ND	12.6	5000
XHE-III-49	1.3	5.5	4.2	38.7	11.3	85.1
YT-III-25	2.531	5.786	5.691	ND	0.095	ND
SH-I-04	7.3	6.136	5.1	ND	7.664	ND
XHE-I-093	2	7.1	8.9	1107	20	1162
RY-008	3.75	7.2	4.14	ND	1.11	44.3
DMH-D-053 (C43H30N6O4)	236	7.4	272	5000	194.2	5000
WY-B-09-1	3.99	8	32	1000	461	2000
HJ-I-037	15.07	8.127	28.29	ND	0.818	ND
DMCM	5.69	8.29	4	ND	1.04	134
SH-I-89S	12.78	8.562	8.145	ND	3.23	ND
XLi223 C22H20BrN3O2	14	8.7	18	1000	10	2000
CM-A82a	2.78	8.93	24.51	1000	7.49	1000
QH-II-063	9.4	9.3	31	ND	7.7	3000
	9.4	9.3	31	ND	7.7	3000
XHE-II-017	3.3	10	7	258	17	294
TG-4-29	8.3	10.2	6.9	ND	0.4	7.61
MLT-II-16	5.05	10.41	18.4	ND	260	10000
JC184 C13H9BrN2OS	9.606	10.5	ND	ND	6.709	ND
ZG-168	11.2	10.7	9.2	ND	0.47	9.4
XHE-II-073A (R ENRICHED)	5.9	11	10	15	1.18	140
XLI-8TC	21.52	11.01	2.155	ND	4.059	ND
SH-I-030	14.42	11.04	19.09	ND	1.89	ND
XLI-348	13.56	11.17	1.578	ND	82.05	ND
ZG-208	9.7	11.2	10.9	ND	0.38	4.6
YT-TC-3	141.4	11.43	118.1	ND	29.22	ND
YCT-5	2.2	11.46	16.3	ND	200	10000
MLT-II-18	3.4	11.7	11	ND	225	10000
XHE-II-O53-ACID	50.35	11.8	44	ND	5.9	5000
SHU-1-19	4	12	7	48	14	84
RY-067	21	12	10	ND	0.37	42

Table 6: Continued.

Cook code[a]	$\alpha1$	$\alpha2$	$\alpha3$	$\alpha4$	$\alpha5$	$\alpha6$
DM-III-01 (C18H12N3O2Br)	5000	12	ND	ND	4.73	5000
MLT-II-18	3.9	12.2	24.4	ND	210	10000
SH-053-2′F	21.99	12.34	34.9	ND	0.671	ND
WYS13 C20H18N2O3	2.442	13	27.5	ND	163	5000
PWZ-085	4.86	13	8.5	ND	0.55	40
MMB-III-14	13	13	6.9	333	1.1	333
RY-061	17	13	6.7	ND	0.3	31
WZ-113	19.2	13.2	13.4	ND	11.5	300
YT-II-83	32.74	13.22	24.1	ND	3.548	ND
DM-II-30 (C20H13N3O2BrF3)	17.6	13.4	28.51	ND	7.8	5000
LJD-III-15E	1.93	14	19	ND	70.8	1000
YT-III-272	295.9	14.98	10.77	ND	103.3	ND
BCCt	0.72	15	18.9	ND	110.8	5000
XHE-II-006b	3.7	15	12	1897	144	1000
ABECARNIL	12.4	15.3	7.5	ND	6	1000
MLT-II-34	7.04	15.95	22.3	ND	158	1000
MSA-IV-35	2.1	16	21	ND	995	3000
JYI-04 (C21H23N3O3)	28.3	16	ND	ND	0.51	1.57
PS-1-35 C23H22N5OBr	ND	16.03	24.41	ND	ND	ND
ZG69A	6.8	16.3	9.2	ND	0.85	54.6
ZG-69a (Ro15-1310)	6.8	16.3	9.2	ND	0.85	54.6
YT-III-42	382.9	16.83	44.04	ND	9.77	ND
XHE-I-065	7.2	17	18	500	57	500
XHE-II-073B (S-ENRICHED)	11	17	12	33	2.1	269
TJH-IV-51	2.39	17.4	14.5	ND	316	10000
SH-I-047	1710	17.52	1222	ND	1519	ND
XLi343 C20H19ClN2OSi	6.375	17.71	ND	ND	150.5	ND
XHE-II-002	8.3	18	13	3.9	1.5	11
YT-III-38	1461	18.21	14.63	ND	3999	
JYI-72 (C22H21N4SiF)	48.5	18.5	ND	ND	11.5	5000
MSR-I-032	6.2	18.7	4	ND	3.3	74.9
JC208 C15H10N2OS	22.42	18.89	ND	ND	5.039	ND
diazepam	14	20	15	ND	11	ND

[a]Affinity of compounds at $GABA_A$/BzR recombinant subtypes was measured by competition for [^{3}H]flunitrazepam or [^{3}H] Ro15-4513 binding to HEK cell membranes expressing human receptors of compositions $\alpha1\beta3\gamma2$, $\alpha2\beta3\gamma2$, $\alpha3\beta3\gamma2$, $\alpha4\beta3\gamma2$, $\alpha5\beta3\gamma2$, and $\alpha6\beta3\gamma2$ [22, 139]. Data represent the average of at least three determinations with a SEM of ±5%. ND: not determined.

included volume overlay that the L_2 pocket is deeper for the $\alpha5$ subtype, as determined previously [13, 21–23, 110, 119]. The new L_4 pocket can be distinguished as the new yellow region of the $\alpha5\beta3\gamma2$ subtype which is due to recently designed R-isomers by Huang [135], Poe and Li.

17. The $\alpha6\beta3\gamma2$ Receptor Subtype

See Table 10 and Figures 46 and 47.

18. Updates to the Previous Model

In addition to the newly discovered L_4 pocket, the updated library of binding affinity led to two specific updates in the previous model (Figure 48).

19. QSAR

A nontraditional quantitative structure activity relationship (QSAR) approach was executed to observe steric and electrostatic preferences for each receptor subtype. A subset of the compounds used in each subtype pharmacophore/receptor model were chosen with a good cross section of scaffold variety. The compounds used in the COMFA maps are the imidazobenzodiazepines published previously [110, 137] and additionally alternative scaffolds which bound with <20 nM at the respective subtype [22].

The interest here was in creation of steric and electrostatic maps of the comparative molecular field analyses (COMFA) created from molecular spreadsheets. A variety of compounds selective for each subtype were selected and placed into a dataset used to build the CoMFA models. Activities (K_i

Table 7: Ligands with potent affinity for $\alpha 3$; ligands bound with K_i values <20 nM at this subtype. The structures of these ligands are in the Ph.D. thesis of Clayton (2011) [22].

Cook code[a]	$\alpha 1$	$\alpha 2$	$\alpha 3$	$\alpha 4$	$\alpha 5$	$\alpha 6$
QH-II-085	0.08	0.06	0.02	ND	0.08	ND
SH-TSC-2 (BCCT)	0.03	0.0419	0.035	ND	69.32	ND
QH-II-092	0.07	0.03	0.04	ND	0.17	ND
QH-II-077	0.06	0.08	0.05	ND	0.12	4
YT-II-76	95.34	2.797	0.056	ND	0.04	ND
PWZ-007A	0.11	0.1	0.09	ND	0.2	10
XLI-286	0.051	0.064	0.118	ND	0.684	ND
QH-II-090 (CGS-8216)	0.05	0.08	0.12	ND	0.25	17
PWZ-0071	0.23	0.17	0.12	ND	0.44	17.31
JYI-57	0.076	0.076	0.131	ND	0.036	ND
BRETAZENIL	0.35	0.64	0.2	ND	0.5	12.7
PZII-028	0.2	ND	0.2	ND	0.32	1.9
QH-II-075	0.18	0.21	0.25	ND	1.3	40
JYI-42	0.257	0.146	0.278	ND	0.256	ND
XHE-II-024	0.09	0.18	0.32	14	0.24	11
SH-I-048A	0.774	0.1723	0.383	ND	0.11	ND
JYI-55	41.39	ND	0.504	ND	24.75	ND
JYI-47	2.759	2.282	0.511	ND	0.427	ND
DM-239	1.5	ND	0.53	ND	0.14	6.89
WY-B-15	0.92	0.83	0.58	2080	4.42	646
JYI-64 (C17H12N4FBr)	0.305	1.111	0.62	ND	0.87	5000
DM-II-90 (C17H12N4BrCl)	0.505	1	0.63	ND	0.37	5000
QH-146	0.49	ND	0.76	ND	7.7	10000
PZII-029	0.34	ND	0.79	ND	0.52	10
WYS19 C26H32N2O4Si	ND	ND	0.89	ND	ND	ND
XHE-III-06a	1	2	1	5	1.8	37
Ro15-1788	0.8	0.9	1.05	ND	0.6	148
MLT-I-70	1.1	1.2	1.1	ND	40.3	1000
XHE-III-04	1.2	2	1.1	219	0.4	500
FG8205	0.4	2.08	1.16	ND	1.54	227
PWZ-009A1	1.34	1.31	1.26	ND	0.84	2.03
alprazolam	0.8	0.59	1.43	ND	1.54	10000
XLI-348	13.56	11.17	1.578	ND	82.05	ND
QH-II-082	1.7	1.8	1.6	ND	6.1	100
WY-TSC-4 (WYS8)	0.007	0.99	1.63	ND	51.04	ND
SPH-121	0.14	1.19	1.72	ND	4	479
XLi-JY-DMH ANX3	3.3	0.58	1.9	ND	4.4	5000
MMB-III-016	3	1.97	2	1074	0.26	211
MMB-III-16	3	1.97	2	1074	0.26	211
XLI-8TC	21.52	11.01	2.155	ND	4.059	ND
6-PBC	0.49	1.21	2.2	ND	2.39	1343
YT-III-271	32.54	1.26	2.35	ND	103	ND
Ro15-4513	3.3	2.6	2.5	ND	0.26	3.8
TG-4-29	2.8	3.9	2.7	2.1	0.18	3.9
TG-II-82	1.6	2.9	2.8	ND	1	1000
OMB-18	3.9	1.2	3.4	1733	0.8	5
YT-II	6.932	0.8712	3.518	ND	5.119	ND

Table 7: Continued.

Cook code[a]	α1	α2	α3	α4	α5	α6
PS-1-34B C20H17N4BrO	ND	4.198	3.928	ND	ND	ND
DMCM	5.69	8.29	4	ND	1.04	134
MSR-I-032	6.2	18.7	4	ND	3.3	74.9
RY-008	3.75	7.2	4.14	ND	1.11	44.3
XHE-III-49	1.3	5.5	4.2	38.7	11.3	85.1
JYI-60 (C17H11N2OF)	3.73	1.635	4.3	ND	1.7	5000
FLUNITRAZEPAM	2.2	2.5	4.5	ND	2.1	2000
XLI-317	60.24	24.05	4.562	ND	0.295	ND
QH-II-080b	3	3.7	4.7	ND	24	1000
SPH-165	0.63	2.79	4.85	ND	10.4	1150
SH-I-04	7.3	6.136	5.1	ND	7.664	ND
SVO-8-30	1.1	5.3	5.3	2.8	0.6	15
WY-B-99-1	4.4	4.5	5.58	2000	47	2000
YT-III-25	2.531	5.786	5.691	ND	0.095	ND
BCCE	1.2	4.9	5.7	ND	26.8	2700
MMB-II-90	20	24	5.7	9	0.25	36
TC-YT-II-76	101.1	1.897	5.816	ND	11.99	ND
ZK 93423	4.1	4.2	6	ND	4.5	1000
RY-061	17	13	6.7	ND	0.3	31
JYI-54 (C24H15N3O3F4)	2.89	172	6.7	ND	57	1890
TG-4-29	8.3	10.2	6.9	ND	0.4	7.61
MMB-III-14	13	13	6.9	333	1.1	333
XHE-II-017	3.3	10	7	258	17	294
SHU-1-19	4	12	7	48	14	84
XHE-III-13	7.3	ND	7.1	880	1.6	311
DM-215	6.74	ND	7.42	ND	0.293	8.28
ABECARNIL	12.4	15.3	7.5	ND	6	1000
SVO-8-14	8	25	8	6.9	0.9	14
XHE-III-24	0.25	ND	8	222	10	328
SH-I-89S	12.78	8.562	8.145	ND	3.23	ND
PWZ-085	4.86	13	8.5	ND	0.55	40
XHE-I-093	2	7.1	8.9	1107	20	1162
ZG-168	11.2	10.7	9.2	ND	0.47	9.4
ZG69A	6.8	16.3	9.2	ND	0.85	54.6
ZG-69a (Ro15-1310)	6.8	16.3	9.2	ND	0.85	54.6
ZG-234	7.25	22.14	9.84	ND	0.3	5.25
XHE-II-073A (R ENRICHED)	5.9	11	10	15	1.18	140
RY-067	21	12	10	ND	0.37	42
XHE-III-14	2.6	ND	10	13	2	7
YT-III-272	295.9	14.98	10.77	ND	103.3	ND
SPH-38	2	5.4	10.8	ND	18.5	3000
ZG-208	9.7	11.2	10.9	ND	0.38	4.6
MLT-II-18	3.4	11.7	11	ND	225	10000
DM-II-33 (C20H13N3O2BrCl3)	88.6	85	11.6	ND	26.2	5000
JYI-59 (C22H13N3O2F4)	1.08	2.6	11.82	ND	11.5	5000
XHE-II-006b	3.7	15	12	1897	144	1000
XHE-II-073B (S-ENRICHED)	11	17	12	33	2.1	269
CM-B44 (ss)	32	43	12	379	4.3	485

Table 7: Continued.

Cook code[a]	α1	α2	α3	α4	α5	α6
WYSC1 C16H16N2O2	1.094	5.44	12.3	ND	69.8	21.2
JYI-48	75.59	90.68	12.78	ND	31.28	ND
XHE-II-002	8.3	18	13	3.9	1.5	11
RY-076	26	27	13	ND	0.7	22
WZ-113	19.2	13.2	13.4	ND	11.5	300
SH-I-085	11.08	4.866	13.75	ND	0.24	ND
CM-E10	23	26	14	215	0.51	96
TJH-IV-51	2.39	17.4	14.5	ND	316	10000
YT-III-38	1461	18.21	14.63	ND	3999	ND
CM-A87	1.62	4.54	14.73	1000	4.61	1000
diazepam	14	20	15	ND	11	ND
RY-053	49	29	15	ND	1	46
YCT-5	2.2	11.46	16.3	ND	200	10000
RY-098	10.1	22.2	16.5	ND	1.68	100
PWZ-096	11.1	36	16.9	ND	1.07	51.5
XLi223 C22H20BrN3O2	14	8.7	18	1000	10	2000
XHE-I-065	7.2	17	18	500	57	500
SH-I-02B	29.82	1315	18	ND	74.05	ND
MLT-II-16	5.05	10.41	18.4	ND	260	10000
RY-024 C19H19N3O3	26.9	26.3	18.7	ND	0.4	5.1
BCCt	0.72	15	18.9	ND	110.8	5000
LJD-III-15E	1.93	14	19	ND	70.8	1000
CM-E09b	20	22	19	55	0.45	69
RY-I-31	10	45	19	ND	6	1000
SH-I-030	14.42	11.04	19.09	ND	1.89	ND
YT-III-23	19.83	23.65	19.87	ND	1.105	ND
XHE-II-006a	4.7	4.4	20	1876	89	3531
OMB-19	22	4.6	20	3333	3.5	40
XHE-III-06b	32	33	20	299	28.6	740

[a]Affinity of compounds at $GABA_A$/BzR recombinant subtypes was measured by competition for [^{3}H]flunitrazepam or [^{3}H] Ro15-4513 binding to HEK cell membranes expressing human receptors of compositions $\alpha1\beta3\gamma2$, $\alpha2\beta3\gamma2$, $\alpha3\beta3\gamma2$, $\alpha4\beta3\gamma2$, $\alpha5\beta3\gamma2$, and $\alpha6\beta3\gamma2$ [22, 139]. Data represent the average of at least three determinations with a SEM of ±5%. ND: not determined.

values) were converted to logarithmic units for this study. A CoMFA descriptor set was created based on the –log (K_i) of over 70 structures. The goal was to derive an alternative three-dimensional shape of the receptor using biological activity of the most selective compounds. Structures were determined by crystal structure where available or by calculation. Charges were provided based on the Gasteiger-Huckel model. Conformations were kept consistent based on previous studies of low energy conformations [110]. It should be noted that this was not a traditional QSAR study as nonselective compounds were excluded. Therefore, K_i values did not cross 3 log units. This was acceptable since the goal was not to create a predictive QSAR predictive algorithm, rather a map of the receptor based on sterics and electrostatics. Hydrogen acceptor radii were set to 3.0 and the hydrogen donor radii were set to 2.6 based on recommendations from Certara (Tripos). Analyses were executed using PLS (partial least squares). The details of modeling will be further discussed in the SI.

For each of the following QSAR models (Figures 49–64), green areas represent desirable steric bulk and yellow represents undesirable steric bulk. Positive electrostatic contributions are represented by blue and negative electrostatic contributions are represented by red.

20. The $\alpha1\beta3\gamma2$ Receptor Subtype

See Figures 49–52.

21. The $\alpha2\beta3\gamma2$ Receptor Subtype

See Figures 53–56.

Table 8: Ligands with potent affinity for $\alpha 4$; ligands bound with K_i values <20 nM at this subtype. The structures of these ligands are in the Ph.D. thesis of Clayton (2011) [22].

Cook code[a]	$\alpha 1$	$\alpha 2$	$\alpha 3$	$\alpha 4$	$\alpha 5$	$\alpha 6$
CM-D45 C19H21N3O4	90.5	65.5	30.3	0.15	1.65	0.23
CM-D44	34.3	56.3	20.7	0.33	0.57	0.92
XHE-III-74	77	105	38	0.42	2.2	5.8
TG-4-29	2.8	3.9	2.7	2.1	0.18	3.9
SVO-8-30	1.1	5.3	5.3	2.8	0.6	15
XHE-II-002	8.3	18	13	3.9	1.5	11
XHE-III-06a	1	2	1	5	1.8	37
RY-080 C17H15N3O3	28.4	21.4	25.8	5.3	0.49	28.8
TG-4-39	1.6	34	24	5.6	1.4	23
SVO-8-14	8	25	8	6.9	0.9	14
RY-023 C22H27N3O3Si	197	142.6	255	7.8	2.61	58.6
MMB-II-90	20	24	5.7	9	0.25	36
XHE-III-14	2.6		10	13	2	7
XHE-II-024	0.09	0.18	0.32	14	0.24	11
XHE-II-073A (R ENRICHED)	5.9	11	10	15	1.18	140
SVO-8-67	7	41	26	15	2.3	191
CM-B3li (ss)	90	184	78	18	4.9	121
SVO-8-20	11	40	28	19	8.6	138

[a] Affinity of compounds at $GABA_A$/BzR recombinant subtypes was measured by competition for [^{3}H]flunitrazepam or [^{3}H] Ro15-4513 binding to HEK cell membranes expressing human receptors of compositions $\alpha 1\beta 3\gamma 2$, $\alpha 2\beta 3\gamma 2$, $\alpha 3\beta 3\gamma 2$, $\alpha 4\beta 3\gamma 2$, $\alpha 5\beta 3\gamma 2$, and $\alpha 6\beta 3\gamma 2$ [22, 139]. Data represent the average of at least three determinations with a SEM of ±5%. ND: not determined.

22. The $\alpha 3\beta 3\gamma 2$ Receptor Subtype

See Figures 57–60.

23. The $\alpha 5\beta 3\gamma 2$ Receptor Subtype

From the CoMFA maps several observations (Figure 65) can be made. The yellow steric regions near L_3 in the $\alpha 5\beta 3\gamma 2$ map are unique. This illustrated that, in general, benzodiazepines lacking a pendant phenyl are more suited to targeting the $\alpha 5$ subtype. The L_{Di} region of the $\alpha 1$ subtype is most tolerable for compounds with steric interactions in this location while the $\alpha 3$ subtype receptor compounds prefer no steric interaction in this location. Negative electrostatics are most preferred by the L_3 pocket of the $\alpha 2$ and $\alpha 5$ receptors. In general, the $\alpha 1$ subtype receptor prefers molecules without a dipole. It should be noted that none of the analogs are ionic in nature and the charges for this model were provided by the Gasteiger-Huckel model. For this reason more emphasis is placed on the steric relationships which exclude interactions in the pharmacophores. In the future a QSAR study which includes nonbinding benzodiazepines in the data set along with activity data will permit the creation of a predictive algorithm which will be very useful in lead targeting (see Figures 61–65).

24. Conclusion

Benzodiazepines, β-carbolines, and other classes of compounds readily target the $GABA_A$ receptors. The difficulty is finding subtype selective ligands, since there is no crystal structure of the Bz/$GABA_A$-ergic site itself, just one composed of five beta-subunits which has no Bz site to date. The $\alpha 5$-BzR/$GABA_A$ subunit has recently been shown to be important in the search to treat numerous cognition-based illnesses including Alzheimer's, schizophrenia, bipolar, and depression, as well as more recently a bronchodilator, potentially important in the treatment of asthma. As an inverse agonist, PWZ-029 was able to counteract the memory-impairing effects of scopolamine, a muscarinic antagonist, in both object recognition tests and object retrieval tests in rodents, and was active in primates, as well as samaritan Alzheimer's rats. The implications of these tests point to a use as a possible treatment for Alzheimer's disease. The docking of PWZ-029 in the $\alpha 5\gamma 2$ $GABA_A$R-subunit details the interactions between the pharmacophore/receptor model binding site and this important negative allosteric modulator. Furthermore, $\alpha 5$-BzR/$GABA_A$ positive allosteric modulator, SH-053-2′F-R-CH_3, was shown to reverse deleterious effects in the MAM-model of schizophrenia. The recent discovery of $\alpha 5$-$GABA_A$R in airway smooth muscle by Emala et al. has also lead to the testing of SH-053-2′F-R-CH_3 as a bronchodilator. This SH-053-2′F-R-CH_3 was found to be effective in relaxing preconstricted airway smooth muscle, as well as attenuating calcium-ion entry through the plasma membrane. In addition, XLi-093 (an $\alpha 5$ receptor antagonist), a potently binding $\alpha 5$-subtype selective bivalent ligand, has been shown to inhibit the $\alpha 5$-cognition deficits effected by diazepam and is a very good $\alpha 5$ benzodiazepine receptor site antagonist. It has also been shown to reverse the effects of $\alpha 5$ PAMs and NAMs in both rodent and primate models. These findings led to the exploration of the $\alpha 5$-binding pocket in the Milwaukee-based pharmacophore.

New features have been introduced to the unified pharmacophore/receptor model based on many substance classes that act at the diazepam sensitive and diazepam insensitive BzR binding sites of $GABA_A$ receptors. The major new feature identified for the $\alpha 5\beta 3\gamma 2$ receptor was a new L_4 pocket which was found by using pendant 6-phenyl benzodiazepines with a R-CH_3 at the prochiral center at C4. Further enhancement of potency was achieved by addition of 2′-F or 2′-N substituent in the pendant phenyl ring at C-6. While these changes have led to enhanced subtype selective ligands, the overall development guided by this pharmacophore model described here has led to new agents with varying, fascinating pharmacological profiles, ranging from use in cognition-based diseases such as Alzheimer's and schizophrenia, to use as a bronchodilator. This research on updating the Milwaukee-based pharmacophore/receptor model can be used in the rational design for improving the selectivity of $\alpha 5$ ligands. As the library of compounds increases, the data which follows can then be further evaluated and can lead to more insight to the identification of the possible roles each individual residue may have with the binding pocket.

Table 9: Ligands with potent affinity for $\alpha 5$; ligands bound with K_i values <20 nM at this subtype. The structures of these ligands are in the Ph.D. thesis of Clayton (2011) [22].

Cook code[a]	$\alpha 1$	$\alpha 2$	$\alpha 3$	$\alpha 4$	$\alpha 5$	$\alpha 6$
JYI-57	0.076	0.076	0.131	ND	0.036	ND
YT-II-76	95.34	2.797	0.056	ND	0.04	ND
QH-II-085	0.08	0.06	0.02	ND	0.08	ND
YT-III-25	2.531	5.786	5.691	ND	0.095	ND
SH-I-048A	0.774	0.1723	0.383	ND	0.11	ND
QH-II-077	0.06	0.08	0.05	ND	0.12	4
DM-239	1.5	ND	0.53	ND	0.14	6.89
QH-II-092	0.07	0.03	0.04	ND	0.17	ND
TG-4-29	2.8	3.9	2.7	2.1	0.18	3.9
SH-I-75	1487	989.9	773	ND	0.1825	ND
PWZ-007A	0.11	0.1	0.09	ND	0.2	10
XHE-II-024	0.09	0.18	0.32	14	0.24	11
SH-I-085	11.08	4.866	13.75	ND	0.24	ND
MMB-II-90	20	24	5.7	9	0.25	36
QH-II-090 (CGS-8216)	0.05	0.08	0.12	ND	0.25	17
JYI-42	0.257	0.146	0.278	ND	0.256	ND
MMB-III-016	3	1.97	2	1074	0.26	211
MMB-III-16	3	1.97	2	1074	0.26	211
Ro15-4513	3.3	2.6	2.5	ND	0.26	3.8
DM-215	6.74	ND	7.42	ND	0.293	8.28
XLI-317	60.24	24.05	4.562	ND	0.295	ND
RY-061	17	13	6.7	ND	0.3	31
ZG-234	7.25	22.14	9.84	ND	0.3	5.25
PZII-028	0.2	ND	0.2	ND	0.32	1.9
RY-067	21	12	10	ND	0.37	42
DM-II-90 (C17H12N4BrCl)	0.505	1	0.63	ND	0.37	5000
ZG-208	9.7	11.2	10.9	ND	0.38	4.6
XHE-III-04	1.2	2	1.1	219	0.4	500
TG-4-29	8.3	10.2	6.9	ND	0.4	7.61
RY-024 C19H19N3O3	26.9	26.3	18.7	ND	0.4	5.1
JYI-47	2.759	2.282	0.511	ND	0.427	ND
PWZ-0071	0.23	0.17	0.12	ND	0.44	17.31
CM-E09b	20	22	19	55	0.45	69
ZG-168	11.2	10.7	9.2	ND	0.47	9.4
RY-080 C17H15N3O3	28.4	21.4	25.8	5.3	0.49	28.8
BRETAZENIL	0.35	0.64	0.2	ND	0.5	12.7
CM-E10	23	26	14	215	0.51	96
JYI-04 (C21H23N3O3)	28.3	16	ND	ND	0.51	1.57
PZII-029	0.34	ND	0.79	ND	0.52	10
PWZ-085	4.86	13	8.5	ND	0.55	40
JYI-70 (C19H13N4F)	6.3	2.1	ND	ND	0.56	5000
CM-D44	34.3	56.3	20.7	0.33	0.57	0.92
SVO-8-30	1.1	5.3	5.3	2.8	0.6	15
Ro15-1788	0.8	0.9	1.05	ND	0.6	148
XLi268 C17H13BrN4	2.8145	0.6862	ND	ND	0.6243	ND
ZG-63A	17.3	21.6	29.1	ND	0.65	4
SH-053-2′F	21.99	12.34	34.9	ND	0.671	ND
XLI-286	0.051	0.064	0.118	ND	0.684	ND
SH-I-S66	22.93	30.36	55.26	ND	0.69	ND

Table 9: Continued.

Cook code[a]	α1	α2	α3	α4	α5	α6
RY-076	26	27	13	ND	0.7	22
DM-173	13.1	ND	38.1	ND	0.78	118
OMB-18	3.9	1.2	3.4	1733	0.8	5
HJ-I-037	15.07	8.127	28.29	ND	0.818	ND
PWZ-009A1	1.34	1.31	1.26	ND	0.84	2.03
ZG69A	6.8	16.3	9.2	ND	0.85	54.6
ZG-69a (Ro15-1310)	6.8	16.3	9.2	ND	0.85	54.6
JYI-64 (C17H12N4FBr)	0.305	1.111	0.62	ND	0.87	5000
SVO-8-14	8	25	8	6.9	0.9	14
JYI-03 (C21H21N3O3)	185.4	107	ND	ND	0.954	3.34
TG-II-82	1.6	2.9	2.8	ND	1	1000
RY-053	49	29	15	ND	1	46
YT-6	15.31	87.8	60.49	ND	1.039	ND
DMCM	5.69	8.29	4	ND	1.04	134
PWZ-096	11.1	36	16.9	ND	1.07	51.5
MMB-III-14	13	13	6.9	333	1.1	333
YT-III-23	19.83	23.65	19.87	ND	1.105	ND
RY-008	3.75	7.2	4.14	ND	1.11	44.3
XLI-2TC	3.442	1.673	44.08	ND	1.121	ND
XHE-II-073A (R ENRICHED)	5.9	11	10	15	1.18	140
QH-II-075	0.18	0.21	0.25	ND	1.3	40
RY-054	59	44	27	ND	1.3	126
TG-4-39	1.6	34	24	5.6	1.4	23
XHE-II-002	8.3	18	13	3.9	1.5	11
RY-031 (RY-10)	20.4	27	26.1	ND	1.5	176
FG8205	0.4	2.08	1.16	ND	1.54	227
alprazolam	0.8	0.59	1.43	ND	1.54	1000
XHE-III-13	7.3	ND	7.1	880	1.6	311
CM-D45 C19H21N3O4	90.5	65.5	30.3	0.15	1.65	0.23
RY-098	10.1	22.2	16.5	ND	1.68	100
YT-5	0.421	0.6034	36.06	ND	1.695	ND
JYI-60 (C17H11N2OF)	3.73	1.635	4.3	ND	1.7	5000
RY-033	14.8	56	25.3	ND	1.72	22.9
XHE-III-06a	1	2	1	5	1.8	37
SH-I-030	14.42	11.04	19.09	ND	1.89	ND
XLi352 C18H13ClN2O	1.56	0.991	ND	ND	1.957	ND
XLi351 C21H21ClN2OSi	1.507	0.967	ND	ND	1.985	ND
XHE-III-14	2.6	ND	10	13	2	7
DM-II-72 (C15H10N20BrCl)	5000	1.37	ND	ND	2.02	5000
XHE-II-073B (S-ENRICHED)	11	17	12	33	2.1	269
FLUNITRAZEPAM	2.2	2.5	4.5	ND	2.1	2000
XHE-III-74	77	105	38	0.42	2.2	5.8
SVO-8-67	7	41	26	15	2.3	191
6-PBC	0.49	1.21	2.2	ND	2.39	1343
RY-058	86	40	85	ND	2.4	150
ZG-224	17.1	33.7	50	ND	2.5	31.7
RY-066	83	60	48	ND	2.6	180
RY-023 C22H27N3O3Si	197	142.6	255	7.8	2.61	58.6
XLi350 C17H11ClN2O	1.224	1.188	ND	ND	2.9	ND
JYI-32 (C20H15N3O2BrF)	3.07	4.96	ND	ND	2.92	52.24

Table 9: Continued.

Cook code[a]	α1	α2	α3	α4	α5	α6
SH-I-89S	12.78	8.562	8.145	ND	3.23	ND
MSR-I-032	6.2	18.7	4	ND	3.3	74.9
OMB-19	22	4.6	20	3333	3.5	40
ZG-213	12.8	49.8	30.2	ND	3.5	22.5
YT-II-83	32.74	13.22	24.1	ND	3.548	ND
RY-059	89	70	91	ND	3.7	301
SPH-121	0.14	1.19	1.72	ND	4	479
RY-047	200	124	79	ND	4	340
XLI-8TC	21.52	11.01	2.155	ND	4.059	ND
YT-I-38	945.9	326.8	245.9	ND	4.07	ND
DM-146	6.44	ND	148	ND	4.23	247
CM-B44 (ss)	32	43	12	379	4.3	485
CM-B47	32	63	34	2007	4.4	717
XLi-JY-DMH ANX3	3.3	0.58	1.9	ND	4.4	5000
WY-B-15	0.92	0.83	0.58	2080	4.42	646
ZK 93423	4.1	4.2	6	ND	4.5	1000
JYI-12 (C19H16N3O3F3)	91	39	ND	ND	4.5	6.8
CM-A87	1.62	4.54	14.73	1000	4.61	1000
DM-III-01 (C18H12N3O2Br)	5000	12	ND	ND	4.73	5000
RY-057	73	85	97	ND	4.8	333
JYI-15 (C19H14N3O3F3)	205	812	ND	ND	4.8	22
CM-B31i (ss)	90	184	78	18	4.9	121
RY-079	121.1	141.9	198.4	159	5	113.7
JC208 C15H10N2OS	22.42	18.89	ND	ND	5.039	ND
YT-II	6.932	0.8712	3.518	ND	5.119	ND
XLi270 C19H14N4	36.39	25.81	ND	ND	5.291	ND
XHE-I-051	35	39	42	ND	5.3	979
MMB-II-87	200	333	107	109	5.4	333
XLI-210	231	661	2666	ND	5.4	54.22
XHE-II-O53-ACID	50.35	11.8	44	ND	5.9	5000
ABECARNIL	12.4	15.3	7.5	ND	6	1000
RY-I-31	10	45	19	ND	6	1000
QH-II-082	1.7	1.8	1.6	ND	6.1	100
SH-TSC-1 (PWZ-029)	362.4	180.3	328.2	ND	6.185	ND
XHE-II-065	1000	409	216	37	6.4	175
JYI-49 (C20H12N3O2F4Br)	1.87	2.38	ND	ND	6.7	3390
JC184 C13H9BrN2OS	9.606	10.5	ND	ND	6.709	ND
QH-II-066	76.3	42.1	47.4	2000	6.8	3000
XLI-381	619.9	285.6	3639	ND	7.051	ND
RY-071	19	56	91	ND	7.2	266
RY-I-28	283	318	102	ND	7.2	61
CM-A82a	2.78	8.93	24.51	1000	7.49	1000
YT-III-31	36.39	67.85	129.7	ND	7.59	ND
SH-I-04	7.3	6.136	5.1	ND	7.664	ND
QH-146	0.49	ND	0.76	ND	7.7	1000
QH-II-063	9.4	9.3	31	ND	7.7	3000
JC221 ANX1	106.175	49.405	182	ND	7.7495	362
DM-II-30 (C20H13N3O2BrF3)	17.6	13.4	28.51	ND	7.8	5000
SH-TS-CH_3	107.2	50.09	20.95	ND	8.068	ND
RY-073	156	88	122	ND	8.5	267

Table 9: Continued.

Cook code[a]	α1	α2	α3	α4	α5	α6
SVO-8-20	11	40	28	19	8.6	138
SHU-221-1	66	41	43	3000	9	3000
YT-III-231	51.09	61.46	26.34	ND	9.124	ND
CM-E09a	176	192	122	490	9.2	718
DM-139	5.8	ND	169	ND	9.25	325
YT-III-42	382.9	16.83	44.04	ND	9.77	ND
CD-214	16.4	48.2	42.5	ND	9.8	168
XHE-III-24	0.25	ND	8	222	10	328
XLi223 C22H20BrN3O2	14	8.7	18	1000	10	2000
SPH-165	0.63	2.79	4.85	ND	10.4	1150
JYI-01 (C19H20N3O3Br)	59.2	159	96	ND	10.6	2.88
diazepam	14	20	15	ND	11	ND
XHE-III-49	1.3	5.5	4.2	38.7	11.3	85.1
WZ-113	19.2	13.2	13.4	ND	11.5	300
JYI-59 (C22H13N3O2F4)	1.08	2.6	11.82	ND	11.5	5000
JYI-72 (C22H21N4SiF)	48.5	18.5	ND	ND	11.5	5000
TC-YT-II-76	101.1	1.897	5.816	ND	11.99	ND
JYI-10 (C17H13N3O3F3Br)	5000	368	ND	ND	12.3	23
WZ-069	40	30.5	38.5	ND	12.6	1000
JYI-06 (C23H23N3O4)	16.5	5.48	5000	ND	12.6	5000
RY-072	220	150	184	ND	12.7	361
JYI-14 (C17H14N3O3F3)	32	25	ND	ND	13	565
XHE-II-053	287	45	96	1504	13.8	1000
Xli-347 C34H28N6O7	828.05	690.2	ND	ND	13.87	ND
SHU-1-19	4	12	7	48	14	84
CM-C28 (SR)	176	752	244	290	14	141
CM-E11	333	308	161	394	14	750
XHE-II-012	49	24	31	1042	14	2038
MMB-III-018	117	140	78	3500	14	976
MMB-III-18	117	140	78	3500	14	976
CM-B31c (ss)	118	319	173	37	15	137
CM-B45	230	557	336	265	15	230
XLI-093	1000	1000	858	1550	15	2000
DM-II-20 (C22H14N3O2F3)	54.3	27.14	35.68	ND	15.35	5000
XLi269 C22H22N4Si	221.8	154.2	ND	ND	15.51	ND
SH-O53-S-CH_3-2′F	350	141	1237	ND	16	5000
JYI-13 (C21H16N3O4F3)	5000	63.7	ND	ND	16	8.38
CM-B34	472	451	223	114	17	175
XHE-II-017	3.3	10	7	258	17	294
JC222 C16H12N2OS	86.7	45.11	ND	ND	17.63	ND
SPH-38	2	5.4	10.8	ND	18.5	3000
WZ-070	72.7	30.7	53.2	ND	18.6	300
RY-069	692	622	506	ND	19	1000
SH-053-2′F-S-CH_3	468.2	33.27	291.5	ND	19.2	ND
XHE-I-093	2	7.1	8.9	1107	20	1162

[a]Affinity of compounds at $GABA_A$/BzR recombinant subtypes was measured by competition for [^{3}H]flunitrazepam or [^{3}H] Ro15-4513 binding to HEK cell membranes expressing human receptors of compositions $\alpha1\beta3\gamma2$, $\alpha2\beta3\gamma2$, $\alpha3\beta3\gamma2$, $\alpha4\beta3\gamma2$, $\alpha5\beta3\gamma2$, and $\alpha6\beta3\gamma2$ [22, 139]. Data represent the average of at least three determinations with a SEM of ±5%. ND: not determined.

Table 10: Ligands with potent affinity for $\alpha 6$; ligands bound with K_i values <20 nM at this subtype. The structures of these ligands are in the Ph.D. thesis of Clayton (2011) [22].

Cook code[a]	$\alpha 1$	$\alpha 2$	$\alpha 3$	$\alpha 4$	$\alpha 5$	$\alpha 6$
CM-D45 C19H21N3O4	90.5	65.5	30.3	0.15	1.65	0.23
CM-D44	34.3	56.3	20.7	0.33	0.57	0.92
JYI-04 (C21H23N3O3)	28.3	16	ND	ND	0.51	1.57
PZII-028	0.2	ND	0.2	ND	0.32	1.9
PWZ-009A1	1.34	1.31	1.26	ND	0.84	2.03
JYI-01 (C19H20N3O3Br)	59.2	159	96	ND	10.6	2.88
JYI-03 (C21H21N3O3)	185.4	107	ND	ND	0.954	3.34
Ro15-4513	3.3	2.6	2.5	ND	0.26	3.8
TG-4-29	2.8	3.9	2.7	2.1	0.18	3.9
JYI-11 (C22H22N3O3F3Si)	5000	5000	ND	ND	648	3.97
QH-II-077	0.06	0.08	0.05	ND	0.12	4
ZG-63A	17.3	21.6	29.1	ND	0.65	4
ZG-208	9.7	11.2	10.9	ND	0.38	4.6
OMB-18	3.9	1.2	3.4	1733	0.8	5
RY-024 C19H19N3O3	26.9	26.3	18.7	ND	0.4	5.1
ZG-234	7.25	22.14	9.84	ND	0.3	5.25
XHE-III-74	77	105	38	0.42	2.2	5.8
JYI-12 (C19H16N3O3F3)	91	39	ND	ND	4.5	6.8
DM-239	1.5	ND	0.53	ND	0.14	6.89
XHE-III-14	2.6	ND	10	13	2	7
TG-4-29	8.3	10.2	6.9	ND	0.4	7.61
DM-215	6.74	ND	7.42	ND	0.293	8.28
JYI-13 (C21H16N3O4F3)	5000	63.7	ND	ND	16	8.38
CGS9895	0.21	ND	ND	ND	ND	9.3
ZG-168	11.2	10.7	9.2	ND	0.47	9.4
PWZ-007A	0.11	0.1	0.09	ND	0.2	10
PZII-029	0.34	ND	0.79	ND	0.52	10
XHE-II-024	0.09	0.18	0.32	14	0.24	11
XHE-II-002	8.3	18	13	3.9	1.5	11
BRETAZENIL	0.35	0.64	0.2	ND	0.5	12.7
JYI-19 (C23H23N3O3S)	2.176	205	ND	ND	34	12.7
SVO-8-14	8	25	8	6.9	0.9	14
SVO-8-30	1.1	5.3	5.3	2.8	0.6	15
WYS10 C14H9F3N2O2	0.88	36	25.6	ND	548.7	15.3
QH-II-090 (CGS-8216)	0.05	0.08	0.12	ND	0.25	17
PWZ-0071	0.23	0.17	0.12		0.44	17.31

[a]The affinity of compounds at $GABA_A$/BzR recombinant subtypes was measured by competition for [^{3}H]flunitrazepam binding to HEK cell membranes expressing human receptors of compositions $\alpha 1\beta 3\gamma 2$, $\alpha 2\beta 3\gamma 2$, $\alpha 3\beta 3\gamma 2$, $\alpha 4\beta 3\gamma 2$, $\alpha 5\beta 3\gamma 2$, and $\alpha 6\beta 3\gamma 2$ [139]. Data represent the average of at least three determinations with a SEM of ±5%. ND: not determined.

The X-ray structure determination of the $\alpha 5\beta 3\gamma 2$ GABA(A) receptor is eagerly awaited, while that with five $\beta 3$-subunits has been reported recently (Miller and Aricescu, *Nature* 2014). It is hoped that the proposed orientation may be used by others to gain additional insight into the potential mechanisms underlying binding and modulation at the Bz site, all of which will lead to a better understanding of the structure and function of GABA(A) receptors, ultimately targeted toward treatment of diseases.

25. Synthesis of Ligands with $\alpha 5$ BzR Subtype Selectivity

Briefly, bromoacetyl bromide was added to 2-aminobenzophenone **44**, followed by treatment with methanol, which had been saturated with ammonia (g) under the cooling of an ice-water bath. The benzodiazepine, **45**, was brominated to provide **46** and then reacted with ethyl isocyanoacetate to generate the imidazobenzodiazepine, **47**. A much better one-pot process has now been devised using KtBuO at −30°C [140]. The bromide **48** was subjected to a Stille-type coupling to give DM-I-81 (**9**) [126]. This route (Scheme 1) can be executed on several hundred gram scales.

The benzodiazepine monomers were prepared by the method of Fryer and Gu [89, 141]. The isatoic anhydride was heated with sarcosine in dimethyl sulfoxide to provide amide **49**. Bromination of **49** in a mixture of acetic acid, bromine, and sodium acetate afforded the corresponding monosubstituted bromide **50** in good yield. Deprotonation of **50** with lithium diisopropyl amide (LDA) in THF was followed by treatment with diethyl chlorophosphate to provide the intermediate enol phosphate. The enol phosphate was stirred with a solution of ethyl isocyanoacetate and LDA to yield the imidazo congener. Again, a better one-pot procedure has been developed using KtBuO at −30°C in place of LDA at 0°C. A Heck type coupling reaction was employed with the bromide **51** with bis(acetate)bis(triphenylphosphine)palladium(II) to provide the TMS-acetylene **52**. Treatment of **52** with Bu_4NF removed the trimethylsilyl group. Hydrolysis of the ester function of **53** provided the acid **54** in excellent yield and this material was dried scrupulously and subjected to a standard CDI-mediated coupling reaction to furnish bivalent ligand XLi-093 (**4**). The imidazobenzodiazepine diethyl diester XLi-356 (**10**) was obtained from XLi-093 (Scheme 2) in high yield *via* catalytic hydrogenation (Pd/C, H_2).

26. Synthesis of Bivalents

Inverse agonist **53** was synthesized via the reported procedure. Hydrolysis of the ester function of **53** provided the acid **54** in excellent yield. This material was dried scrupulously and was subjected to a standard CDI-mediated coupling reaction to furnish bivalent ligands **4**, **55**, and **56** in 60% yield (Scheme 3) [13].

The acid **57**, obtained from the ester **47**, which was available from the literature [13], was stirred with CDI in DMF, followed by stirring with the required diol and DBU to provide bromide substituted dimers **58** or **59**, respectively. They were converted into the trimethylsilylacetylenyl **60** or **61**, respectively, under standard conditions (Pd-mediated, Heck-type coupling) [142]. The bisacetylene **62** or **63** (individually) was easily obtained by treatment of the trimethylsilyl ligand **60** or **61** with fluoride anion, as shown in Scheme 4.

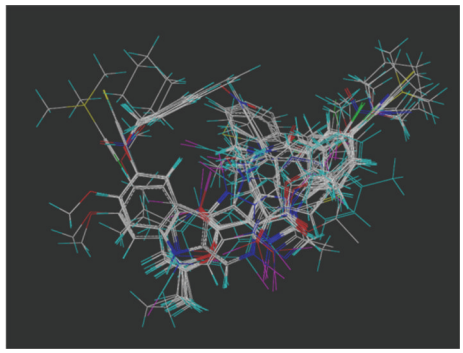

Figure 34: Overlay of selected compounds for $\alpha 1\beta 3\gamma 2$ subtype from Table 5.

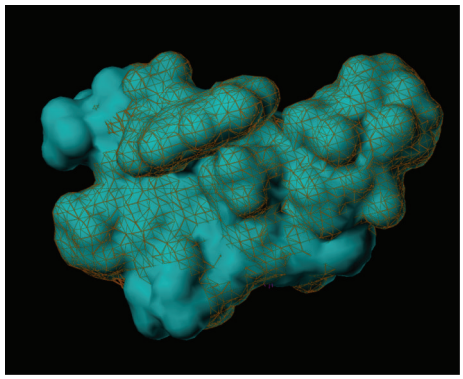

Figure 35: Updated $\alpha 1\beta 3\gamma 2$ subtype (blue solid) overlaid with the previous model (red wire). Overlap identified where wire and solid overlap.

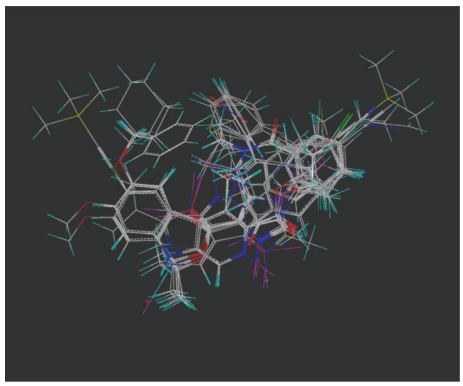

Figure 36: Overlay of compounds selective for $\alpha 2\beta 3\gamma 2$ subtype.

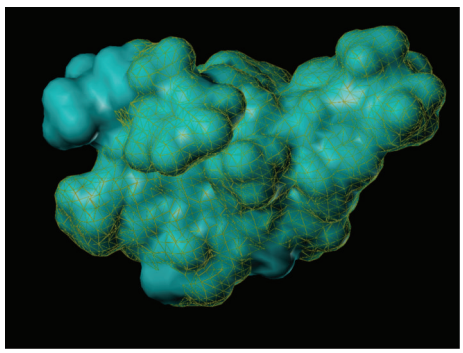

Figure 37: Updated $\alpha 2\beta 3\gamma 2$ subtype (solid) overlaid with the previous model (red wire). Overlap identified where wire and solid overlap.

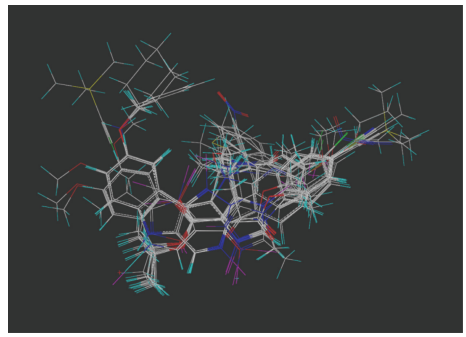

Figure 38: Overlay of compounds selective for $\alpha 3\beta 3\gamma 2$ subtype.

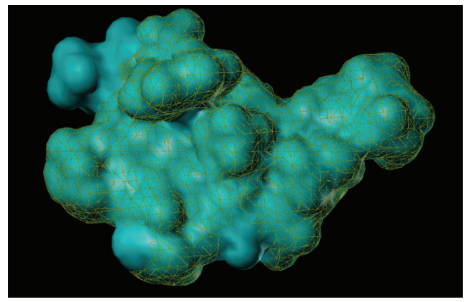

Figure 39: Updated $\alpha 3\beta 3\gamma 2$ subtype (blue solid) overlaid with the previous model (red wire). Overlap identified where wire and solid overlap.

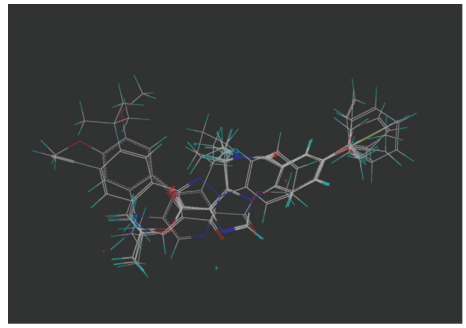

Figure 40: Overlay of selected compounds selective for $\alpha 4\beta 3\gamma 2$ subtype.

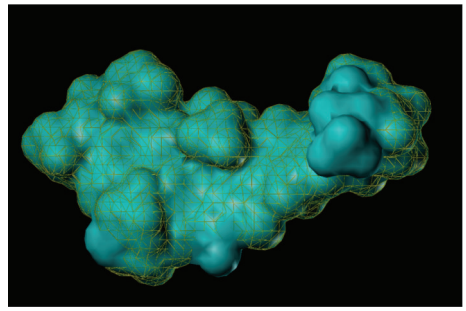

Figure 41: Updated $\alpha 4\beta 3\gamma 2$ subtype (blue solid) overlaid with the previous model (yellow wire). Overlap identified where wire and solid overlap.

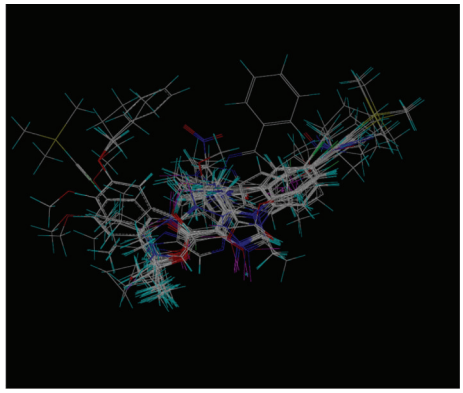

Figure 42: Overlay of selected compounds selective for $\alpha5\beta3\gamma2$ subtype.

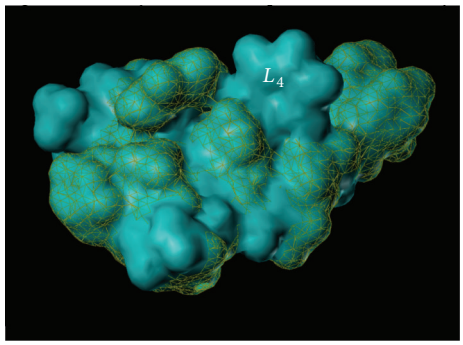

Figure 43: Updated $\alpha5\beta3\gamma2$ subtype (blue solid) overlaid with the previous model (yellow wire). Overlap identified where wire and solid overlap.

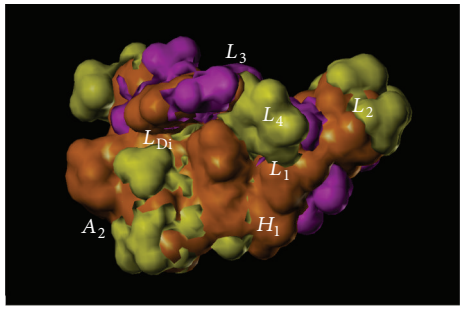

Figure 44: Overlay of the $\alpha5\beta3\gamma2$ receptor (yellow) subtype with the $\alpha1\beta3\gamma2$ receptor (magenta) subtype. Orange surfaces indicate overlapping regions.

27. Materials, Methods, and Experimental

27.1. Materials and General Instrumentation. Chemicals were purchased from Aldrich Chemical Co. or Tokyo Chemical Industries and were used without further purification except where otherwise noted. Anhydrous THF was distilled from sodium/benzophenone ketyl. TLC analyses were carried out on Merck Kieselgel 60 F_{254}, and flash column chromatography was performed on silica gel 60b purchased from E. M. Laboratories. Melting points were taken on a Thomas-Hoover melting point apparatus or an Electrothermal Model IA8100 digital melting point apparatus and are reported uncorrected. NMR spectra were recorded on a Bruker 300 or 500 MHz multiple-probe spectrometer. Infrared spectra were recorded on a Nicolet DX FTIR BX V5.07 spectrometer or a Mattson Polaris IR-10400 instrument. Low-resolution mass spectral data (EI/CI) were obtained on a Hewlett-Packard 5985B GC-mass spectrometer, while high resolution mass spectral data were taken on a VG autospectrometer (Double Focusing High Resolution GC/Mass Spectrometer, UK). Microanalyses were performed on a CE Elantech EA1110 elemental analyzer. Methods of specific experiments can be found in corresponding cited works.

27.2. Competition Binding Assays. Competition binding assays were performed in a total volume of 0.5 mL of a 50 mM Tris-acetate at 4° degree centigrade for 1 hour using [^{3}H]flunitrazepam as the radioligand. For these binding assays, 20–50 mg of membrane protein harvested with hypotonic buffer (50 mM Tris-acetate pH 7.4 at 4 degree) was incubated with the radiolabel as previously described [139, 143]. Nonspecific binding was defined as radioactivity bound in the presence of 100 μM diazepam and represented less than 20% of total binding. Membranes were harvested with a Brandel cell harvester followed by three ice-cold washes onto polyethyleneimine-pretreated (0.3%) Whatman GF/C filters. Filters were dried overnight and then soaked in Ecoscint A liquid scintillation cocktail (National Diagnostics; Atlanta, GA). Bound radioactivity was quantified by liquid scintillation counting. Membrane protein concentrations were determined using an assay kit from Bio-Rad (Hercules, CA) with bovine serum albumin as the standard.

27.3. Radioligand Binding Assays (Drs. McKernan and Atack) [12]. In brief, the affinity of compounds for human recombinant GABA(A) receptors was measured by competition binding using 0.5 nM [^{3}H]flunitrazepam. Transfected HEK cells (beta2 gamma2 and desired alpha subtype) were harvested into phosphate-buffered saline, centrifuged at 3,000 g, and stored at −70°C until required. On the day of the assay, pellets were thawed and resuspended in sufficient volume of 50 mM Tris/acetate (pH 7.4 at 4°C) to give a total binding of approximately 1500–2000 dpm. Nonspecific binding was defined in the presence of 100 mM (final concentration) diazepam. Test compounds were dissolved in DMSO at a concentration of 10 mM and diluted in assay buffer to give an appropriate concentration range in the assay, such that the final DMSO concentration in the assay was always less than 1%. Total assay volume was 0.5 mL and assays were carried out in 96-well plates and incubation time started by the addition of 0.1 mL of resuspended cell membranes. Following incubation for 1 hour at 4°C, assays were terminated by filtration through GF/B filters, washed with 10 mL ice cold buffer, dried, and then counted using a liquid scintillation counter. The percentage of inhibition of [^{3}H]flunitrazepam binding, the IC_{50}, and the K_i values were calculated using the Activity Base Software Package (ID Business Solutions,

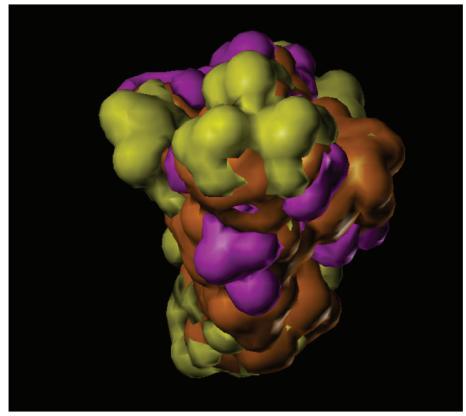

Figure 45: Overlay of the $\alpha5\beta3\gamma2$ receptor (yellow) subtype with the $\alpha1\beta3\gamma2$ receptor (magenta) subtype (Figure 44 rotated 90°). Orange surfaces indicate overlapping regions.

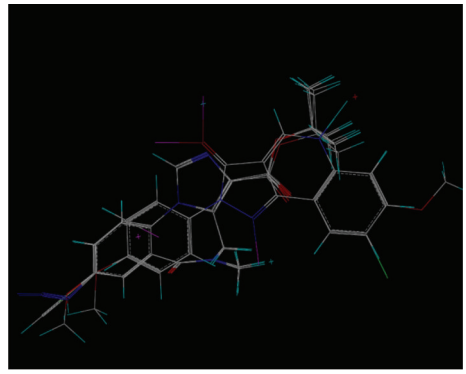

Figure 46: Overlay of selected compounds selective for $\alpha6\beta3\gamma2$ subtype.

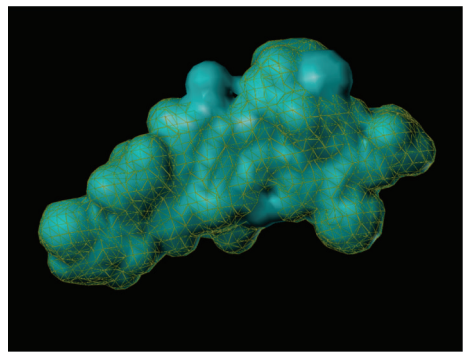

Figure 47: Updated $\alpha6\beta3\gamma2$ subtype (blue solid) overlaid with the previous model (yellow wire). Overlap identified where wire and solid overlap.

Guildford, UK) according to the Cheng-Prusoff equation [143]. We have previously reported the synthesis of the following.

1,3-Bis(8-acetyleno-5,6-dihydro-5-methyl-6-oxo-4H-imidazo[1,5a][1,4]benzodiazepine-3-carboxy) propyl diester ***4*** (XLi-093) (Procedure A), experimental details previously reported [17].

1,5-Bis(8-acetyleno-5,6-dihydro-5-methyl-6-oxo-4H-imidazo[1,5a][1,4]benzodiazepine-3-carboxy) pentyl diester ***56*** (XLi-210), experimental details previously reported [17].

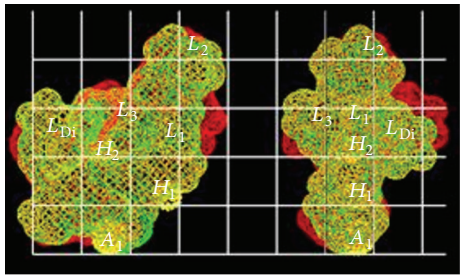

(a) Orthogonal views of the overlap (yellow) volumes of $\alpha1\beta3\gamma2$ (red) and $\alpha2\beta3\gamma2$ (green)

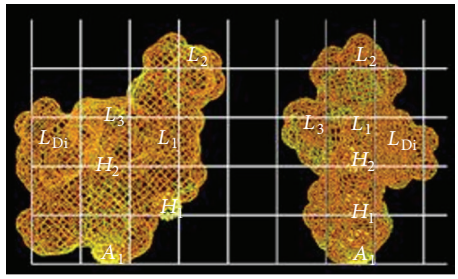

(b) Orthogonal views of the overlap (yellow) volumes of $\alpha2\beta3\gamma2$ (red) and $\alpha3\beta3\gamma2$ (green)

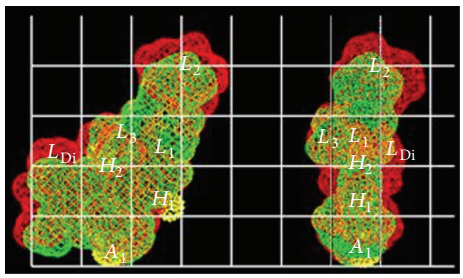

(c) Orthogonal views of the overlap (yellow) volumes of $\alpha4\beta3\gamma2$ (red) and $\alpha6\beta3\gamma2$ (green)

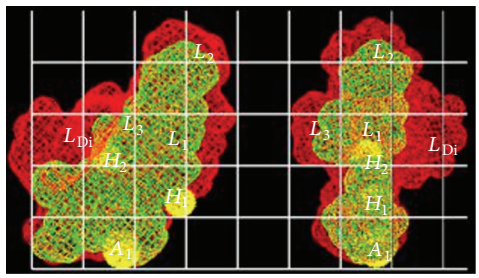

(d) Orthogonal views of the overlap (yellow) volumes of $\alpha1\beta3\gamma2$ (red) and $\alpha6\beta3\gamma2$ (green)

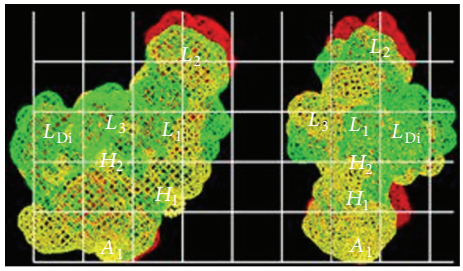

(e) Orthogonal views of the overlap (yellow) volumes of $\alpha5\beta3\gamma2$ (red) and $\alpha1\beta3\gamma2$ (green)

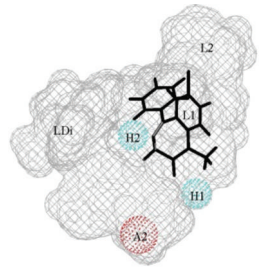

(f) Diazepam and the unified pharmacophore descriptors

FIGURE 48: The previous benzodiazepine subtype selective receptor pharmacophore models [23]. (1) The L_2 region in the $\alpha5$ subtype is larger than the $\alpha1$ subtypes. This is a key result. It is the principle difference between $\alpha5$ subtypes compared to $\alpha2$ and $\alpha3$ subtypes, but especially in regard to $\alpha1$ subtypes (L_2 smaller in $\alpha1$). (2) The L_3 region is larger in the $\alpha5$ subtype as compared to the $\alpha1$, $\alpha2$, $\alpha3$, $\alpha4$, and $\alpha6$ BzR sites. R analogs of benzodiazepines with pendant phenyls had increased affinity to $\alpha5$ supporting the larger L_3 pocket in this receptor subtype, while S isomers bound to $\alpha2$, $\alpha3$, and $\alpha5$ subtypes because of different conformational constraints.

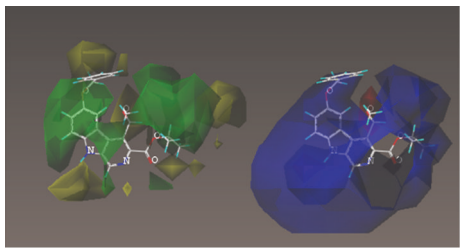

FIGURE 49: Steric (left) and electrostatic maps of the $\alpha1\beta3\gamma2$ receptor subtype shown in the transparent mode as seen from the classic perspective.

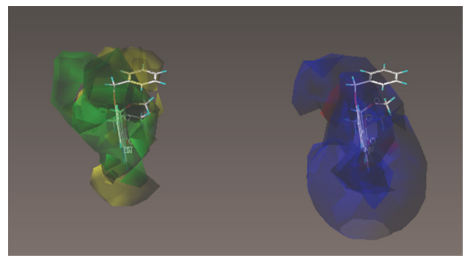

FIGURE 50: Steric (left) and electrostatic maps of the $\alpha1\beta3\gamma2$ receptor subtype shown in the transparent mode as seen from the classic perspective (Figure 45) rotated 90°.

1,3-Bis(8-ethyl-5,6-dihydro-5-methyl-6-oxo-4H-imidazo[1,5a][1,4]benzodiazepine-3-carboxy) propyl diester ***10*** (Xli-356), experimental previously published [144].

Bis(8-acetyleno-5,6-dihydro-5-methyl-6-oxo-4H-imidazo[1,5a][1,4]benzodiazepine-3-carboxy) dimethyl glycol dies-

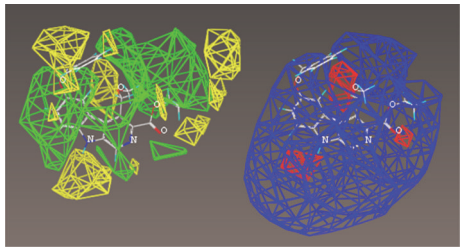

Figure 51: Steric (left) and electrostatic maps of the $\alpha 1\beta 3\gamma 2$ receptor subtype shown in line mode as seen from the classic perspective.

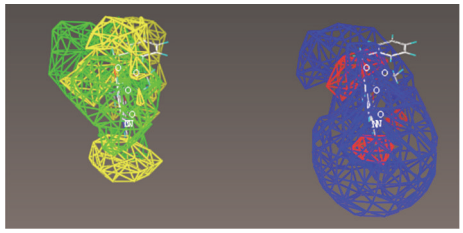

Figure 52: Steric (left) and electrostatic maps of the $\alpha 1\beta 3\gamma 2$ receptor subtype shown in line mode as seen from the classic perspective rotated 90°.

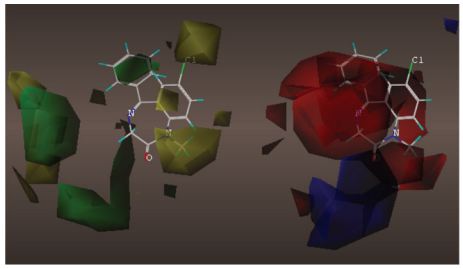

Figure 53: Steric (left) and electrostatic maps of the $\alpha 2\beta 3\gamma 2$ receptor subtype shown in the transparent mode as seen from the classic perspective.

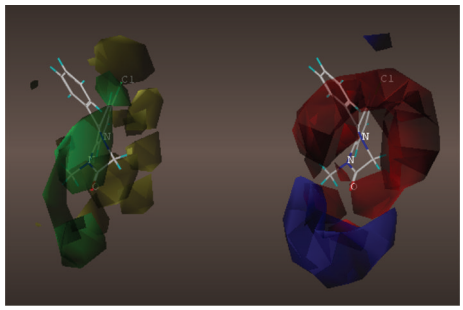

Figure 54: Steric (left) and electrostatic maps of the $\alpha 2\beta 3\gamma 2$ receptor subtype shown in the transparent mode as seen from the classic perspective rotated 90°.

ter **55** (Xli-374), experimental details previously reported [17].

8-Bromo-6-phenyl-4H-benzo[f]imidazo[1,5-a][1,4]diazepine-3-carboxylic acid **57**, experimental details previously reported [17].

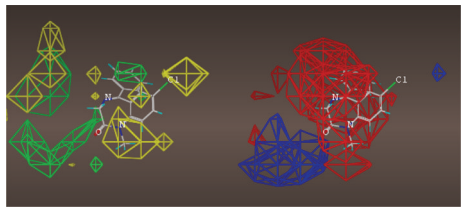

Figure 55: Steric (left) and electrostatic maps of the $\alpha 2\beta 3\gamma 2$ receptor subtype shown in line mode as seen from the classic perspective.

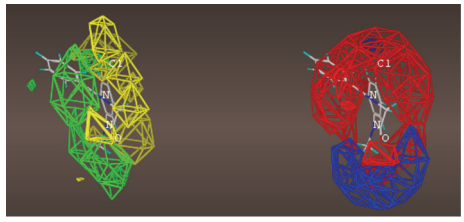

Figure 56: Steric (left) and electrostatic maps of the $\alpha 2\beta 3\gamma 2$ receptor subtype shown in line mode as seen from the classic perspective rotated 90°.

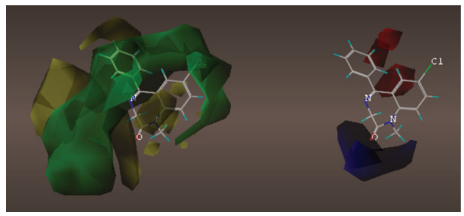

Figure 57: Steric (left) and electrostatic maps of the $\alpha 3\beta 3\gamma 2$ receptor subtype shown in the transparent mode as seen from the classic perspective.

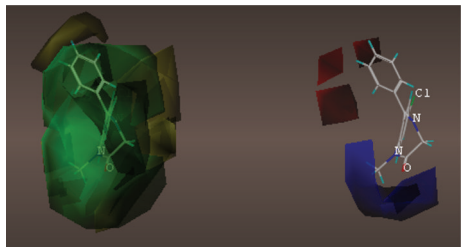

Figure 58: Steric (left) and electrostatic maps of the $\alpha 3\beta 3\gamma 2$ receptor subtype shown in the transparent mode as seen from the classic perspective rotated 90°.

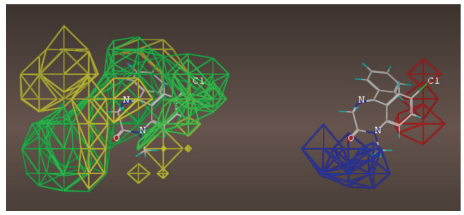

Figure 59: Steric (left) and electrostatic maps of the $\alpha 3\beta 3\gamma 2$ receptor subtype shown in line mode as seen from the classic perspective.

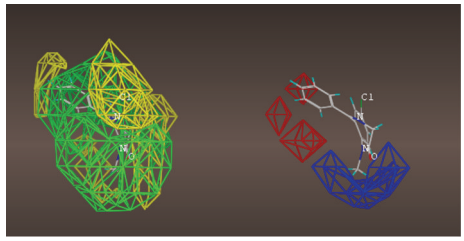

Figure 60: Steric (left) and electrostatic maps of the $\alpha 3\beta 3\gamma 2$ receptor subtype shown in line mode as seen from the classic perspective rotated 90°.

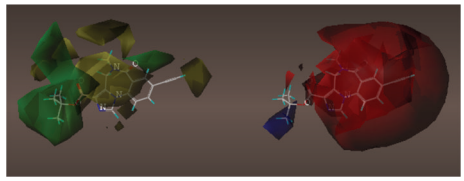

Figure 61: Steric (left) and electrostatic maps of the $\alpha 5\beta 3\gamma 2$ receptor subtype shown in the transparent mode as seen from the classic perspective.

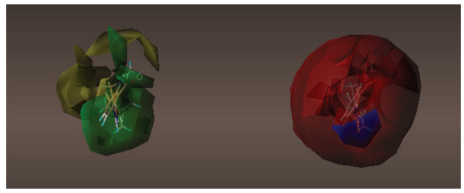

Figure 62: Steric (left) and electrostatic maps of the $\alpha 5\beta 3\gamma 2$ receptor subtype shown in the transparent mode as seen from the classic perspective rotated 90°.

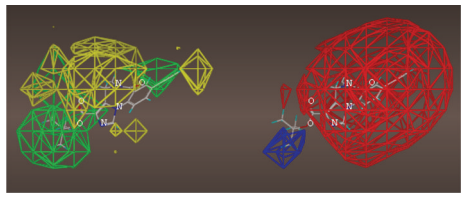

Figure 63: Steric (left) and electrostatic maps of the $\alpha 5\beta 3\gamma 2$ receptor subtype shown in line mode as seen from the classic perspective.

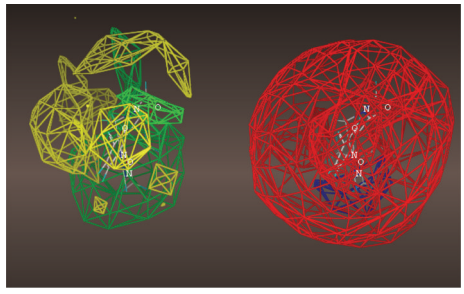

Figure 64: Steric (left) and electrostatic maps of the $\alpha 5\beta 3\gamma 2$ receptor subtype shown in line mode as seen from the classic perspective rotated 90°.

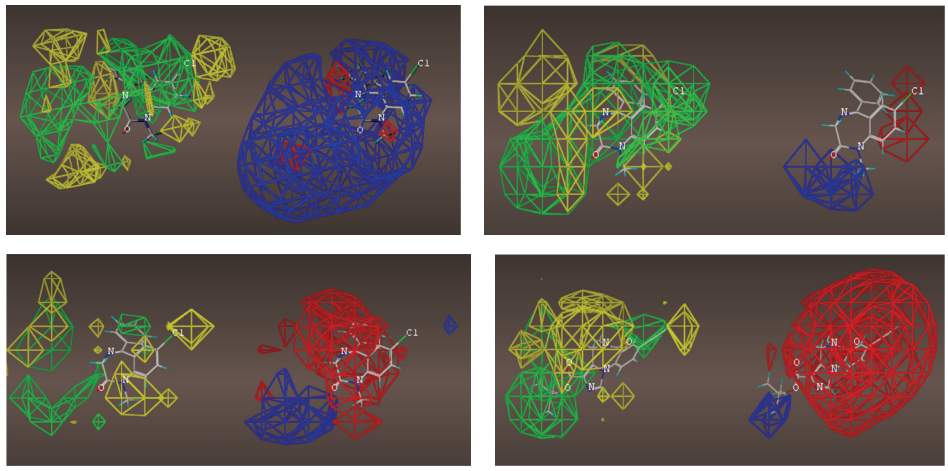

Figure 65: Clockwise from the top left, line maps of the $\alpha 1\beta 3\gamma 2$, $\alpha 2\beta 3\gamma 3$, $\alpha 3\beta 3\gamma 2$, and $\alpha 5\beta 3\gamma 2$ CoMFA.

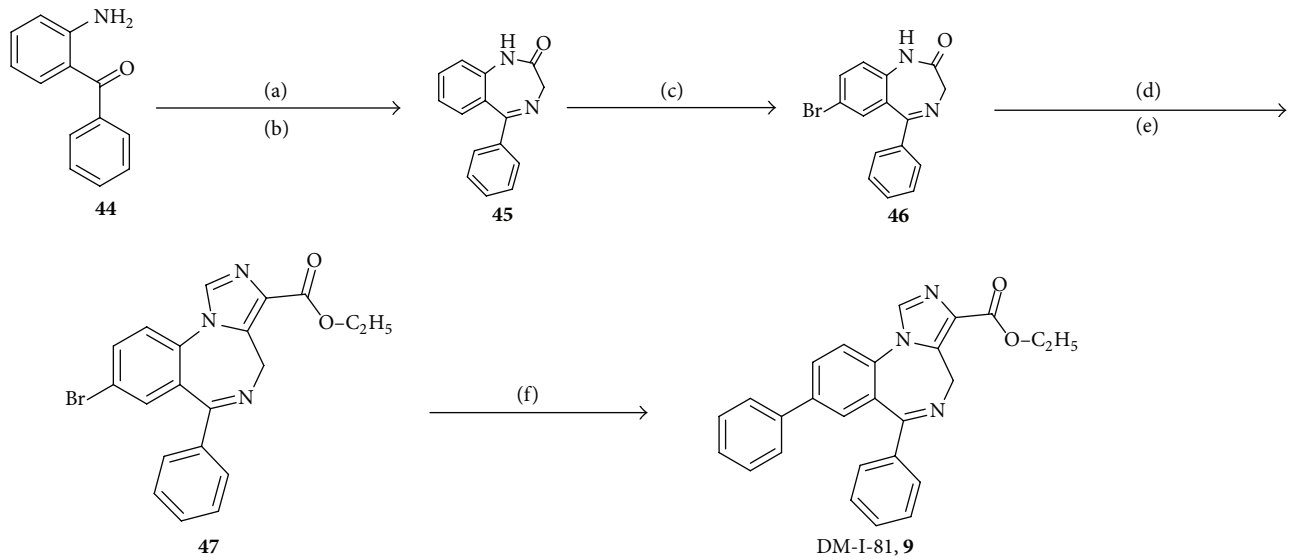

Scheme 1: Synthesis of 8-substituted imidazobenzodiazepines following chemistry earlier developed by Sternbach, Fryer et al. *Reagents and Conditions*. (a) Bromoacetyl bromide, sodium bicarbonate, and chloroform; (b) ammonia (anhydrous), methanol, and reflux; (c) bromine, sulfuric acid, and acetic acid; (d) sodium hydride, diethyl chlorophosphate, and tetrahydrofuran; (e) sodium hydride, ethyl isocyanoacetate, and tetrahydrofuran, −30°C to r.t.; (f) tributyl(phenyl)stannane, $Pd(PPh_3)_4$.

1,3-Bis(8-bromo-6-phenyl-4H-benzo[f]imidazo[1,5-a][1,4]diazepine-3-carboxy) propyl diester ***59*** (DMH-D-070) (Procedure B), experimental details previously reported [17].

1,3-Bis(8-trimethylsilylacetylenyl-6-phenyl-4H-benzo[f]imidazo[1,5-a][1,4]-diazepine-3-carboxy) propyl diester ***61*** (DMH-D-048) (Procedure C), experimental details previously reported [17].

1,3-Bis(8-acetylenyl-6-phenyl-4H-benzo[f]imidazo[1,5-a][1,4]diazepine-3-carboxy) propyl diester ***63*** (DMH-D-053): experimental details previously reported [17].

Bis(8-bromo-6-phenyl-4H-benzo[f]imidazo[1,5-a][1,4]diazepine-3-carboxy) diethylene glycol diester ***58*** (DM-III-93), experimental details previously reported [17].

Bis(8-trimethylsilylacetylenyl-6-phenyl-4H-benzo[f]imidazo[1,5-a][1,4]diazepine-3-carboxy) diethylene glycol diester ***60*** (DM-III-94), experimental details previously reported [17].

Bis(8-acetylenyl-6-phenyl-4H-benzo[f]imidazo[1,5-a][1,4]diazepine-3-carboxy) diethylene glycol diester ***62*** (DM-III-96), experimental details previously reported [17].

Abbreviations

APD: Antipsychotic drug
ASM: Airway smooth muscle
BS: Binding site
BZD, Bz: Benzodiazepine
BzR: Benzodiazepine receptor
DA: Dopamine
DAPI: 4′,6-Diamidino-2-phenylindole

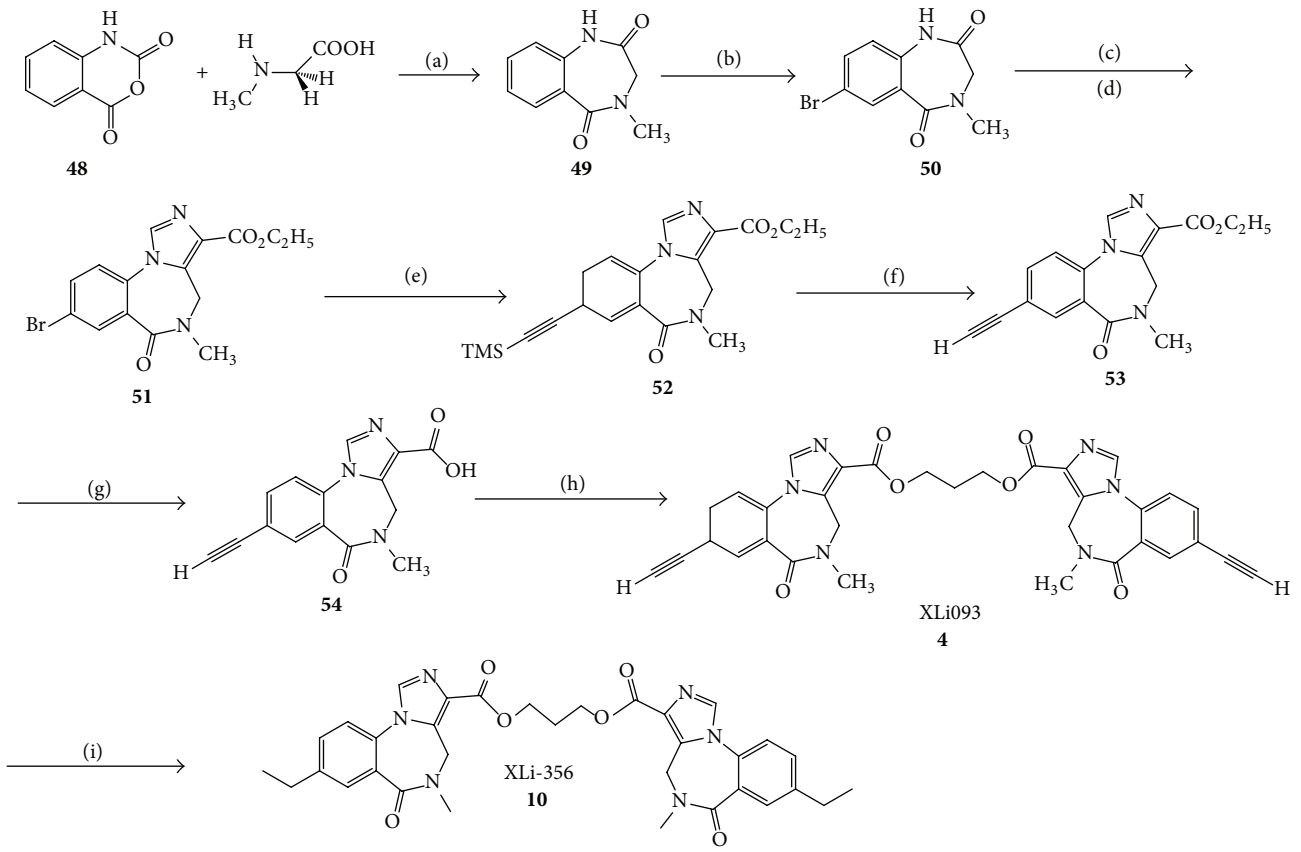

Scheme 2: Synthesis of 8-substituted imidazobenzodiazepine bivalent ligands. *Reagents and Conditions*. (a) DMSO, 180°C, 90%; (b) bromine, sodium acetate, and acetic acid, r.t., 80%; (c) LDA, THF, and diethyl chlorophosphate, 0°C; (d) LDA, THF, and ethyl isocyanoacetate; (e) trimethylsilyl acetylene, $Pd(OAc)_2(PPh_3)_2$, triethylamine, acetonitrile, and reflux, 80%; (f) tetrabutylammonium fluoride, THF, and H_2O, r.t., 88%; (g) 2N NaOH and ethanol, 70°C, 90%; (h) CDI, DMF, $HO(CH_2)_3OH$, and DBU, 60%; (i) Pd/C, H_2, ethanol, and DCM, 90%.

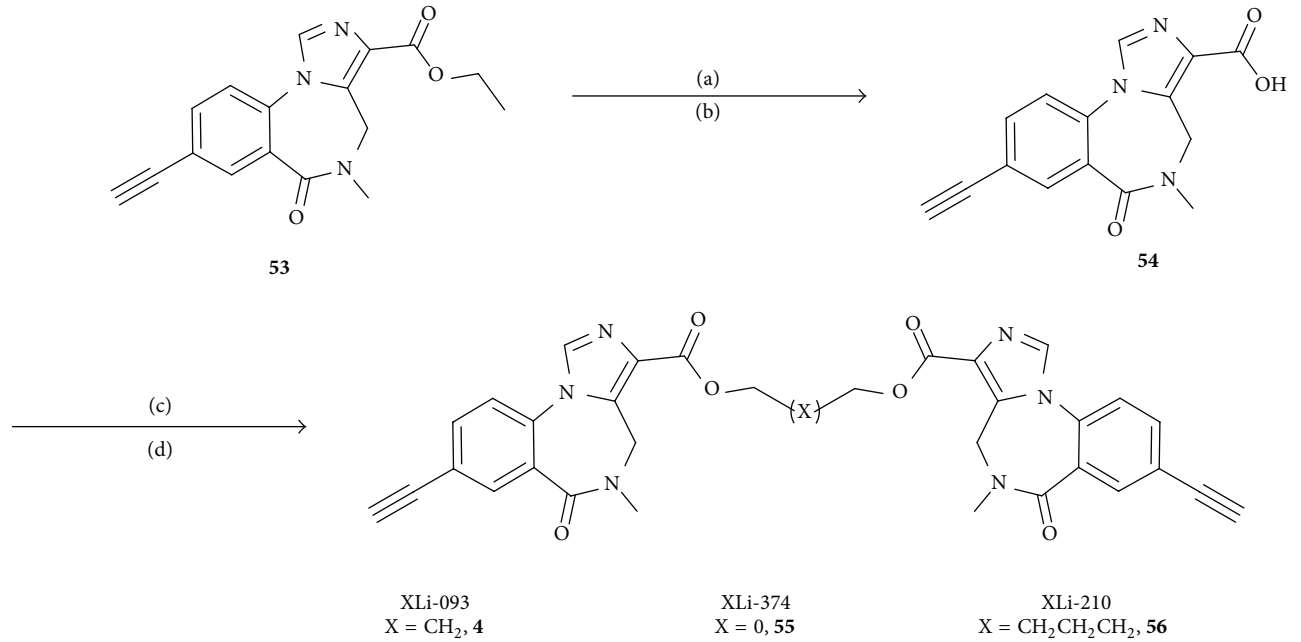

Scheme 3: Synthesis of bivalent analogs of XLi-093 (**4**). *Reagents and Conditions*. (a) 2 M NaOH, EtOH, 70°C; (b) 10% aq HCl; (c) CDI, DMF; (d) diol, DBU.

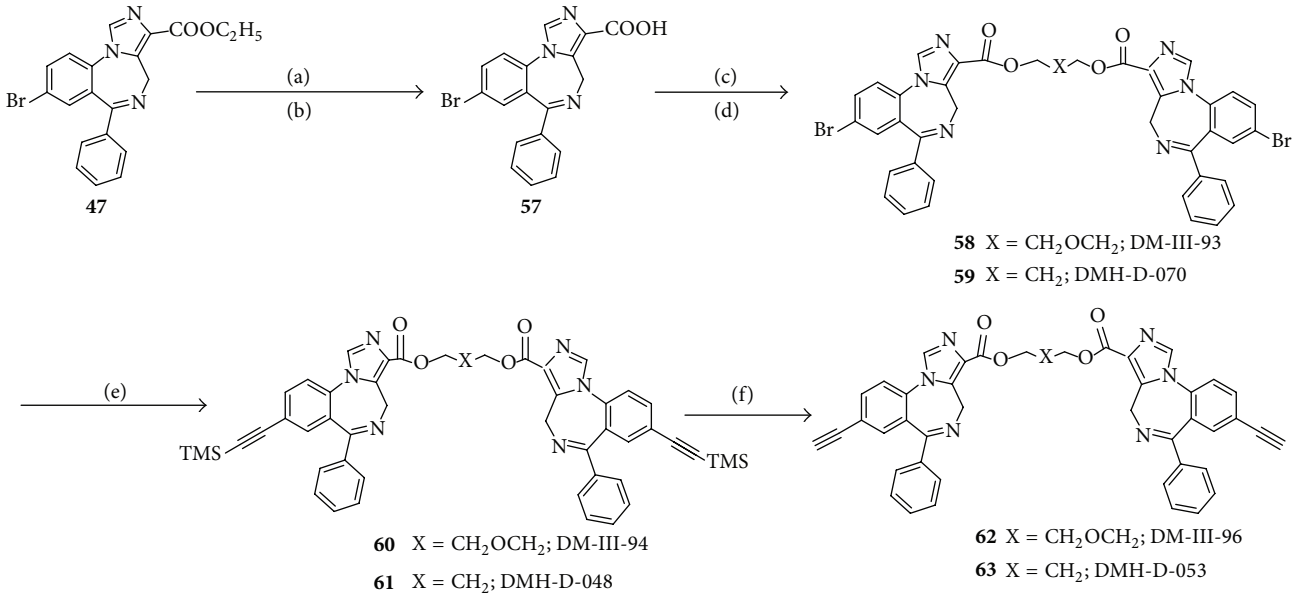

Scheme 4: Synthesis of bivalent analogues of DMH-D-053 (**63**). *Reagents and Conditions*. (a) 2 N NaOH, EtOH, and reflux; (b) 10% aq. HCl; (c) CDI, DMF; (d) diol, DBU; (e) trimethylsilylacetylene, $Pd(OAc)_2(PPH_3)_2$, Et_3N, CH_3CN, and reflux; (f) TBAF∗0.5H_2O, THF, −78°C.

GABA:	Gamma amino butyric acid
$GABA_A$:	Gamma amino butyric acid A
$GABA_AR$:	Gamma amino butyric acid A receptor
HAL:	Haloperidol
HEK:	Human embryonic kidney
HPC:	Hippocampal
LTK:	Leukocyte tyrosine kinase
MAM:	Methylazoxymethanol
NAM:	Negative allosteric modulator
QSAR:	Quantitative structure-activity relationship
PAM:	Positive allosteric modulator
PV:	Parvalbumin
SAL:	Saline
SH-053:	SH-053-2′F-R-CH_3
SMA:	Smooth muscle actin
TTX:	Tetrodotoxin
VTA:	Ventral tegmental area.

Conflict of Interests

The authors declare that there is no conflict of interests regarding the publication of this paper.

Authors' Contribution

Terry Clayton and Michael M. Poe contributed equally to this work.

Acknowledgments

The authors gratefully acknowledge the work of Dr. Ruth McKernan and Dr. Bryan Roth for receptor binding. This was supported by NS-076517, MH-096463, NIA AG-039511, and AG-048446. The authors acknowledge support from the Milwaukee Institute for Drug Design.

References

[1] P. S. Miller and A. R. Aricescu, "Crystal structure of a human $GABA_A$ receptor," *Nature*, vol. 512, no. 7514, pp. 270–275, 2014.

[2] K. H. Backus, M. Arigoni, U. Drescher et al., "Stoichiometry of a recombinant $GABA_A$ receptor deduced from mutation-induced rectification," *Neuroreport*, vol. 5, no. 3, pp. 285–288, 1993.

[3] H. Möhler, "Brain disorders and novel therapeutics," *Chimia*, vol. 58, no. 10, pp. 718–720, 2004.

[4] H. Möhler, J.-M. Fritschy, F. Crestani, T. Hensch, and U. Rudolph, "Specific $GABA_A$ circuits in brain development and therapy," *Biochemical Pharmacology*, vol. 68, no. 8, pp. 1685–1690, 2004.

[5] U. Rudolph and H. Möhler, "Analysis of $GABA_A$ receptor function and dissection of the pharmacology of benzodiazepines and general anesthetics through mouse genetics," *Annual Review of Pharmacology and Toxicology*, vol. 44, pp. 475–498, 2004.

[6] D. J. Bailey, J. E. Tetzlaff, J. M. Cook, X. He, and F. J. Helmstetter, "Effects of hippocampal injections of a novel ligand selective for the $\alpha5\beta2\gamma2$ subunits of the GABA/benzodiazepine receptor on Pavlovian conditioning," *Neurobiology of Learning and Memory*, vol. 78, no. 1, pp. 1–10, 2002.

[7] T. M. DeLorey, R. C. Lin, B. McBrady et al., "Influence of benzodiazepine binding site ligands on fear-conditioned contextual memory," *European Journal of Pharmacology*, vol. 426, no. 1-2, pp. 45–54, 2001.

[8] M. S. Chambers, J. R. Atack, F. A. Bromidge et al., "6,7-Dihydro-2-benzothiophen-4(5*H*)-ones: a novel class of GABA-A $\alpha5$ receptor inverse agonists," *Journal of Medicinal Chemistry*, vol. 45, no. 6, pp. 1176–1179, 2002.

[9] M. S. Chambers, J. R. Atack, H. B. Broughton et al., "Identification of a novel, selective GABAa $\alpha5$ receptor inverse agonist

which enhances cognition," *Journal of Medicinal Chemistry*, vol. 46, no. 11, pp. 2227–2240, 2003.

[10] C. Sur, K. Quirk, D. Dewar, J. Atack, and R. Mckernan, "Rat and human hippocampal alpha 5 subunit-containing gamma-aminobutyric acid(A) receptors have alpha 5 beta 3 gamma 2 pharmacological characteristics," *Molecular Pharmacology*, vol. 54, no. 5, pp. 928–933, 1998.

[11] M. Sarter, "Taking stock of cognition enhancers," *Trends in Pharmacological Sciences*, vol. 12, pp. 456–461, 1991.

[12] J. R. Atack, L. Alder, S. M. Cook, A. J. Smith, and R. M. McKernan, "In vivo labelling of α5 subunit-containing $GABA_A$ receptors using the selective radioligand [^{3}H]L-655,708," *Neuropharmacology*, vol. 49, no. 2, pp. 220–229, 2005.

[13] X. Y. Li, H. Cao, C. C. Zhang et al., "Synthesis, in vitro affinity, and efficacy of a bis 8-ethynyl-4*H*-imidazo[1,5α]-[1,4]benzodiazepine analogue, the first bivalent α5 subtype selective BzR/$GABA_A$ antagonist," *Journal of Medicinal Chemistry*, vol. 46, no. 26, pp. 5567–5570, 2003.

[14] X. Li, *Synthesis of selective ligands for GABAA/benzodiazepine receptors [Ph.D. thesis]*, University of Wisconsin-Milwaukee, Milwaukee, Wis, USA, 2004.

[15] A. H. Abadi, S. Lankow, B. Hoefgen, M. Decker, M. U. Kassack, and J. Lehmann, "Dopamine/serotonin receptor ligands, part III: synthesis and biological activities of 7,7′-alkylene-bis-6,7,8,9,14,15-hexahydro-5H-benz[d]indolo[2,3-g]azecines—application of the bivalent ligand approach to a novel type of dopamine receptor antagonist," *Archiv der Pharmazie*, vol. 335, no. 8, pp. 367–373, 2002.

[16] W. Yin, F. Rivas, R. Furtmueller et al., "Synthesis, in-vitro affinity and efficacy of the first bivalent alpha 5 subtype selective BzR/GABA(A) antagonist," in *Proceedings of the 2004 Neuroscience Meeting*, San Diego, Calif, USA, 2004.

[17] D. Han, F. Holger Försterling, X. Li et al., "A study of the structure-activity relationship of GABAA-benzodiazepine receptor bivalent ligands by conformational analysis with low temperature NMR and X-ray analysis," *Bioorganic and Medicinal Chemistry*, vol. 16, no. 19, pp. 8853–8862, 2008.

[18] D. M. Han, F. H. Försterling, X. Y. Li, J. R. Deschamps, H. Cao, and J. M. Cook, "Determination of the stable conformation of $GABA_A$-benzodiazepine receptor bivalent ligands by low temperature NMR and X-ray analysis," *Bioorganic & Medicinal Chemistry Letters*, vol. 14, no. 6, pp. 1465–1469, 2004.

[19] C. C. Zhang, *Structure Activity Relationships and Cytotoxic Activity of Analogs of Tryprostatin A and B. Preparation of Irreversible Inhibitors for Studies of Mechanism and Action. II. Pharmacophore Receptor Models of GABA(A)/BzR*, University of Wisconsin-Milwaukee, Milwaukee, Wis, USA, 2004.

[20] R. Y. Liu, R. J. Hu, P. W. Zhang, P. Skolnick, and J. M. Cook, "Synthesis and pharmacological properties of novel 8-substituted imidazobenzodiazepines: high-affinity, selective probes for α5-containing GABAA receptors," *Journal of Medicinal Chemistry*, vol. 39, no. 9, pp. 1928–1934, 1996.

[21] Q. Huang, X. H. He, C. R. Ma et al., "Pharmacophore/receptor models for $GABA_A$/BzR subtypes ($\alpha1\beta3\gamma2$, $\alpha5\beta3\gamma2$, and $\alpha6\beta3\gamma2$) via a comprehensive ligand-mapping approach," *Journal of Medicinal Chemistry*, vol. 43, no. 1, pp. 71–95, 2000.

[22] T. Clayton, *Part I. Unified pharmacophore protein models of the benzodiazepine receptor subtypes. Part II. Subtype selective ligands for alpha5 Gaba(A) /BZ receptors [Ph.D. thesis]*, University of Wisconsin-Milwaukee, Milwaukee, Wis, USA, 2011.

[23] T. Clayton, J. L. Chen, M. Ernst et al., "An updated unified pharmacophore model of the benzodiazepine binding site on γ-aminobutyric acida receptors: correlation with comparative models," *Current Medicinal Chemistry*, vol. 14, no. 26, pp. 2755–2775, 2007.

[24] M. M. Savić, T. Clayton, R. Furtmüller et al., "PWZ-029, a compound with moderate inverse agonist functional selectivity at GABA-A receptors containing alpha5 subunits, improves passive, but not active, avoidance learning in rats," *Brain Research*, vol. 1208, pp. 150–159, 2008.

[25] M. Milić, T. Timić, S. Joksimović et al., "PWZ-029, an inverse agonist selective for α5 GABAA receptors, improves object recognition, but not water-maze memory in normal and scopolamine-treated rats," *Behavioural Brain Research*, vol. 241, no. 1, pp. 206–213, 2013.

[26] J. K. Rowlett, C. A. Moran, T. Clayton, S. Rallapalli, B. Roth, and J. M. Cook, *PWZ-029, An Inverse Agonist Selective for α5 Subunit Containing GABA(A) Receptors, Enhances Performance on an Executive Function Task in Monkeys*, European Behavioral Pharmacology Society, Rome, Italy, 2009.

[27] F. M. Benes, B. Lim, D. Matzilevich, J. P. Walsh, S. Subburaju, and M. Minns, "Regulation of the GABA cell phenotype in hippocampus of schizophrenics and bipolars," *Proceedings of the National Academy of Sciences of the United States of America*, vol. 104, no. 24, pp. 10164–10169, 2007.

[28] L. M. Rimol, C. B. Hartberg, R. Nesvåg et al., "Cortical thickness and subcortical volumes in schizophrenia and bipolar disorder," *Biological Psychiatry*, vol. 68, no. 1, pp. 41–50, 2010.

[29] C. Pantelis, D. Velakoulis, P. D. McGorry et al., "Neuroanatomical abnormalities before and after onset of psychosis: a cross-sectional and longitudinal MRI comparison," *The Lancet*, vol. 361, no. 9354, pp. 281–288, 2003.

[30] S. A. Schobel, M. A. Kelly, C. M. Corcoran et al., "Anterior hippocampal and orbitofrontal cortical structural brain abnormalities in association with cognitive deficits in schizophrenia," *Schizophrenia Research*, vol. 114, no. 1–3, pp. 110–118, 2009.

[31] S. A. Schobel, N. M. Lewandowski, C. M. Corcoran et al., "Differential targeting of the CA1 subfield of the hippocampal formation by schizophrenia and related psychotic disorders," *Archives of General Psychiatry*, vol. 66, no. 9, pp. 938–946, 2009.

[32] A. P. Weiss, D. Goff, D. L. Schacter et al., "Fronto-hippocampal function during temporal context monitoring in schizophrenia," *Biological Psychiatry*, vol. 60, no. 11, pp. 1268–1277, 2006.

[33] R. C. Wolf, A. Höse, K. Frasch, H. Walter, and N. Vasic, "Volumetric abnormalities associated with cognitive deficits in patients with schizophrenia," *European Psychiatry*, vol. 23, no. 8, pp. 541–548, 2008.

[34] H. Moore, J. D. Jentsch, M. Ghajarnia, M. A. Geyer, and A. A. Grace, "A neurobehavioral systems analysis of adult rats exposed to methylazoxymethanol acetate on E17: implications for the neuropathology of schizophrenia," *Biological Psychiatry*, vol. 60, no. 3, pp. 253–264, 2006.

[35] P. Flagstad, A. Mørk, B. Y. Glenthøj, J. Van Beek, A. T. Michael-Titus, and M. Didriksen, "Disruption of neurogenesis on gestational day 17 in the rat causes behavioral changes relevant to positive and negative schizophrenia symptoms and alters amphetamine-induced dopamine release in nucleus accumbens," *Neuropsychopharmacology*, vol. 29, no. 11, pp. 2052–2064, 2004.

[36] D. J. Lodge and A. A. Grace, "Aberrant hippocampal activity underlies the dopamine dysregulation in an animal model of schizophrenia," *The Journal of Neuroscience*, vol. 27, no. 42, pp. 11424–11430, 2007.

[37] D. J. Lodge, M. M. Behrens, and A. A. Grace, "A loss of parvalbumin-containing interneurons is associated with diminished oscillatory activity in an animal model of schizophrenia," *The Journal of Neuroscience*, vol. 29, no. 8, pp. 2344–2354, 2009.

[38] K. M. Gill, D. J. Lodge, J. M. Cook, S. Aras, and A. A. Grace, "A novel α5GABA$_A$R-positive allosteric modulator reverses hyperactivation of the dopamine system in the MAM model of schizophrenia," *Neuropsychopharmacology*, vol. 36, no. 9, pp. 1903–1911, 2011.

[39] W. Zhang, K. F. Koehler, P. Zhang, and J. M. Cook, "Development of a comprehensive pharmacophore model for the benzodiazepine receptor," *Drug Design and Discovery*, vol. 12, no. 3, pp. 193–248, 1995.

[40] W. Zhang, H. Diaz-Arauzo, M. S. Allen, K. F. Koehler, and J. M. Cook, "Chemical and computer assisted development of the inclusive pharmacophore of benzodiazepine receptors," in *Studies in Medicinal Chemistry*, M. I. Choudhary, Ed., p. 303, Harwood Academic Publishers, 1996.

[41] P. W. Zhang, W. J. Zhang, R. Y. Liu, B. Harris, P. Skolnick, and J. M. Cook, "Synthesis and SAR study of novel imidazobenzodiazepines at 'diazepam-insensitive' benzodiazepine receptors," *Journal of Medicinal Chemistry*, vol. 38, no. 10, pp. 1679–1688, 1995.

[42] Q. Huang, E. D. Cox, T. Gan et al., "Studies of molecular pharmacophore/receptor models for GABA(A)/benzodiazepine receptor subtypes: binding affinities of substituted β-carbolines at recombinant $\alpha1\beta3\gamma2$ subtypes and quantitative structure-activity relationship studies via a comparative molecular field analysis," *Drug Design and Discovery*, vol. 16, no. 1, pp. 55–76, 1999.

[43] D. Harris, T. Clayton, J. Cook et al., "Selective influence on contextual memory: physiochemical properties associated with selectivity of benzodiazepine ligands at GABA$_A$ receptors containing the α5 subunit," *Journal of Medicinal Chemistry*, vol. 51, no. 13, pp. 3788–3803, 2008.

[44] D. Rüedi-Bettschen, J. K. Rowlett, S. Rallapalli, T. Clayton, J. M. Cook, and D. M. Platt, "Modulation of α5 subunit-containing GABAA receptors alters alcohol drinking by rhesus monkeys," *Alcoholism: Clinical and Experimental Research*, vol. 37, no. 4, pp. 624–634, 2013.

[45] M. M. Savić, M. M. Milinković, S. Rallapalli et al., "The differential role of alpha1- and alpha5-containing GABAA receptors in mediating diazepam effects on spontaneous locomotor activity and water-maze learning and memory in rats," *International Journal of Neuropsychopharmacology*, vol. 12, no. 9, pp. 1179–1193, 2009.

[46] X. Y. Li, C. R. Ma, X. H. He et al., "Studies in search of diazepam-insensitive subtype selective agents for GABA$_A$/Bz receptors," *Medicinal Chemistry Research*, vol. 11, no. 9, pp. 504–537, 2003.

[47] L. Duggan, M. Fenton, J. Rathbone, R. Dardennes, A. El-Dosoky, and S. Indran, "Olanzapine for schizophrenia," *Cochrane Database of Systematic Reviews*, no. 2, Article ID CD001359, 2005.

[48] J. A. Lieberman, T. S. Stroup, J. P. McEvoy et al., "Effectiveness of antipsychotic drugs in patients with chronic schizophrenia," *The New England Journal of Medicine*, vol. 353, no. 12, pp. 1209–1223, 2005.

[49] K. Komossa, C. Rummel-Kluge, H. Hunger et al., "Olanzapine versus other atypical antipsychotics for schizophrenia," *Cochrane Database of Systematic Reviews*, no. 3, Article ID CD006654, 2010.

[50] K. Komossa, C. Rummel-Kluge, H. Hunger et al., "Zotepine versus other atypical antipsychotics for schizophrenia," *Cochrane Database of Systematic Reviews*, no. 1, p. CD006628, 2010.

[51] K. Komossa, C. Rummel-Kluge, H. Hunger et al., "Amisulpride versus other atypical antipsychotics for schizophrenia," *Cochrane Database of Systematic Reviews*, no. 1, p. CD006624, 2010.

[52] K. Komossa, C. Rummel-Kluge, F. Schmid et al., "Quetiapine versus other atypical antipsychotics for schizophrenia," *Cochrane Database of Systematic Reviews*, no. 1, Article ID CD006625, 2010.

[53] C. Sur, L. Fresu, O. Howell, R. M. McKernan, and J. R. Atack, "Autoradiographic localization of α5 subunit-containing GABA(A) receptors in rat brain," *Brain Research*, vol. 822, no. 1-2, pp. 265–270, 1999.

[54] H. L. June, S. C. Harvey, K. L. Foster et al., "GABAA receptors containing α5 subunits in the CA1 and CA3 hippocampal fields regulate ethanol-motivated behaviors: an extended ethanol reward circuitry," *The Journal of Neuroscience*, vol. 21, no. 6, pp. 2166–2177, 2001.

[55] A. Lingford-Hughes, S. P. Hume, A. Feeney et al., "Imaging the GABA-benzodiazepine receptor subtype containing the alpha5-subunit in vivo with [11C]Ro15 4513 positron emission tomography," *Journal of Cerebral Blood Flow and Metabolism*, vol. 22, no. 7, pp. 878–889, 2002.

[56] B. Hutcheon, J. M. Fritschy, and M. O. Poulter, "Organization of GABAA receptor alpha-subunit clustering in the developing rat neocortex and hippocampus," *European Journal of Neuroscience*, vol. 19, no. 9, pp. 2475–2487, 2004.

[57] B. Ramos, J. F. Lopez-Tellez, J. Vela et al., "Expression of α5 GABAA receptor subunit in developing rat hippocampus," *Developmental Brain Research*, vol. 151, no. 1-2, pp. 87–98, 2004.

[58] S. K. Towers, T. Gloveli, R. D. Traub et al., "Alpha5 subunit-containing GABAA receptors affect the dynamic range of mouse hippocampal kainate-induced gamma frequency oscillations in vitro," *Journal of Physiology*, vol. 559, no. 3, pp. 721–728, 2004.

[59] S. A. Heldt and K. J. Ressler, "Forebrain and midbrain distribution of major benzodiazepine-sensitive GABAA receptor subunits in the adult C57 mouse as assessed with in situ hybridization," *Neuroscience*, vol. 150, no. 2, pp. 370–385, 2007.

[60] C. Papatheodoropoulos and E. Koniaris, "α5GABAA receptors regulate hippocampal sharp wave-ripple activity in vitro," *Neuropharmacology*, vol. 60, no. 4, pp. 662–673, 2011.

[61] K. M. Gill, J. M. Cook, M. M. Poe, and A. A. Grace, "Prior antipsychotic drug treatment prevents response to novel antipsychotic agent in the methylazoxymethanol acetate model of schizophrenia," *Schizophrenia Bulletin*, vol. 40, no. 2, pp. 341–350, 2014.

[62] C. C. Kaczorowski and J. F. Disterhoft, "Memory deficits are associated with impaired ability to modulate neuronal excitability in middle-aged mice," *Learning and Memory*, vol. 16, no. 6, pp. 362–366, 2009.

[63] C. C. Kaczorowski, E. Sametsky, S. Shah, R. Vassar, and J. F. Disterhoft, "Mechanisms underlying basal and learning-related intrinsic excitability in a mouse model of Alzheimer's disease," *Neurobiology of Aging*, vol. 32, no. 8, pp. 1452–1465, 2011.

[64] C. C. Kaczorowski, S. J. Davis, and J. R. Moyer Jr., "Aging redistributes medial prefrontal neuronal excitability and impedes extinction of trace fear conditioning," *Neurobiology of Aging*, vol. 33, no. 8, pp. 1744–1757, 2012.

[65] S. I. Rallapalli, *Synthesis of Agents to Enhance Cognition. II. Synthesis of Indole Alkaloids*, University of Wisconsin-Milwaukee, 2014.

[66] P. J. Barnes, "Biochemistry of asthma," *Trends in Biochemical Sciences*, vol. 16, pp. 365–369, 1991.

[67] D. W. Cockcroft, "Clinical concerns with inhaled β2-agonists: adult asthma," *Clinical Reviews in Allergy and Immunology*, vol. 31, no. 2-3, pp. 197–208, 2006.

[68] R. W. Morton, M. L. Everard, and H. E. Elphick, "Adherence in childhood asthma: the elephant in the room," *Archives of Disease in Childhood*, vol. 99, no. 10, pp. 949–953, 2014.

[69] N. S. Jentzsch, P. Camargos, E. S. C. Sarinho, and J. Bousquet, "Adherence rate to beclomethasone dipropionate and the level of asthma control," *Respiratory Medicine*, vol. 106, no. 3, pp. 338–343, 2012.

[70] E. K. Chu and J. M. Drazen, "Asthma: one hundred years of treatment and onward," *The American Journal of Respiratory and Critical Care Medicine*, vol. 171, no. 11, pp. 1202–1208, 2005.

[71] G. Gallos, N. R. Gleason, Y. Zhang et al., "Activation of endogenous GABAA channels on airway smooth muscle potentiates isoproterenol-mediated relaxation," *The American Journal of Physiology—Lung Cellular and Molecular Physiology*, vol. 295, no. 6, pp. L1040–L1047, 2008.

[72] K. Mizuta, D. Xu, Y. Pan et al., "GABAA receptors are expressed and facilitate relaxation in airway smooth muscle," *The American Journal of Physiology—Lung Cellular and Molecular Physiology*, vol. 294, no. 6, pp. L1206–L1216, 2008.

[73] M. M. Savić, T. Clayton, R. Furtmüller et al., "PWZ-029, a compound with moderate inverse agonist functional selectivity at $GABA_A$ receptors containing α5 subunits, improves passive, but not active, avoidance learning in rats," *Brain Research*, vol. 1208, pp. 150–159, 2008.

[74] M. M. Savić, S. Huang, R. Furtmüller et al., "Are GABAA receptors containing alpha5 subunits contributing to the sedative properties of benzodiazepine site agonists?," *Neuropsychopharmacology*, vol. 33, no. 2, pp. 332–339, 2008.

[75] G. Gallos, G. T. Yocum, M. E. Siviski et al., "Selective targeting of the α5 subunit of $GABA_A$ receptors relaxes airway smooth muscle and inhibits cellular calcium handling," *American Journal of Physiology—Lung Cellular and Molecular Physiology*, vol. 308, no. 9, pp. L931–L942, 2015.

[76] M. S. Allen, Y.-C. Tan, M. L. Trudell et al., "Synthetic and computer-assisted analyses of the pharmacophore for the benzodiazepine receptor inverse agonist site," *Journal of Medicinal Chemistry*, vol. 33, no. 9, pp. 2343–2357, 1990.

[77] M. S. Allen, T. J. Hagen, M. L. Trudell, P. W. Codding, P. Skolnick, and J. M. Cook, "Synthesis of novel 3-substituted β-carbolines as benzodiazepine receptor ligands: probing the benzodiazepine receptor pharmacophore," *Journal of Medicinal Chemistry*, vol. 31, no. 9, pp. 1854–1861, 1988.

[78] H. Diaz-Arauzo, G. E. Evoniuk, P. Skolnick, and J. M. Cook, "The agonist pharmacophore of the benzodiazepine receptor. Synthesis of a selective anticonvulsant/anxiolytic," *Journal of Medicinal Chemistry*, vol. 34, no. 5, pp. 1754–1756, 1991.

[79] H. Diaz-Arauzo, K. F. Koehler, T. J. Hagen, and J. M. Cook, "Synthetic and computer assisted analysis of the pharmacophore for agonists at benzodiazepine receptors," *Life Sciences*, vol. 49, no. 3, pp. 207–216, 1991.

[80] W. J. Zhang, K. F. Koehler, B. Harris, P. Skolnick, and J. M. Cook, "Synthesis of benzo-fused benzodiazepines employed as probes of the agonist pharmacophore of benzodiazepine receptors," *Journal of Medicinal Chemistry*, vol. 37, no. 6, pp. 745–757, 1994.

[81] M. L. Trudell, S. L. Lifer, Y.-C. Tan et al., "Synthesis of substituted 7,12-dihydropyrido[3,2-b:5,4-b′]diindoles: rigid planar benzodiazepine receptor ligands with inverse agonist/antagonist properties," *Journal of Medicinal Chemistry*, vol. 33, no. 9, pp. 2412–2420, 1990.

[82] M. L. Trudell, A. S. Basile, H. E. Shannon, P. Skolnick, and J. M. Cook, "Synthesis of 7,12-dihydropyrido[3,4-b:5,4-b′]diindoles. A novel class of rigid, planar benzodiazepine receptor ligands," *Journal of Medicinal Chemistry*, vol. 30, no. 3, pp. 456–458, 1987.

[83] M. J. Frisch, G. W. Trucks, M. Head-Gordon et al., *Gaussian 92*, Gaussian, Pittsburgh, Pa, USA, 1992, http://www.lct.jussieu.fr/manuels/Gaussian98/00000119.htm.

[84] M. L. I. Trudell, *The synthesis and study of the pharmacologic activity of 7,12 dihydropyrido[3,2 b:5,4 b′]diindoles. A novel class of rigid, planar benzodiazepine receptor ligands. II. The total synthesis of the indole alkaloid, (±) suaveoline [Ph.D. thesis]*, University of Wisconsin-Milwaukee, Milwaukee, Wis, USA, 1989.

[85] W. Yin, S. Majumder, T. Clayton et al., "Design, synthesis, and subtype selectivity of 3,6-disubstituted β-carbolines at Bz/GABA(A)ergic receptors. SAR and studies directed toward agents for treatment of alcohol abuse," *Bioorganic and Medicinal Chemistry*, vol. 18, no. 21, pp. 7548–7564, 2010.

[86] D. Han, F. H. Forsterling, X. Li, J. Deschamps, H. Cao, and J. M. Cook, "Study of the structure activity relationships of $GABA_A$-benzodiazepine receptor ligands by low termperature NMR spectroscopy and X-ray analysis," in *Proceedings of the 227th ACS National Meeting*, Anaheim, Calif, USA, March-April 2004.

[87] B. D. Fischer, S. C. Licata, H. Zhou et al., "Anxiolytic-like effects of 8-acetylene imidazobenzodiazepines in a rhesus monkey conflict procedure," *Neuropharmacology*, vol. 59, no. 7-8, pp. 612–618, 2010.

[88] W. Haefely, E. Kyburz, M. Gerecke, and H. Mohler, "Recent advances in the molecular pharmacology of benzodiazepine receptors and in the structure—activity relationships of their agonist and antagonists," in *Advances in Drug Research*, vol. 99, pp. 165–322, Academic Press, New York, NY, USA, 1985.

[89] R. I. Fryer, Z.-Q. Gu, and C.-G. Wang, "Synthesis of novel, substituted 4H-imidazo[1,5-a][1,4]benzodiazepines," *Journal of Heterocyclic Chemistry*, vol. 28, no. 7, pp. 1661–1669, 1991.

[90] R. I. Fryer, P. Zhang, R. Rios, Z.-Q. Gu, A. S. Basile, and P. Skolnick, "Structure-activity relationship studies at the benzodiazepine receptor (Bzr)—a comparison of the substituent effects of pyrazoloquinolinone analogs," *Journal of Medicinal Chemistry*, vol. 36, no. 11, pp. 1669–1673, 1993.

[91] F. M. Rivas, C. R. Edwankar, J. M. Cook et al., "Antiseizure activity of novel γ-aminobutyric acid (A) receptor subtype-selective benzodiazepine analogues in mice and rat models," *Journal of Medicinal Chemistry*, vol. 52, no. 7, pp. 1795–1798, 2009.

[92] J. M. Cook, D. Han, X. He et al., "Anxiolytic agents with reduced sedative and ataxic effects," 7119196 B2, 2006.

[93] J. M. Cook, H. Zhao, S. Huang, P. S. Sarma, and C. C. Zhang, "Stereospecific anxiolytic and anticonvulsant agents with reduced muscle-relaxant, sedative-hypnotic and ataxic effects," US Patent 2006004945, 2007.

[94] R. I. Fryer, *Comprehensive Medicinal Chemistry*, vol. 99, Pergamon Press, Oxford, UK, 1989.

[95] H. O. Villar, M. F. Davies, G. H. Loew, and P. A. Maguire, "Molecular models for recognition and activation at the benzodiazepine receptor: a review," *Life Sciences*, vol. 48, no. 7, pp. 593–602, 1991.

[96] H. O. Villar, E. T. Uyeno, L. Toll, W. Polgar, M. F. Davies, and G. H. Loew, "Molecular determinants of benzodiazepine receptor affinities and anticonvulsant activities," *Molecular Pharmacology*, vol. 36, no. 4, pp. 589–600, 1989.

[97] G. M. Crippen, "Distance geometry analysis of the benzodiazepine binding site," *Molecular Pharmacology*, vol. 22, no. 1, pp. 11–19, 1982.

[98] A. K. Ghose and G. M. Crippen, "Modeling the benzodiazepine receptor binding site by the general three-dimensional structure-directed quantitative structure-activity relationship method REMOTEDISC," *Molecular Pharmacology*, vol. 37, no. 5, pp. 725–734, 1990.

[99] P. W. Codding and A. K. S. Muir, "Molecular structure of Ro15-1788 and a model for the binding of benzodiazepine receptor ligands. Structural identification of common features in antagonists," *Molecular Pharmacology*, vol. 28, no. 2, pp. 178–184, 1985.

[100] A. K. S. Muir and P. W. Codding, "Structure-activity studies of β-carbolines. 3. Crystal and molecular structures of methyl β-carboline-3-carboxylate," *Canadian Journal of Chemistry*, vol. 63, no. 10, pp. 2752–2756, 1985.

[101] M. G. Codding, A. W. Roszak, M. B. Szkaradzinska, J. M. Cook, and L. J. Aha, *Modeling of the Benzodiazepine Receptor Using Structural and Theoretical Characterization of Novel Beta-Carbolines*, Elsevier Science, Amsterdam, The Netherlands, 1989.

[102] V. Ferretti, P. Gilli, and P. A. Borea, "Structural features controlling the binding of β-carbolines to the benzodiazepine receptor," *Acta Crystallographica Section B: Structural Science*, vol. 60, no. 4, pp. 481–489, 2004.

[103] P. A. Borea, G. Gilli, V. Bertolasi, and V. Ferretti, "Stereochemical features controlling binding and intrinsic activity properties of benzodiazepine-receptor ligands," *Molecular Pharmacology*, vol. 31, no. 4, pp. 334–344, 1987.

[104] V. Bertolasi, V. Feretti, G. Gilli, and P. A. Borea, "Stereochemistry of benzodiazepine-receptor ligands.1. Structure of methyl beta-carboline-3-carboxylate (beta-CCM), $C_{13}H_{10}N_2O_2$," *Acta Crystallographica Section C: Crystal Structure Communications*, vol. 40, p. 1981, 1984.

[105] V. Ferretti, V. Bertolasi, G. Gilli, and P. A. Borea, "Structures of two 2-arylpyrazolo[4,3-c]quinolin-3-ones: CGS8216, $C_{16}H_{11}N_3O$, and CGS9896, $C_{16}H_{10}ClN_3O$," *Acta Crystallographica Section C: Crystal Structure Communications*, vol. 41, no. 1, pp. 107–110, 1985.

[106] S. Tebib, J.-J. Bourguignon, and C.-G. Wermuth, "The active analog approach applied to the pharmacophore identification of benzodiazepine receptor ligands," *Journal of Computer-Aided Molecular Design*, vol. 1, no. 2, pp. 153–170, 1987.

[107] C. R. Gardner, "A review of recently-developed ligands for neuronal benzodiazepine receptors and their pharmacological activities," *Progress in Neuropsychopharmacology and Biological Psychiatry*, vol. 16, no. 6, pp. 755–781, 1992.

[108] M. S. Allen, A. J. LaLoggia, L. J. Dorn et al., "Predictive binding of β-carboline inverse agonists and antagonists via the CoMFA/GOLPE approach," *Journal of Medicinal Chemistry*, vol. 35, no. 22, pp. 4001–4010, 1992.

[109] Q. Huang, E. Cox, T. Gan et al., "Studies of molecular pharmacophore/receptor models for $GABA_A$/benzodiazepine receptor subtypes: binding affinities of substituted β-carbolines at recombinant alpha x beta 3 gamma 2 subtypes and quantitative structure-activity relationship studies via a comparative molecular field analysis," *Drug Design and Discovery*, vol. 16, no. 1, pp. 55–76, 1999.

[110] X. He, Q. Huang, C. Ma, S. Yu, R. McKernan, and J. M. Cook, "Pharmacophore/receptor models for GABA(A)/BzR $\alpha 2\beta 3\gamma 2$, $\alpha 3\beta 3\gamma 2$ and $\alpha 4\beta 3\gamma 2$ recombinant subtypes. Included volume analysis and comparison to $\alpha 1\beta 3\gamma 2$, $\alpha 5\beta 3\gamma 2$ and $\alpha 6\beta 3\gamma 2$ subtypes," *Drug Design and Discovery*, vol. 17, no. 2, pp. 131–171, 2000.

[111] E. D. Cox, H. Diaz-Arauzo, Q. Huang et al., "Synthesis and evaluation of analogues of the partial agonist 6- (propyloxy)-4-(methoxymethyl)-β-carboline-3-carboxylic acid ethyl ester (6-PBC) and the full agonist 6-(benzyloxy)-4-(methoxymethyl)-β-carboline-3-carboxylic acid ethyl ester (Zk 93423) at wild type and recombinant GABA(A) receptors," *Journal of Medicinal Chemistry*, vol. 41, no. 14, pp. 2537–2552, 1998.

[112] M. J. Martin, M. L. Trudell, H. D. Araúzo et al., "Molecular yardsticks—rigid probes to define the spatial dimensions of the benzodiazepine receptor binding site," *Journal of Medicinal Chemistry*, vol. 35, no. 22, pp. 4105–4117, 1992.

[113] K. Naryanan and J. M. Cook, "Probing the dimensions of the benzodiazepine receptor inverse agonist site," *Heterocycles*, vol. 31, no. 2, pp. 203–209, 1990.

[114] S. P. Hollinshead, M. L. Trudell, P. Skolnick, and J. M. Cook, "Structural requirements for agonist actions at the benzodiazepine receptor: studies with analogues of 6-(benzyloxy)-4-(methoxymethyl)-beta-carboline-3-carboxylic acid ethyl ester," *Journal of Medicinal Chemistry*, vol. 33, no. 3, pp. 1062–1069, 1990.

[115] J. M. Cook, H. Diaz-Arauzo, and M. S. Allen, "Inverse agonists: probes to study the structure, topology and function of the benzodiazepine receptor," in *Proceedings of the 51st Annual Scientific Meeting*, L. S. Harris, Ed., National Institute on Drug Abuse Research Monograph, pp. 133–139, The College on Problems of Drug Dependence, 1991.

[116] R. Trullas, H. Ginter, B. Jackson et al., "3-Ethoxy-beta-carboline: a high affinity benzodiazepine receptor ligand with partial inverse agonist properties," *Life Sciences*, vol. 43, no. 15, pp. 1189–1197, 1988.

[117] M. Cain, R. W. Weber, F. Guzman et al., "β-Carbolines: synthesis and neurochemical and pharmacological actions on brain benzodiazepine receptors," *Journal of Medicinal Chemistry*, vol. 25, no. 9, pp. 1081–1091, 1982.

[118] X. H. He, C. C. Zhang, and J. M. Cook, "Model of the BzR binding site: correlation of data from site-directed mutagenesis and the pharmacophore/receptor model," *Medicinal Chemistry Research*, vol. 10, no. 5, pp. 269–308, 2001.

[119] Q. Huang, R. Y. Liu, P. W. Zhang et al., "Predictive models for $GABA_A$/benzodiazepine receptor subtypes: studies of quantitative structure-activity relationships for imidazobenzodiazepines at five recombinant $GABA_A$/benzodiazepine receptor subtypes [$\alpha x\beta 3\gamma 2$ ($x = 1$–3, 5, and 6)] via comparative molecular field analysis," *Journal of Medicinal Chemistry*, vol. 41, no. 21, pp. 4130–4142, 1998.

[120] R. Y. Liu, P. W. Zhang, T. Gan, R. M. McKernan, and J. M. Cook, "Evidence for the conservation of conformational topography at five major GABA(A)/benzodiazepine receptor subsites. Potent affinities of the (S)-enantiomers of framework-constrained 4,5-substituted pyrroloimidazo-benzodiazepines," *Medicinal Chemistry Research*, vol. 7, no. 1, pp. 25–35, 1997.

[121] Q. Huang, W. Zhang, R. Liu, R. M. McKernan, and J. M. Cook, "Benzo-fused benzodiazepines employed as topological probes

for the study of benzodiazepine receptor subtypes," *Medicinal Chemistry Research*, vol. 6, no. 6, pp. 384–391, 1996.

[122] S. Yu, X. H. He, C. R. Ma, R. McKernan, and J. M. Cook, "Studies in search of α2 selective ligands for GABAA/BzR receptor subtypes. Part I. Evidence for the conservation of pharmacophoric descriptors for DS subtypes," *Medicinal Chemistry Research*, vol. 9, no. 3, pp. 186–202, 1999.

[123] S. Arbilla, H. Depoortere, P. George, and S. Z. Langer, "Pharmacological profile of the imidazopyridine zolpidem at benzodiazepine receptors and electrocorticogram in rats," *Naunyn-Schmiedeberg's Archives of Pharmacology*, vol. 330, no. 3, pp. 248–251, 1985.

[124] G. Wong, K. F. Koehler, P. Skolnick et al., "Synthetic and computer-assisted analysis of the structural requirements for selective, high-affinity ligand binding to diazepam-insensitive benzodiazepine receptors," *Journal of Medicinal Chemistry*, vol. 36, no. 13, pp. 1820–1830, 1993.

[125] A. Camerman and N. Camerman, "Stereochemical basis of anticonvulsant drug action. 2. Molecular structure of diazepam," *Journal of the American Chemical Society*, vol. 94, no. 1, pp. 268–272, 1972.

[126] A. Hempel, N. Camerman, and A. Camerman, "Benzodiazepine stereochemistry: crystal structures of the diazepam antagonist Ro 15-1788 and the anomalous benzodiazepine Ro 5-4864," *Canadian Journal of Chemistry*, vol. 65, no. 7, pp. 1608–1612, 1987.

[127] S. Neidle, G. D. Webster, G. B. Jones, and D. E. Thurston, "Structures of two DNA minor-groove binders, based on pyrrolo[2,1-c][1,4]-benzodiazepines," *Acta Crystallographica Section C: Crystal Structure Communications*, vol. 47, no. 12, pp. 2678–2680, 1991.

[128] T. A. Halgren, "Merck molecular force field. V. Extension of MMFF94 using experimental data, additional computational data, and empirical rules," *Journal of Computational Chemistry*, vol. 17, no. 5-6, pp. 616–641, 1996.

[129] T. A. Halgren, "Merck molecular force field. III. Molecular geometries and vibrational frequencies for MMFF94," *Journal of Computational Chemistry*, vol. 17, no. 5-6, pp. 553–586, 1996.

[130] T. A. Halgren, "Merck molecular force field. II. MMFF94 van der Waals and electrostatic parameters for intermolecular interactions," *Journal of Computational Chemistry*, vol. 17, no. 5-6, pp. 520–552, 1996.

[131] T. A. Halgren, "Merck molecular force field. I. Basis, form, scope, parameterization, and performance of MMFF94," *Journal of Computational Chemistry*, vol. 17, no. 5-6, pp. 490–519, 1996.

[132] T. A. Halgren and R. B. Nachbar, "Merck molecular force field. IV. Conformational energies and geometries for MMFF94," *Journal of Computational Chemistry*, vol. 17, no. 5-6, pp. 587–615, 1996.

[133] H. L. June, S. C. Harvey, K. L. Foster et al., "$GABA_A$ receptors containing α5 subunits in the CA1 and CA3 hippocampal fields regulate ethanol-motivated behaviors: an extended ethanol reward circuitry," *Journal of Neuroscience*, vol. 21, no. 6, pp. 2166–2177, 2001.

[134] B. J. Kaminski, M. L. Van Linn, J. M. Cook, W. Yin, and E. M. Weerts, "Effects of the benzodiazepine GABAA α1-preferring ligand, 3-propoxy-β-carboline hydrochloride (3-PBC), on alcohol seeking and self-administration in baboons," *Psychopharmacology*, vol. 227, no. 1, pp. 127–136, 2013.

[135] S. Huang, *Synthesis of Optically Active Subtype Selective Benzodiazepine Receptor Ligands*, University of Wisconsin, Milwaukee, Wis, USA, 2007.

[136] M. M. Savić, S. Majumder, S. Huang et al., "Novel positive allosteric modulators of $GABA_A$ receptors: do subtle differences in activity at α1 plus α5 versus α2 plus α3 subunits account for dissimilarities in behavioral effects in rats?" *Progress in Neuro-Psychopharmacology and Biological Psychiatry*, vol. 34, no. 2, pp. 376–386, 2010.

[137] M. Ernst, D. Brauchart, S. Boresch, and W. Sieghart, "Comparative modeling of GABAA receptors: limits, insights, future developments," *Neuroscience*, vol. 119, no. 4, pp. 933–943, 2003.

[138] B. L. Roth, "Ki determinations were generously provided by the National Institute of Mental Health's Psychoactive Drug Screening Program," Contract # HHSN-271-2013-00017-C (NIMH PDSP), The NIMH PDSP, 2013, https://pdspdb.unc.edu/pdspWeb/.

[139] M. S. Choudhary, S. Craigo, and B. L. Roth, "Identification of receptor domains that modify ligand binding to 5-hydroxytryptamine2 and 5-hydroxytryptamine1c serotonin receptors," *Molecular Pharmacology*, vol. 42, no. 4, pp. 627–633, 1992.

[140] J. Yang, Y. Teng, S. Ara, S. Rallapalli, and J. M. Cook, "An improved process for the synthesis of 4H-imidazo[1,5-a][1,4]benzodiazepines," *Synthesis*, no. 6, pp. 1036–1040, 2009.

[141] Z.-Q. Gu, G. Wong, C. Dominguez, B. R. De Costa, K. C. Rice, and P. Skolnick, "Synthesis and evaluation of imidazo[1,5-a][1,4]benzodiazepine esters with high affinities and selectivities at 'diazepam-insensitive' benzodiazepine receptors," *Journal of Medicinal Chemistry*, vol. 36, no. 8, pp. 1001–1006, 1993.

[142] J. Buckingham, *Dictionary of Organic Compounds*, vol. 2, Chapman & Hall, New York, NY, USA, 1982.

[143] C. Yung-Chi and W. H. Prusoff, "Relationship between the inhibition constant (KI) and the concentration of inhibitor which causes 50 per cent inhibition (I50) of an enzymatic reaction," *Biochemical Pharmacology*, vol. 22, no. 23, pp. 3099–3108, 1973.

[144] J. M. Cook, T. Clayton, Y. T. Johnson, S. Rallapalli, and D. Han, "GABAergic agents to treat memory deficits," US Patent 2010/0130479 A1, 2010.